Univerzita Karlova v Praze

Přírodovědecká fakulta

Doktorský studijní program: geologie

Mgr. Zuzana Burdíková

Aktuoekologie krytének ve sladkovodním a půdním prostředí v interakci s houbami & jejich analýza novými mikroskopickými technikami

Actuoecology of testate amoebae in fresh water and soil environment in interaction with fungi & their analysis with new microscopic techniques

Disertační práce

Školitelka: Doc. Katarína Holcová, CSc.

Praha, 2012

Školitelka: Doc. RNDr. Katarína Holcová, CSc., Přírodovědecká fakulta UK v Praze, Ústav geologie a paleontologie

Konzultantka: RNDr. Lucie Kubínová, CSc., Fyziologický ústav AVČR v.v.i., Oddělení biomatematiky

Poděkování

Děkuji své školitelce Doc. RNDr. Kataríně Holcové, CSc. a RNDr. Lucii Kubínové, CSc. za odborné vedení, pomoc a veškerou podporu, kterou mi poskytovaly během mé práce.

Dále děkuji RNDr. Martinu Vohníkovi, PhD. za pomoc při experimentální práci a vytvoření příjemného prostředí na pracovišti. Rovněž děkuji Mgr. Ondřeji Hudečkovi za pomoc s konečnou úpravou disertační práce, své rodině, manželovi Mgr. Zdeňku Švindrychovi a dceři Janě za trpělivost a podporu, která mi umožnila mou disertační práci zdárně vypracovat.

Je mou milou povinností poděkovat také Československé mikroskopické společnosti a Evropské mikroskopické společnosti za částečné financování nákladů, spojených se zahraničními prezentacemi dosažených výsledků.

Prohlašuji, že jsem závěrečnou práci zpracovala samostatně a že jsem uvedla všechny použité informační zdroje a literaturu. Tuto disertační práci ani její podstatnou část jsem nepředložila k získání jiného nebo stejného akademického titulu. Prohlášení spoluautorů jsou připojena ve zvláštní příloze, která není součástí disertační práce.

Mgr. Zuzana Burdíková V Praze, 4. 1. 2012

ABSTRAKT

Tato disertační práce se zabývá studiem krytének ve vztahu k jejich přirozenému biotopu a možností analýzy krytének pokročilými mikroskopickými technikami. Hlavní výzkum se opírá o původní publikované vědecké články, ty jsou zařazeny do tří samostatných kapitol (Část I, Část II & Část III) a každá je opatřena úvodem.

(Část I) Metodická část disertační práce se věnuje využití pokročilých mikroskopických technik používaných k rozšíření rozsahu ekologických analýz. Zejména přesné rozlišení živých a mrtvých jedinců ve vzorku, přesné měření biomasy uvnitř schránky či vizualizace cytoplazmy mohou výrazně ovlivnit výsledky ekologických studií. Jako hlavní metody analýzy krytének byly použity nově konfokální a dvoufotonová mikroskopie. Tyto pokročilé mikroskopické metody umožnily zkoumat podrobně morfologii krytének. Údaje mohou mít vliv na taxonomii a ekofyziologii, včetně využití krytének jako bioindikátoru znečištění.

(Část II) Aktuoekologická analýza se zaměřuje na výkyvy ve složení společenstva krytének ve sladkovodním ekosystému, jmenovitě Komořanských tůňkách v Praze, v průběhu roku. Změny v druhovém složení krytének jsou korelovány se současně zaznamenávanými limnologickými parametry jako je teplota, pH, koncentrace těžkých kovů (Ni, Cd, Pb, Mn, As) nebo polycyklických aromatických uhlovodíků a dalších chemických látek (NH_4^+, NO_3^-, P).
Údaje získané v mělkých tůňkách ukázaly, že ekologické preference nároky rodu *Arcella* a rodu *Difflugia* se zdají být v opozici.

(Část III) Složitější ekologické interakce byly studovány zkoumáním interakce v mykorhizosféře evropských rhododendronů mezi kryténkami a erikoidně mykorhizními houbami a DSE-asociací, pojmenované podle hub, které ji tvoří (*Dark Septate Endophytes*). Možná role krytének jako zdroje živin pro hostitelské rostliny je diskutována. Další studie se zaměřuje na interakci mezi kryténkami a myceliem saprotrofních hub kolonizujících opad borovice lesní (*Pinus sylvestris*). Analýzou bylo zjištěno, že saprofytické/parazitické houby interagují s kryténkami ve

smrkovém opadu. Půdní houby tak nepřímo ovlivňují bakteriální populace v hyphosféře. Tato interakce zahrnuje mykofágy, houbové parazity a dekompozici schránek krytének.

Abstract

The present thesis focuses on testate amoebae (TA) and their relationship to their natural environment, as well as on relevant microscopic imaging methods. The bulk of the data has been published in original scientific papers and is compiled into three separate chapters (Pt I, Pt II & Pt III), each annotated by a brief introduction.

(Pt I) The methods section is devoted to specialized microscopic techniques employed to broaden the scope of the ecological analyses. In particular, precise discrimination between live and dead individuals, biomass determination inside individual tests and a multi-modal visualization of the cytoplasm and organelles enhance the data. Laser scanning confocal microscopy and two-photon microscopy are the main imaging modalities employed to study TA morphology in detail. The data have implications for taxonomy and ecophysiology, including the use of TA as bioindicators of pollution.

(Pt II) An actuoecological analysis focuses on the seasonal variability of TA species composition in a freshwater ecosystem, namely the Komořany ponds in Prague, during the course of the year. The species composition variation is correlated to simultaneously recorded limnological parameters such as temperature, pH, contamination by (heavy) metals (As, Cd, Mn, Ni, Fe, Pb), polycyclic aromatic hydrocarbons (PAH) and other chemical species (NH_4^+, NO_3^-, P). For example, the data obtained in shallow ponds revealed that the ecological preferences of *Arcella* and *Difflugia* genera are more-or-less opposite.

(Pt III) More complex ecological interactions were studied by investigating the interaction in the mycorhizosphere of European rhododendrons between TA and ericoid mycorrhizal fungi (ErMF) and dark septate endophytes (DSE) fungi. The possible role of TA as a source of nutrients for the host plant is discussed. Another study focuses on the interactions between TA and saprotrophic fungi mycelium colonizing Scots pine (*Pinus sylvestris* L.). The analysis of TA species composition data revealed that the saprotrophic/parasitic fungi do indeed interact with TA. Soil fungi interact with TA indirectly by affecting the bacterial population in the hyphosphere. This interaction involves mycophagy, fungal parasites and TA test decomposition.

OBSAH

1. PŘEDMLUVA

Tuto disertační práci jsem vypracovala v rámci doktorského studia na Ústavu geologie a paleontologie PřF UK. Vlastní práce probíhala v období 2004-2011 na Ústavu geologie a paleontologie PřF UK, na Oddělení mykorhizních symbióz BÚ AVČR v.v.i. v Průhonicích a Fyziologickém ústavu AVČR v.v.i. v Krči. Mou školitelkou byla Doc. RNDr. Katarína Holcová, CSc. a konzultantkou RNDr. Lucie Kubínová, CSc.

Předkládaná DP je sepsána v českém jazyce se shrnutím v angličtině. Detailní popis konkrétních experimentálních metod a postupů, výsledky, poděkování a finanční podpora jsou uvedeny v jednotlivých manuskriptech/publikacích. Práce je zakončena shrnutím dosažených výsledků, jejich obecnou diskuzí a závěrem. Seznam literatury na konci práce obsahuje pouze články ještě neuvedené v jednotlivých manuskriptech/publikacích. Praktická část této disertační práce je rozdělena do tří částí, jejichž centrálním motivem je zkoumání ekologie krytének pomocí nejrůznějších přístupů:

Část I: Analýza krytének novými mikroskopickými technikami

Tato část obsahuje jeden původní článek:

Článek 1: *Burdíková Z, Čapek M, Ostašov P, Machač J, Pelc R, Mitchell EAD, Kubínová L. 2010. Testate amoebae examined by confocal and two-photon microscopy: implications for taxonomy and ecophysiology. Microscopy and Microanalysis 16: 735–746*

Část II: Aktuoekologie krytének sladkovodního prostředí

Tato část obsahuje jeden původní manuskript:

Článek 2: *Burdíková Z, Čapek M, Švindrych Z, Gryndler M, Kubínová L, Holcová K. Ecology of testate amoebae in the Komořany Pools of the Vltava Basin. Manuskript v tisku v časopise Microbial Ecology*

Část III: Interakce mezi kryténkami a mykorhizními a saprotrofními houbami

Tato část obsahuje dva původní články:

Článek 3: *Vohník M, Burdíková Z, Albrechtová J, Vosátka M. 2009 Testate amoebae vs. mycorrhizal fungi: a possible novel interaction in the mycorhizosphere*

of ericaceous plants? Microbial Ecology 57: 203–214

Článek 4: *Vohník M, Burdíková Z, Vyhnal A, Koukol O. 2011. Interactions between testate amoebae and saprotrophic microfungi in a Scots pine litter microcosm. Microbial Ecology 61: 660-668*

2. ÚVOD

2.1. Morfologie a fyziologie krytének

Kryténky (TA) (Arcellinida a Euglyphida) jsou polyfyletickou skupinou jednobuněčných améboidních organismů obklopených schránkou o velikosti 10 až 400 µm. Schránka má obvykle jeden otvor pro pseudopodia a je formována bílkovino-chitinózní hmotou produkovanou cytoplazmou krytének (Bartoš, 1954). Bílkovinná hmota je základní složkou schránky většiny krytének (Moraczewski 1969, Lamentowicz a Mitchell, 2005), existují ale i schránky tvořené jiným materiálem. Rozlišujeme čtyři hlavní typy schránek: bílkovinné, vápnité, křemité (druhy, které vylučují jejich pravidelné křemičité části schránky, tzv. idiosomy) a aglutinované (druhy, jejichž schránky obsahují cizí částečky nerostů, tzv. xenosomy) (Wanner, 1999). Velikost schránky poskytuje důležitá limnologická data; schránky krytének po nepohlavním dělení již nerostou (Penard, 1902), vyhodnocení střední velikosti schránek v populaci tak může poskytnout užitečné informace o životním prostředí (Dallimore et al., 2000). U krytének rozlišujeme vnější ektoplazmu a vnitřní endoplazmu. Pseudopodia jsou tvořena většinou ektoplazmou, vnitřní část může být tvořena endoplazmou (Medioli a Scott, 1988).

Kryténky se rozmnožují nepohlavně binárním dělením, pohlavní rozmnožování je relativně řídké (Medioli a Scott, 1988). Během reprodukce je velikost dceřiné schránky určována objemem cytoplazmy a množstvím dostupné potravy v období před reprodukcí. Velikost schránky také ovlivňuje řada abiotických faktorů, např. teplota vody (Medioli a Scott, 1988). Většina krytének se živí bakteriemi, řasami a houbami, některé druhy jsou predátoři (Gilbert, 2003; Yeates, 1995; Ogden, 1990). U některých druhů (např. *Hyalosphenia papilio*) jsou v těle přítomny symbiotické bakterie a tyto kryténky se vyživují mixotrofně. Při nepříznivých podmínkách kryténky vytvářejí cysty, pomocí nichž se také pasivním transportem kosmopolitně šíří.

2.2. Význam krytének pro aktuoekologii

Mezi hlavní důvody zvýšeného zájmu o kryténky patří jejich kosmopolitní rozšíření, vysoká abundance a vynikající zachování především v sedimentu pozdních čtvrtohor a holocénu (Patterson et al. 1985) a to nejčastěji v sedimentech jezer, rašelinišť a řek (Medioli a Scott, 1988,

Warner, 1990, Warner a Charman, 1994). Nejstarší nálezy popisují Porter a Knoll (2000) z proterozoika v Grand Canyon v Arizoně, USA. V České republice jsou doloženy nejstarší nálezy z karbonu (namur) Vašíčkem a Růžičkou (1957), dále z cenomanu české křídové pánve (Bubík, 1997). Přehled o fosilních nálezech ve světě shrnuje Medioli et al. (1990). Nejčastěji se uchovávají schránky či křemité destičky. Vzhledem k jednoduché morfologii jsou fosilní skupiny velmi podobné svým moderním příbuzným (Patterson, 2002). Studie fosilních společenstev krytének naznačují, že jsou citlivé na epizodně antropogenní narušení zahrnující změny v trofickém statusu jezer spojené s rozšířením hnojiv (Sageman, 1997).

Kryténky osidlují širokou paletu sladkovodních prostředí (jezera, rybníky, potoky, řeky) a také podmáčená prostředí (rašeliniště, slatiniště, vlhkou půdu, kůru stromů); pouze malé množství druhů se vyskytuje v brakických podmínkách. Kryténky jsou kosmopolitně rozšířeny od tropických až po polární oblasti (Ogden a Headley, 1980). Jako vhodná pro studie zabývající se paleoekologií ponejvíce kvartéru se ukázala aplikace současných ekologických poznatků z oblasti taxonomie a ekologie krytének, jež byla korelována s mnoha environmentálními parametry jako je např. eutrofizace (Schönborn, 1990), změny teploty vody (Collins et al., 1990), salinita (Roe, 2006) a pH (Escobar, 2008). Společenstva krytének bývají silně ovlivněna obsahem fosforu, jehož zvýšené hladiny odráží eutrofický status jezer, dále také charakterem substrátu, celkovým obsahem organických látek a kontaminací prostředí těžkými kovy (Roe, 2010).

Kryténky se běžně používají jako modelové organismy v populační ekologii, ekotoxikologii a paleoekologii, zejména díky relativně snadnému sběru a identifikaci (Booth, 2002; Mitchell et al, 1999; Payne a Mitchell, 2007). Mohou sloužit jako spolehlivý ukazatel prostředí s nízkým pH, ve kterém mají schránky ostatních modelových skupin (měkkýši, lasturnatky) tendenci se rozpouštět (Escobar, 2008). Řada studií používá kryténky jako bioindikátory změny hladiny moře (Scott a Medioli, 1980, Charman et al., 1998; Scott et al., 2001), paleohydrologie a paleoklimatu (Tolonen, 1986; Warner a Charman, 1994), či limnologických ukazatelů jako teplota, pH, koncentrace kyslíku nebo množství těžkých kovů (Reinhard et al., 1998; Patterson a Kumar, 2002; Escobar, 2008).

3. ČÁST I: ANALÝZA KRYTÉNEK NOVÝMI MIKROSKOPICKÝMI TECHNIKAMI

3.1. Mikroskopické metody studia krytének

Důležitým předpokladem pro úspěšné použití krytének v ekologickém a paleoekologickém výzkumu je jejich správné taxonomické zařazení, které je i v dnešní době založeno především na struktuře schránky a cytoplazmy (Ogden a Headley, 1980). Pro mnoho taxonů však struktura cytoplasmy, počet jader či typy pseudopodií ještě nebyly pozorovány (Meisterfeld, 2002a, 2002b). Na druhou stranu, současné studie kombinující morfologická a molekulární data odhalily neočekávanou diverzitu mezi kryténkami; jemné morfologické rozdíly, které nejsou většinou viditelné pod světelným mikroskopem, se ukázaly být taxonomicky významné (Todorov, 2009; Heger, 2010). Dosud však bohužel chybí relativně přístupná metodika, jež by na tyto skutečnosti reagovala a umožnila badatelům získat co nejpřesnější taxonomická data, která by mohla být použita pro další ekologické aplikace.

3.1.2. Skenovací elektronová mikroskopie

Pravděpodobně nejefektivnější zobrazovací technikou používanou při studiu krytének je skenovací elektronová mikroskopie (SEM). Tato technika je ideální pro vizualizaci povrchu schránek krytének a jejich taxonomicky významných morfologických detailů. Schránky je před použitím této techniky nejdříve nutno pokovit; v poslední době se také u některých novějších SEM mikroskopů používá environmentální mód (např. Olympus ESEM), jenž umožňuje studium nezkolabovaných schránek bez pokovení a tím dovoluje zobrazit více jemnějších detailů. Hlavní nevýhodou SEM je její relativně vysoká finanční náročnost a také delší doba přípravy vzorků.

3.1.3. Optická mikroskopie

Ke studiu struktury schránek krytének jsou v praxi nejspíš nejčastěji používány různé optické kontrastní metody. Nezastupitelnou úlohu zde mají fázový a diferenciální interferenční kontrast (DIC) (Murphy, 2001), lze také využít výhod digitální holografické mikroskopie, moderní adaptace interferenční mikroskopie (Charriere et al., 2006), zejména pokud potřebujeme měřit biomasu uvnitř schránky nebo vytvářet 3D rekonstrukce. Nevýhodou digitální holografické mikroskopie je nízké rozlišení a relativní časová a finanční náročnost, zejména v porovnání s fázovým kontrastem či DIC.

3.1.4. Konfokální mikroskopie

Nové cenné poznatky o vnitřní struktuře krytének přinesly až pokročilé optické mikroskopické metody – konfokální a dvoufotonová fluorescenční mikroskopie. Jejich hlavní výhodou je možnost studovat vnitřní uspořádání živých jedinců v přirozeném prostředí a stanovit objem jejich biomasy. Konfokální mikroskopie (Confocal Laser Scanning Microscopy - CLSM) se snaží odstranit jeden z nedostatků klasické optické mikroskopie, konkrétně nízký kontrast způsobený pronikáním světla z částí vzorku mimo zaostřenou rovinu pozorování do výsledného obrazu. V běžné optické mikroskopii je totiž osvětleno celé zorné pole vzorku a rozptýlené světlo nebo vyzářená fluorescence z rovin mimo zaostřenou rovinu (tzv. nežádoucí signál) přispívá do výsledného obrazu téměř stejnou měrou, jako užitečný signál, tedy světlo pocházející ze zaostřené roviny. Problém nežádoucího signálu lze vyřešit dvěma způsoby: eliminací zdroje nežádoucího signálu - světlo přichází jen ze zaostřené roviny (Total Internal Reflection Fluorescence Microscopy, Two Photon Excitation Microscopy, případně použití velmi tenkých vzorků) nebo tzv. konfokálním snímáním.

V konfokálním mikroskopu je vzorek osvětlen bodovým zdrojem světla a signál ze vzorku je snímán bodovým detektorem, najednou je tedy možné zobrazit jeden bod ze zaostřené roviny vzorku. Celý obraz se získá posouváním tohoto bodu pomocí zrcátek (skenováním) podobně, jako je v obrazovkách analogových televizí magneticky vychylován elektronový paprsek. Velikost tohoto bodu pak určuje rozlišení mikroskopu. Mikroskop je "konfokální" v tom smyslu, že bodový zdroj světla i bodový detektor jsou zobrazeny objektivem do jednoho a téhož bodu ve vzorku. Z principu je také zřejmé, že světlo z nezaostřených rovin (pod nebo nad rovinou zaostření) je blokováno konfokální clonkou a neprojde na detektor. Tím je zajištěno podstatné zlepšení rozlišení v ose vzorku oproti běžné optické mikroskopii, a to až na hodnoty pod 1 μm, rozlišení v rovině vzorku pod 0,5 μm, v závislosti na použitém objektivu a vlnových délkách světla.

Jako zdroj světla se nejčastěji používá sada laserů pro excitaci běžných fluorescenčních barev a jako detektor pak fotonásobič nebo lavinová fotodioda doplněné vhodnými filtry nebo difrakční mřížkou (popř. hranolem) pro pružnou volbu spektrálního rozsahu detekce. Celý mikroskop je řízen počítačem, který také vytváří výsledný obraz vzorku.

3.1.5. Dvoufotonová mikroskopie

Každý laserový skenovací konfokální mikroskop lze též použít pro dvoufotonovou mikroskopii (Two Photon Excitation Microscopy - TPEM); nutnou modifikací je jen připojení speciálního pulzního laseru. Ve dvoufotonovém mikroskopu není třeba využít konfokálního principu (lze vynechat konfokální clonku detektoru), protože fluorescence pochází jen ze zaostřené roviny. Při dvoufotonové excitaci absorbuje molekula barviva energii dvou fotonů. Vlnová délka excitačního světla je tedy přibližně dvojnásobná oproti normální excitační vlnové délce daného barviva a spadá tedy většinou do blízké infračervené oblasti. Tato dvoufotonová excitace je také velmi málo pravděpodobná, je tedy potřeba řádově vyšších intenzit osvětlení vzorku, které jsou dosažitelné jen při použití velmi krátkých pulzů (kolem 100 fs = 10^{-13} s). A nakonec, rozdíl od normální excitace je dvoufotonová excitace nelineární - její intenzita závisí na druhé mocnině intenzity dopadajícího světla, tedy fluorescence vychází hlavně z míst, kde je dopadající světlo neintenzivnější, tj. z ohniska. Fluorescence z míst nad a pod ohniskem je potlačena. Rozlišení dvoufotonového mikroskopu je o něco horší, než u konfokálního mikroskopu, důvodem je hlavně dlouhá vlnová délka excitačního světla. Ta má však tu výhodu, že lépe proniká biologickými vzorky, je tedy možné zkoumat tlusté a méně průsvitné vzorky.

3.2. Zpracování obrazových dat

Dalším krokem je zpracování dat získaných těmito metodami, nabízejí se stereologické metody a 3D rekonstrukce. Posunem vzorku ve směru optické osy je totiž možné snadno získat jednotlivé optické řezy vzorkem, které jsou přesně slícované a bez deformací.

3D rekonstrukce je pokročilá počítačová grafická metoda, která umožňuje z řady optických řezů vytvořit prostorový model zkoumaného objektu a nahlížet pak na něj z libovolného úhlu. Stereologické metody na druhou stranu umožňují pomocí poměrně jednoduchých výpočtů určit důležité vlastnosti vzorku a jeho částí, jako jsou rozměry, velikosti ploch a objem. Právě pro ekologické studie je jedním z důležitých parametrů množství biomasy uvnitř schránky krytének, které se dá poměrně přesně určit pomocí stereologického zpracování snímků z konfokálního nebo dvoufotonového mikroskopu.

V rámci své disertační práce jsem se zabývala analýzou krytének pokročilými mikroskopickými technikami a možnostmi jejich využití v ekologických výzkumech. Výsledkem

bylo zobrazení vnitřních struktur krytének, optimalizace postupu rozlišení živých a mrtvých jedinců ve vzorku a navržení postupu měření biomasy krytének uvnitř schránky. Výsledky této práce jsem opublikovala v jednom vědeckém článku.

3.3. ***Článek 1: Testate Amoebae Examined by Confocal and Two-Photon Microscopy: Implications for Taxonomy and Ecophysiology (publikováno v časopise Microscopy and Microanalysis 16(6):735-746, 2010)***

Testate amoebae examined by confocal and two-photon microscopy: Implications for taxonomy and ecophysiology

Running head: Confocal Microscopy Study of Testate Amoebae

Zuzana Burdíková[1,2], Martin Čapek[1,3], Pavel Ostašov[1], Jiří Machač[4], Radek Pelc[1], Edward A.D. Mitchell[5], Lucie Kubínová[1]

1. Institute of Physiology, Academy of Sciences of the Czech Republic, v.v.i., Vídeňská 1083, CZ-14220 Prague 4, Czech Republic

2. Institute of Geology and Paleontology, Faculty of Science, Charles University, Albertov 6, CZ-12843 Prague 2, Czech Republic

3. Faculty for Biomedical Engineering, Czech Technical University in Prague, nám. Sítná 3105, CZ-27201 Kladno, Czech Republic

4. Institute of Botany, Academy of Sciences of the Czech Republic, v.v.i., Zamek 1, Lesní CZ-322, 25243 Průhonice, Czech Republic

5. Laboratory of Soil Biology, University of Neuchâtel, Rue Emile-Argand 11, CH-2009 Neuchâtel, Switzerland

Corresponding author: Zuzana Burdíková, tel.: +420 296443769, fax: +420 296442488, e-mail: burdikova@biomed.cas.cz.

Keywords: testate amoebae, confocal microscopy, environmental scanning electron microscopy, taxonomy, ecophysiology

Abstract:

Testate amoebae (TA) are a group of free-living protozoa, important in ecology and paleoecology. Testate amoebae taxonomy is mainly based on the morphological features of the shell, as examined by means of light microscopy (LM) or (environmental) scanning electron microscopy (SEM). We explored the potential applications of confocal laser scanning microscopy (CLSM), two photon excitation microscopy (TPEM), phase contrast, differential interference contrast (DIC Nomarski) and polarization microscopy to visualize TA shells and inner structures of living cells, which is not possible by SEM or ESEM. Images captured by CLSM and TPEM were utilized to create 3D visualizations and to evaluate biovolume inside the shell by stereological methods, to assess the function of TA in ecosystems. To the best of author's knowledge the present report is the first to employ fluorescent probes, CLSM, TPEM, 3D reconstructions and stereological methods to visualize TA. This approach significantly broadens the understanding of TA cell and shell morphology, and inner structures including organelles and symbionts, with potential implications for taxonomy and ecophysiology.

ABBREVIATIONS:

CLSM – confocal laser scanning microscopy

DIC – differential interference contrast

ESEM – environmental scanning electron microscopy

LM – light microscopy

SEM – scanning electron microscopy

TA – testate amoeba(e)

TPEM – two- photon excitation microscopy

INTRODUCTION

Testate amoebae (TA) belong a polyphyletic group of unicellular eucaryotes (ca. 10-400 µm) protected by a shell (test). The shell enclosing the cell plasma usually has a single aperture for the pseudopodia, rarely two apertures. A proteinaceous organic matrix is the basic shell component (Meisterfeld, 2002a, 2000b). There are four main shell types: proteinaceous, calcareous, siliceous (species secreting their own regular siliceous shell plates, so-called idiosomes), agglutinated (species incorporating extraneous mineral particles, so-called xenosomes, into their shells structure) (Wanner, 1999). Despite the presence of an opaque shell, some testate amoeba species have photosynthetic symbionts and are thus mixotrophic (Meisterfeld, 2002a, 2000b).

Testate amoebae are commonly used as model organisms in population ecology, ecotoxicology, ecology, paleoecology and evolutionary biology. They are useful bioindicators of natural ecological gradients, environmental stress or pollution in both aquatic and terrestrial ecosystems (Booth, 2002; Mitchell et al., 2008; Foissner, 1997, 1999; Patterson et al. 1996, 2002). In most aquatic and terrestrial ecosystems TA also play an important role in the cycling of nutrients, especially C, N, and Si. (Aoki et al., 2007; Wilkinson, 2008; Schröter et al., 2003; Schönborn, 1983, 1992; Vohník et al., 2009).

A prerequisite for the use of TA in ecological and paleoecological studies is a sound taxonomy. TA taxonomy is mainly based on the shell structure (Ogden & Hedley, 1980). Indeed, in a number of taxa the cytoplasm, the nuclei and types of pseudopodia have not been observed yet (Meisterfeld, 2002a, 2000b). Recent studies combining morphological and molecular data have revealed an unexpected diversity among the testate amoebae, thus illustrating their role as a model group to study evolutionary processes such as marine-terrestrial transitions. Subtle morphological differences that are typically invisible under light microscopy were shown be of taxonomical significance (Todorov et al., 2009; Heger et al., 2010).

Ecological studies aiming to establish the contribution of TA to biomass or nutrient cycling require a reliable estimate of cell volume (e.g. Gilbert et al., 1998; Schröder et al., 2003;

Mitchell et al., 2003). The volume of biomass inside the shells can be calculated by applying an appropriate conversion factor (Madrid & Felice, 2005) or calculated assuming that the TA shells can be approximated by simple geometrical shapes (Gilbert et al., 1998). The accuracy of these approaches is limited (Charière et al., 2006).

There has been a growing demand to revise the taxonomy of testate amoebae and to develop new optical methods for their reliable identification (Mitchell & Gilbert, 2010). Apart from scanning electron microscopy (SEM) as the most common technique, the ideal imaging setup should distinguish the relevant morphological features without requiring an excessively complex preparation and handling. To some extent, the optical contrasting modalities such as phase contrast, DIC (Murphy, 2001) or digital holographic microscopy, a modern adaptation of interference microscopy (Charriere et al., 2006) can be utilized, as demonstrated in TA (Beyens and Meisterfeld, 2001, Charriere et al., 2006). If biovolume estimations and/or 3D reconstructions are required confocal or two-photon microscopy represents a convenient solution.

The aim of the present study is to explore the potential of CLSM and TPEM together with 3D reconstructions and stereological measurements for the study of testate amoebae morphology. Phase contrast, differential interference contrast (DIC Nomarski, polarization microscopy) and (E)SEM were employed as well. The data have implications for taxonomy and ecophysiology. To the best of the authors' knowledge, the present study is the first of its kind, as applied to testate amoebae.

MATERIALS AND METHODS

Specimens

Samples of TA were collected from four pools of Komořany ponds near Vltava River, 1-2 m from the river, in Prague, Czech Republic. TA from Komořany pools were studied without fixation and stored in their natural environment (water) for not more than four hours before image acquisition. Samples from the Alps and Jura Mountains (Switzerland) and from *Sphagnum* moss

areas of the Šumava Mountains (Czech Republic) were studied both before and after a paraformaldehyde fixation. A list of all examined species is shown in Table 1.

The fixation was a performed by gentle centrifugation followed by replacing the resulting supernatant by 4% paraformaldehyde (45 min at room temperature). After fixation the specimen was centrifuged again and supernatant replaced by filtered water (20 µm mesh) obtained from the place of sampling.

TA were labeled by 15 fluorescent markers: DAPI (D1306), Er-Tracker Blue- White DPX (E12353), Hoechst (H21486), LysoTracker Red DND (L7528), MitoTracker (M22426), AlexaFluor 633 phalloidin (A22284), SYTO 16 (S 7578), Texas Red C_2-imde, TMRE (T-699) (Invitrogen, Eugene, OR, USA), and acid fuchsine (84600), aniline blue (ANILO1600), BCECF-AM (B8806), $DiOC_3(3)$, FITC 46952 and propidium iodide (70335) (Sigma-Aldrich, USA). Details about the fluorescent probes are listed in Table 2. We were also checking the autofluorescence of TA and chlorophyll-a inside TA (mixotrophic species).

For DAPI, Hoechst, propidium iodide and AlexaFluor 633 phalloidin staining, the TA were fixed and treated with 0.1% Triton X-100 (5 min at room temperature) to permeabilize the plasma membrane. The samples were then centrifuged, Triton X-100 aspired and the samples suspended in water. The TA samples were stained as specified in Table 2, centrifuged in Eppendorf tubes (12,100 rpm for 45 s, RCF ca 9,000 g), supernatant removed and replaced with filtered water (20 µm mesh) from the place of sampling. The centrifugation was performed three times, in order to remove any excessive probe. Afterwards, the TA suspension in water was mounted between a microscope slide and a cover slip sealed together with nail varnish.

Optical contrasting modalities

All images shown in Fig. 1 were acquired with Olympus DP70 digital camera fitted to Olympus BX60 upright microscope equipped with U-UCD8 universal condenser (NA 0.90 in a dry "TLD" mode).

Conventional phase-contrast with no special modifications was employed. Polarization microscopy was performed in a simple way, with the specimen placed between crossed or nearly crossed polarizers; no other optical elements were present. Differential interference contrast (DIC Nomarski) images were optimized by adjusting the position of the Wollaston prism in a DIC slider (U-DICT type), thus setting an optimal bias retardation, depending on the optical thickness of the object (testate amoeba). Two objective lenses were used: UPlanFl 40x/0.75 Ph2 (Fig. 1b) and UPlanFl 20x/0.50 (all other images).

Except for Figs. 1f and 1h, all images shown in Fig. 1 are processed ones obtained from raw images acquired at a series of focal planes, by employing a DeepFocus module of QuickPHOTO Micro software.

Scanning and environmental scanning microscopy (SEM and ESEM)

A scanning electron microscope FEI Quanta 200 was used as described in (Michels, 2005), either in SEM or ESEM mode.

For the SEM (high-vacuum) mode, the fixed shells were critical point dried or partially dried, mounted on metal stubs with a double-sided adhesive conductive tape (carbon tape) and coated with gold (4 min at 20mA in a vacuum of about 10 Pa, with argon present) using a model sputter coater. The stubs were then affixed by the carbon tape to a microscope stage. The gold-coated TA shells were observed at 20-30 kV in a high vacuum mode, using an Everhart-Thornley secondary electron detector (ETD).

For the environmental SEM (ESEM) mode, the fixed shells were washed in distilled water to remove the fixatives, partially dried and placed on a Peltier-cooled stage (JT Manufacturing, USA). To prevent the stub from drifting, it was previously covered with the same double-sided adhesive conductive tape (carbon tape) as used in SEM. The TA shells were observed at 20-30 kV, 200 to 400 Pa, and sample temperature of -14°C to -4°C. Alternatively, the pressure was raised up to 1 kPa with no cooling applied. A gaseous secondary electron detector (GSED) was used.

Confocal laser scanning microscopy (CLSM)

Two confocal laser scanning microscope systems were used: [1] Leica TCS SPE based on Leica DM 2500 CSQ V-VIS fluorescent microscope and equipped with four solid state lasers, 405 nm (25 mW), 488 nm (15 mW), 532 nm (15 mW), 635 nm (15 mW)); [2] Leica TCS SP2 AOBS based on Leica DM IRE2 inverted microscope and equipped with continuous lasers 458nm(5mW), 476nm(5mW), 488(20mW), 514nm(20mW); HeNe: 543nm(1.2mW), 633nm(10mW).

The laser power was adjusted to obtain the best images. The laser power amplitude offset and detector gain were manually adjusted prior to image stack collection, so the best combination of black background and avoidance of black pixels and over-saturation in the structures of interest was achieved. The image stacks were obtained by collecting optical sections throughout the entire thickness of the specimen. The images were acquired using scan rates and frame averaging settings to yield the best signal-to-noise ratio within a reasonable collection time. In most cases we used a 20x water immersion planapochromat objective HC PL APO CS (NA = 0.7) and apochromat objective HCX APO CS 63x W CORR / 1.2 – 0.22 wd (NA=1,2).

Due to attenuation of the light arising from deeper parts of the sample, the images in the acquired stack were enhanced by two methods: [1] online method – an intensity compensation feature of Leica Confocal Software (version 2.61, Leica Microsystems GmbH, Heidelberg) in a 'linear-by-gain' mode), adjusting the PMT gain according to the z-coordinate of current image and maintaining the best signal-to-noise ratio throughout the sample; [2] offline method – a custom plug-in for the *Ellipse* modular software package (ViDiTo, Slovakia; www.vidito.com), adjusting the brightness and contrast in an image series so that the effect of light attenuation is minimized (Čapek et al., 2006).

Two-photon excitation microscopy (TPEM)

An above-mentioned confocal microscope (Leica TCS SP2 AOBS) was used in concert with a Ti:Sapphire Chameleon Ultra family femtosecond laser Mira 900 (Coherent, Santa Clara, CA) tunable from 690 to 1040 nm. A two-photon fluorescence signal was collected by an internal

detector placed in the scanning head of the confocal microscope (descanned, backscattering geometry). The detected wavelength by applying lambda scans in order to maximize the fluorescence signal of the sample. The average laser power on the sample was in the order of miliwatts.

3D visualization

CLSM and TPEM provided a series of perfectly aligned optical sections of TA cells. To visualize them as 3D objects, we used the *Ellipse* software package (ViDiTo Systems, Košice, Slovakia) adapted to work with a specialized VolumePro 1000 board (www.terarecon.com), performing volume rendering of digital scalar data in real time (Čapek et al., 2009).

Stereological measurement

The biovolume inside TA shells was determined by the stereological "fakir" method from images acquired by CLSM or TPEM (Cruz-Orive, 1997; Kubínová & Janáček, 2001; Kubínová et al., 2002). The fakir probe (Cruz-Orive, 1997) is a systematic probe consisting of parallel test lines (resembling nails of a fakir's bed and piercing its surface). We applied a highly-efficient spatial grid consisting of three mutually perpendicular halfway shifted fakir probes (Kubínová & Janáček, 1998, 2001, Difato et al., 2004). The TA biovolume (*V*) was estimated by the following formula:

$$estV = \frac{1}{3} \cdot u^2 \cdot (L_1 + L_2 + L_3)$$

where L_i (i=1,2,3) is the total length of object-to-probe intercepts (i-th fakir probe), the object being the biomass boundary, u is the grid constant, i.e. the smallest distance between neighboring parallel lines of the fakir probe. The position of the spatial grid was uniform random (Weibel, 1979).

RESULTS

Basic morphology (optical contrasting modalities)

The testate amoebae architecture was visualized by employing complementary optical contrasting modalities such as phase-contrast (Fig. 1b), polarization (Fig. 1c, 1e, 1g) and DIC

Nomarski (Fig. 1d, 1f, 1h) microscopy. The origin of the optically active objects highlighted in Fig. 1c is unclear and requires further elucidation. Test scales and/or sand grains adsorbed on the test surface are also highlighted by polarization microscopy (Fig. 1e, 1g). The cyst architecture is best visualized by DIC Nomarski imaging (Fig. 1d) while its outline is best rendered by phase-contrast (Fig. 1b). A bright-field image (no optical contrasting, low contrast) is shown for comparison (Fig. 1a).

Observation of testate amoebae surface structures by SEM and ESEM

SEM and ESEM visualize the surface of TA shells at high resolution (Fig. 2c). It is possible to observe the shell coated with sand grains, its structure and typical morphological characteristics (Fig. 2d, 2e).

As ESEM does not require the samples to be metal-coated, frequent artefacts caused by the coating procedure are eliminated. The only requirement is to avoid mechanical or chemical impurities, such as various particles or surface films. ESEM microscopy often yields better-quality images of the shell, plus details just under the shell surface (Fig. 2e), in comparison to SEM. However, SEM or ESEM cannot be applied to visualize living TA.

Fluorescence (data summarized in Table 3)

Labeling of the TA shell with acid fuchsine let us observe secreted scales, or organic or mineral xenosomes used as building blocks of the shell (Fig. 2a, 2d and 2g, 3m). In some cases, the SEM and CLSM images nicely complement each other (Fig. 2). Acid fuchsine also reveals the internal structure of the cell (Fig. 2a, 2b, 2f), and such data can be combined with autofluorescence observations of chlorophyll-a present in endosymbionts (Fig. 3a, 3b).

Fluorescein BCECF-AM labels the cytoplasm in living TA individuals only (Fig. 3c, 3e), a protoplast, most likely of another organism, inside an otherwise empty shell (Fig. 4e) or even cell nuclei during mitosis (Fig. 4f). In living TA, BCECF-AM also stains the shell and its architecture

can be observed in great detail (Fig. 3e, 4c). However, the image is not as sharp as in the case of acid fuchsine. BCECF-AM can also be used to determine cytosolic pH (Fig. 4h).

Propidium iodide stains nucleic acids in dead individuals (Fig. 3h). $DiOC_3(3)$ stains membranes, including those of organelles within the cell. Mitochondria can be specifically labeled by MitoTracker (Fig. 3k) and TMRE (Fig. 3l). Aniline blue visualizes some components of TA shells and appears to be complementary to acid fuchsine (Fig. 3m). Celltracker CMFDA also labels living TA (Fig. 3n). Er-Tracker stains the endoplasmic reticulum of TA (Fig. 3g, 3o). FITC binds to proteins within the cell (Fig. 3p, 5a, 5b). The vacuoles of *Hyalosphenia papilio* labeled by FITC (Fig. 3f) were visualized using a single laser line wavelength (514nm).

Staining by DAPI, LysoTracker, AlexaFluor 633 phalloidin, SYTO 16, Texas Red was unsuccessful (data not shown).

Autofluorescence

Autofluorescence was recorded in *Hyalosphenia papilio* (Fig. 3p), a mixotrophic species (i.e., TA containing endosymbiotic algae). Autofluorescence of chlorophyll-a was recorded at excitation wavelength of 633 nm and emission wavelength range of 650-710 nm (Fig. 3j). This phenomenon could be useful in studies of symbionts inside mixotrophic TA species. No autofluorescence was found in heterotrophic species.

Identification of living and dead TA individuals in sample

A combination of BCECF-AM and propidium iodide fluorescent probes, commonly used to assess cell vitality (King, 2000), can be successfully applied to separate dead and living TA (Fig. 3c, 3e, 3f, 3h, Table 1). While propidium iodide stained nucleic acids in dead cells with a permeabilized membrane, fluorescence of BCECF-AM could only be observed in living cells owing to enzymatic processes that activate the fluorescent probe.

Rose Bengal (rB) is also commonly used to identify dead and living TA individuals (Patterson, 2002). However, no living specimens were detected by rB in our samples from the same locality and time. This may be attributed to generic problems with rB staining as described by Bernhard (2000). Thus, we recommend the BCECF-AM + propidium iodide method over rB staining alone to identify dead/living TA individuals. Separating dead and living TA individuals is important in ecological studies (e.g., Nguyen-Viet, 2008). Moreover, propidium iodide also allows counting nuclei, which is important in taxonomy (Meisterfeld, 2002a, 2000b).

Examination of testate amoebae by TPEM

In small TA species (10-100 µm) with translucent shells standard CLSM yields satisfactory results (Fig. 4g). Problems occur with larger (thicker) species and those that build opaque shells (typically made of agglutinated organic or mineral particles). Since both emission and excitation light is strongly absorbed by the shell and the amoeba itself, CLSM typically makes it possible to acquire TA images from only depths up to 20 µm (Fig. 5a). In deeper layers the images suffer from low signal-to-noise ratio.

These problems are partly solved by TPEM whose excitation light is in the infrared range (700 - 910 nm) capable of penetrating deeper into most biological objects (Fig. 5b), Up to 70 µm in TA. This is sufficient for the vast majority of TA species and enabling biovolume estimation of the amoeba inside the shell, and 3D reconstructions.

3D visualization

3D visualizations based on CLSM and TPEM images (acquired from one direction only) make it possible to examine the object from any angle (Figs. 6a, 6d). Owing to the 3D data it is possible to precisely localize in the amoeba chlorophyll-a (Fig. 6b, 6c) and the activity of non-specific esterases (Fig. 6e, 6f, 6g, 6h).

Stereological volume measurement

The results of biovolume measurement in four specimens of TA are summarized in Table 4. By using the fakir method we were able to evaluate biovolumes with sufficient accuracy while keeping the image acquisition time reasonably short (tens of minutes per one image stack).

DISCUSSION

Future progress in testate amoebae taxonomy and ecology requires a detailed morphological characterization of their shells and cells, as this helps to select the criteria for distinguishing closely related, morphologically similar species. A detailed examination of cell content, e.g., quantification of organelles and (in mixotrophic species) endosymbionts, or biovolume estimation yields information about the physiological state of the amoeba, with implications in ecophysiology and ecotoxicology. Likewise, it is important to reliably recognize living and dead individuals.

The relatively simple optical contrasting modalities such as phase-contrast, DIC-Nomarski or Hoffman modulation contrast reveal the variations of a refractive index within the specimen and are akin to the digital holographic microscopy mentioned towards the end of Discussion. They are particularly suitable for examining non-absorbing objects such as unstained living cells (Murphy, 2001). The structure of the TA shell can often be visualized by a simple polarization microscopy at a negligible cost, owing to the shell's its (bio)mineralized nature (Fig. 1e, 1g). In this context, such modes are complementary with CLSM better capable of visualizing cell components stained with specific fluorescent probes. For example, BCECF-AM binds to the organic part of the TA shell only (e.g., Fig. 4c).

SEM and ESEM are frequently used for taxonomical descriptions of testate amoebae, and less often in ecological studies. They make it possible to examine the surface features of TA at high resolution and a very reasonable depth of field, and to perform quantitative elemental

analyses of shell structures (Ogden & Hedley, 1980; Todorov et al., 2009). However, SEM and ESEM cannot be used to examine living TA or the inner architecture of the amoeba or the shell. Conventional SEM can only operate in a high-vacuum mode, which dictates the rather complex specimen preparation protocol, itself a source of a number of artifacts. ESEM and some of its alternatives, such as variable pressure SEM (VP-SEM), allow the examination of specimens under a wide range of gaseous conditions. These conditions permit an investigation of the biological samples, usually only non-living ones, in a closer-to-natural (uncoated) state, and are applicable to practically any TA shell type. The drawback is a lower image contrast of the uncoated sample.

The fluorescent probes required in CLSM can penetrate into the amoeba only through the shell operculum and some of them thus require a longer loading/staining time. The reproducibility of the labeling protocols is often problematic. For example, *Acantamoeba castellanii* was successfully labeled by Rhodamin tagged–phalloidin complex to visualize actin (González-Robles, 2008). However, we failed to stain TA with this probe.

It is more difficult to stain shell-enclosed TA than naked amoebae or animal cells. The same applies to foraminifera that also build their shells with an operculum. Bernhard, et al. (2004) successfully stained foraminifera by calcein which we have not tested in TA. Instead, we experimented with fluorescein BCECF-AM, a similar type of fluorescent probe. In many cases a trial-and-error approach had to be applied to optimize the labeling protocols in terms of photodamage, toxicity and photobleaching, and ten fluorescent probes were successfully used.

Rose Bengal (rB) is the most commonly used probe to distinguish live/dead shell-enclosed TA or foraminifera cells. rB is a biological dye that is supposed to bind to cytosolic proteins, rendering the cytoplasm in a rose color (Walton, 1952). The main advantages of rB are quick staining and a relatively low price. However, necrotic as well as healthy cytoplasm is stained in foraminifera. It has been shown that rB reacts even weeks or months after individual's death. Moreover, even specimens known to contain dead cells do not always become rB-stained (Martin & Steinker, 1973; Lutze & Altenbach, 1991). Generally, rB should not be used as the only dye to detect live/dead cells (Bernhard, 2000). Sudan black (a lipophilic stain) is yet another

probe that is often used to distinguish live/dead foraminifera, and suffers from the same drawback as rB – staining opaque specimens may yield ambiguous results (Bernhard, 2000).

These problems are absent if a combination of BCECF-AM and propidium iodide is used; live/dead TA are clearly distinguished. BCECF-AM probe is non-fluorescent and membrane-permeable in its basic state. Upon cleavage by non-specific esterases it becomes fluorescent but also membrane impermeable, so it gets trapped in living cells but quickly disappears from dead or membrane-damaged cells. Surprisingly, we observed fluorescence not only inside the living cells, but also on the shells of living amoebae (between idiosomes), perhaps due to non-specific esterases that may be part of the organic (proteinaceous) matrix sustaining the shell. This notion is supported by the fact that the fluorescence was detected on the shells of living TA only.

In mammalian tissues, mitochondria are amongst the first organelles that exhibit distinct structural alterations during necrosis (Raffay & Cohen, 1997). If intact mitochondria are observed in TA, one may conclude that the cell is alive at the time of staining. In our samples differences were encountered in spatial distribution of mitochondria between *Euglypha sp.* (a heterotrophic species) labeled by MitoTracker (Fig. 3k) and *Hyalosphenia papilio* (a mixotrophic species) labeled by TMRE (Fig. 3l). It is premature yet to draw any conclusions about the two nutrition strategies but both of these probes are known to accumulate in active mitochondria only.

To allow determination of the biomass inside the shell an optical diffraction tomography technique based on digital holographic microscopy (DHM) can be utilized. This method, essentially an adaptation of an interference-phase microscopy utilizing coherent light, enables a tomographic reconstruction of the microscopic object with a resolution of ca 1.5 µm in all three directions (Charriere et al., 2006). Very small objects such as organelles or endosymbionts are better modeled by CLSM owing to its better lateral/axial resolution of at least 350/1,000 µm (Diaspro, 2002; Matsumoto, 2002; Pawley, 2006) although in larger specimens such as *Hyalosphenia papilio*, the laser light cannot penetrate sufficiently deep into the amoeba, and TPEM (Denk, 1990; Diaspro, 2002) would have to be employed instead. In DHM, this problem is mitigated simply by rotating the sample.

Nguyen-Viet et al. (2008) evaluated TA biovolumes by assuming they are of regular geometrical shapes. Obviously, this methodology enables fast volume measurements at the expense of accuracy.

CONCLUSION

The present study highlights the advantages and limitations of various specialized microscopic imaging modalities, as applied to testate amoebae morphology. The CLSM and TPEM data are the first of its kind obtained in testate amoebae. Jointly with associated 3D reconstructions and stereological analyses, the multimodal imaging is of potential interest e.g. in taxonomy, ecophysiology or ecotoxicology.

ACKNOWLEDGEMENTS

The authors are grateful to Prof. Jaromír Plášek (Charles University in Prague) and Dr Martin Vohník (Institute of Botany, ACSR) for providing some of the fluorescence probes, and to Zdeněk Švindrych (Charles University in Prague) for a fruitful discussion. The presented study was supported by Academy of Sciences of the Czech Republic (grants No. AV0Z50110509, No. AV0Z10100520 and No.AV0Z60050516), Ministry of Education, Youth and Sports of the Czech Republic (research programs LC06063, MSM6840770012, ESO MNT-ERA ME10069 of MEYS CR, 0021620834), Czech Science Foundation (grant No. 102/08/069) and the Swiss National Science Foundation (grants No: 205321-109709/1 and 205321-109709/2).

REFERENCES

AOKI, Y., HOSHINO, M. & MATSUBARA, T. (2007). Silica and testate amoebae in a soil under pine-oak forest. *Geoderma* **142**, 29–35.

BERNHARD, J.M., BLANKS J.K., HONTZ CH.J. & CHANDLER G.T. (2004). Use of the fluorescent calcite marker calcein to label foraminiferal tests. *J Foraminiferal Res* **2**, 96–101.

BERNHARD, J.M. (2000). Distinguishing live from dead foraminifera: Methods review and proper applications. *Micropaleontology* **46**, Suppl. 1, 38–46.

BEYENS, L., MEISTERFELD, R. (2001). Protozoa: testate amoebae. In *Tracking environmental change using lake sediments: Volume 3: Terrestrial, Algal, and siliceous indicators,* J.P. Smol, H.J. Birks & W.M. Last (eds.), pp. 121–153. Dordrecht, Netherlands: Kluwer Academic Publishers.

BOOTH, R.K. (2002). Testate amoebae as paleoindicators of surface-moisture changes on Michigan peatlands: modern ecology and hydrological calibration. *J Paleolimn* **28**, 329–348.

CRUZ-ORIVE, L.M. (1997). Stereology of single objects. *J Microsc (Oxford, U. K.)* **186**, 93–107.

ČAPEK, M., BRŮŽA, P., JANÁČEK, J., KAREN, P., KUBÍNOVÁ, L. & VÁGNEROVÁ, R. (2009). Volume reconstruction of large tissue specimens from serial physical sections using confocal microscopy and correction of cutting deformations by elastic registration. *Microsc Res Tech* **72**, 110–119.

ČAPEK, M., JANÁČEK, J. & KUBÍNOVÁ, L. (2006). Methods for compensation of the light attenuation with depth of images captured by a confocal microscope. *Microsc Res Tech* **69**, 624–635.

CHARRIERE, F., PAVILLON, N., COLOMB, T., DEPEUSINGE, CH., HEGER, T.J., MITCHELL, E.A.D, MARQUET, P. & RAPPAZ, B. (2006). Living specimen tomography by digital holographic microscopy: morfometry of testate amoeba. *Opt Express* **14,** 7005–7013.

DENK, W., STRICKLER, J.H. & WEBB, W.W. (1990). Two-photon laser scanning fluorescence microscopy. *Science* **248**, 73–76.

DIASPRO, A. (2002). *Confocal and two-photon microscopy: foundations, applications, and advances.* New York: Wiley – Liss.

DIFATO, F., MAZZONE, F., SCAGLIONE, S., FATO, M., BELTRAME, F., KUBÍNOVÁ, L., JANÁČEK, J., RAMOINO, P., VICIDOMINI, G., DIASPRO, A. (2004). Improvement in volume estimation from confocal sections after image deconvolution. *Microsc Res Tech* **64,** 151–155.

FOISSNER, W. (1997). Protozoa as bioindicators in agroecosystems, with emphasis on farming practices, biocides, and biodiversity. *Agric Ecosyst Environ* **62,** 93–103.

FOISSNER, W. (1999). Soil protozoa as bioindicators: pros and cons, methods, diversity, representative examples. *Agric Ecosyst Environ* **74,** 95–112.

GILBERT, D., AMBLARD, C., BOUDIER, G. & FRANCES, A.J. (1998). The microbial loop at the surface of a peatland: Structure, function and impact of nutrient input. *Microb Ecol* **35**, 83–93.

GONZÁLEZ-ROBLES, A., CASTAÑÓN, G., HERNÁNDEZ-RAMÍREZ, V.I., SALAZAR-VILLATORO, L., GONZÁLEZ-LÁZARO, M., OMAÑA-MOLINA, M., TALAMÁS-ROHANA, P. & MARTÍNEZ-PALOMO A. (2008). Acantoamoeba castellanii: Identification and distribution of actin cytoskeleton. *Exp Parasitol* **119**, 411–417.

HEGER, T.J., MITCHELL, E.A.D., TODOROV, M., GOLEMANSKY, V., LARA, E. & PAWLOWSKI, J. (2010). Molecular phylogeny of euglyphid testate amoebae (Cercozoa: Euglyphida) suggest transitions between marine supralittoral and freshwater/terrestrial environments are infrequent. *Mol Phylogenet Evol* **55,** 113–122.

KING, M.A. (2000). Detection of dead cells and measurement of cell killing by flow cytometry. *J Immunol Methods* **234**, 155–166.

KUBÍNOVÁ, L. & JANÁČEK, J. (1998). Estimating surface area by the isotropic fakir method from thick slices cut in an arbitrary direction. *J Microsc (Oxford, U. K.)* **191**, 201–211.

KUBÍNOVÁ, L. & JANÁČEK, J. (2001). Confocal microscopy and stereology: estimating volume, number, surface area and length by virtual test probes applied to three-dimessional images. *Microsc Res Tech* **53**, 425–435.

KUBÍNOVÁ, L., JANÁČEK, J. & KREKULE, I. (2002). Stereological methods for estimating geometrical parameters of microscopic structure by three dimensional imaging. In *Confocal and two photon microscopy: foundations, applications, and advances,* A. Diaspro (Ed.), pp. 299-332. New York: Wiley-Liss.

LUTZE, G.F. & ALTENBACH, A. (1991). Technik und Signifikanz der lebendfarbung foraminiferen mit bengalrose. *Geol Jahr* **A128**, 251–265.

MADRID, R.E. & FELICE, C. J. (2005). Microbial biomass estimation. *Crit Rev Biotechnol* **25**, 97–112.

MARTIN, R.E. & STEINKER, D.C. (1973). Evaluation of techniques for recognition of living foraminifera. *Compass Sigma Gamma Epsilon* **50**, 26–30.

MATSUMOTO, B. (2002). *Cell biological applications of confocal microscopy*, San Diego: Academic Press.

MEISTERFELD, R. (2002). Order Arcellinida Kent, 1880. In *An Illustrated Guide to the Protozoa, 2nd ed.,* Lee, J.J., Leedale, G.F. & Bradbury, P. (Eds.), vol. 2, pp. 827–860. Lawrence, Kansas: Society of Protozoologists.

MEISTERFELD, R. (2002). Testate Amoebae with Filopodia. In *An Illustrated Guide to the Protozoa, Second Edition,* Lee, J.J., Leedale, G.F. & Bradbury, P. (Eds.), vol. 2. pp. 1054–1084. Lawrence, Kansas: Society of Protozoologists.

MICHELS, J. & SCHNACK-SCHIEL, S.B. (2005). Feeding in dominant Antartic copepods - does the morphology of the mandibular gnathobases relate to diet? *Mar Biol (Heidelberg, Ger.)* **146**, 483–495.

MITCHELL, E.A.D., GILBERT, D., BUTTLER, A., AMBLARD, C., GROSVERNIER, P. & GOBAT, J.M. (2003). Structure of microbial communities in *Sphagnum* peatlands and effect of atmospheric carbon dioxide enrichment. *Microb Ecol* **46,** 187–199.

MITCHELL, E.A.D., PAYNE, R. & LAMENTOWICZ, M. (2008). Potential implications of differential preservation of testate amoebae shells for paleoenvironmental reconstruction in peatlands. *J Paleolimn* **40,** 603–618.

MITCHELL, E.A.D. & GILBERT, D. (2010). Present status of testate amoeba research, knowledge gaps and research priorities. Meeting Report: 5th International Symposium on Testate Amoebae (ISTA-5), Montbéliard, France 14-17 September 2009. *Protist* **161,** 337-341.

MITCHELL, E.A.D., CHARMAN, D.J. & WARNER, B.G. (2008). Testate amoebae analysis in ecological

and paleoecological studies of wetlands: past, present and future. *Biodiver Conserv* **17,** 2115–2137.

MURPHY, D.B. (2001). *Fundamentals of Light Microscopy and Electronic Imaging.* New-York: Wiley-Liss.

NGUYEN-VIET, H., BERNARD N., MITCHELL E.A.D., BADOT, P.M. & GILBERT, D. (2008). Effect of lead pollution on testate amoebae communities living in *Sphagnum fallax*: An experimental study. *Ecotoxicol Environ Safe* **69**, 130–138.

OGDEN, C.G. & HEDLEY, R.H. (1980). *An atlas of freshwater testate amoebae*. New-York: Oxford University Press.

PATTERSON, R.T., BARKER, T. & BURBIDGE, S.M. (1996). Arcellaceans (thecamoebians) as proxies of arsenic and mercury contamination in northeastern Ontario lakes. *J Foraminiferal Res* **26,** 172–183.

PATTERSON, R.T., DALBY, A., KUMAR, A., HENDERSON, L.A. & BOUDREAU, R.E.A. (2002). Arcellaceans (thecamoebians) as indicators of land-use change: Settlement history of the Swan Lake area, Ontario as a case study. *J Paleolimn* **28,** 297–316.

PAWLEY, J.B. (2006). Handbook of biological confocal microscopy. New York: Springer.

RAFFAY, M. & COHEN, G.M. (1997). Apoptosis and necrosis in toxicology: a continuum or district modes of cell death? *Pharmacol Ther* **75**, 153–177.

SCHÖNBORN, W. (1983). Relationships between production, mortality and abundance in Testacean (Protozoa) communities in soil. *Pedobiologia* **25,** 403–412.

SCHÖNBORN, W. (1992). The role of protozoan communities in freshwater and soil ecosystems. *Acta Protozool* **31,** 11–18.

SCHRÖTER, D., WOLTERS, V. & DE RUITER, P.C. (2003). C and N mineralisation in the decomposer food webs of a European forest transect. *Oikos* **102**, 294–308.

TODOROV, M., GOLEMANSKI, V., MITCHELL, E.A.D. & HEGER, T.J. (2009). Morphology, biometry, and

taxonomy of freshwater and marine interstitial Cyphoderia (Cercozoa: Euglyphida). *J Eukaryotic Microbiol* **56,** 279–289.

VOHNÍK, M., BURDÍKOVÁ, Z., ALBRECHTOVÁ, J. & VOSÁTKA, M. (2009). Testate amoebae (Arcellinida and Euglyphida) vs. ericoid mycorrhizal and DSE fungi: A possible novel interaction in the mycorrhizosphere of Ericaceous plants? *Microb Ecol* **57**, 203–214.

WALTON, W.R. (1952). Techniques for recognition of living foraminifera. *J Foraminiferal Res* **3**, 56–60.

WANNER, M. (1999). A review on the variability of testate amoebae: methodological approaches, environmental influences and taxonomical implications. *Acta Protozool* **38**, 15–29.

WEIBEL, E.,R. (1979). *Stereological Methods, vol. 1: Practical methods for biological morphometry*. London: Academic Press.

WILKINSON, D.M. (2008). Testate amoebae and nutrient cycling: peering into the black box of soil ecology. *Trends Ecol Evol* **23**, 596–599.

Tables:

Species	Probe /number of examined TA	Number of all/ living TA (staining by P and B probes)
Archerella flavum Archer	A/3	
Arcella vulgaris Ehrenberg ***Arcella discoides*** Ehrenberg	A/3, B/2, C/3, D/1, M/2, P/5, TR/2,	55/7
Assulina sp. ***Assulina muscorum*** Greeff ***Assulina seminulum*** Penard	A/10, B/10, D/10, DI/10, F/10, PH/10, S/1	
Centropyxis sp. ***Centropyxis aculeata*** (Ehrenberg) Stein ***Centropyxis aerophila*** Deflandre ***Centropyxis constricta*** (Ehrenberg) Penard	A/5, AB/3, B/45, D/7, P/6, T/5, TR/8	66/18
Cyclopyxis eurystoma Deflandre ***Cyclopyxis kahli*** Deflandre	B/4, T/7	
Cyphoderia ampulla Ehrenberg		1/1
Difflugia oblonga Ehrenberg	B/3, D/4, H/3, P/3, T/8	21/4
Euglypha sp., ***Euglypha ciliata*** Ehrenberg ***Euglypha compressa*** Carter ***Euglypha strigosa*** Ehrenberg	B/5, C/3, D/2, E/5, H/2, L/5, M/10, P/6, S/1, T/3	31/10
Hyalosphenia papilio Leidy	A/10, B/10, D/10, DI/10, F/10, PH/10, S/3, T/4	
Nebela bohemica Taranek	A/10, B/10, C/3, D/10, DI/10, F/10, PH/10	
Tracheleuglypha dentata Penard	A/3, B/5, D/4, P/3, T/6	21/5
Trinema enchelys Ehrenberg ***Trinema complanatum*** Penard ***Trinema lineare*** Penard	A/10, B/28, D/11, H/3, P/6, T/20, TR/6	68/8
Trigonopyxis arcula Penard	AB/4	

Table 1: A list of observed TA with their description and number of tested species for given fluorescent probes. The first column contains name of the species, while second one contains name of probe used for staining (before slash) and number of examined individuals of given taxa stained with it (after slash). Following notation was used – A (Acid Fuchsine), AB (Aniline Blue), B (BCECF-AM), C (Cell Tracker CMFDA), D (DAPI), DI ($DiOC_3(3)$), E (Er-Tracker Blue-White DPX), F (FITC), H (Hoechst), L (LysoTracker Red DND), M (MitoTracker), P (propidium iodide), PH (AlexaFluor 633 phalloidin), S (SYTO 16), T (TMRE), TR (Texas Red C_2-imde) The third column indicates the overall number of detected individuals of given taxa in phalloidin/BCECF-AM staining experiment (before slash) and number of individuals identified as alive by this method (after slash).

Fluorescent probe	Excitation/ Emission wavelength [nm]	Final concentration	Staining time [min]	Targets of the probes
Acid Fuchsine (84600)	514/600-650	170 µM	10	Chitin, vacuoles, cytoplasm
Aniline Blue (ANILO1600)	405/550-620	135 µM	10	Chitin
BCECF –AM (B8806)	440 and 490/500-600	2 µM	25	Cytoplasm, pH
CellTracker CMFDA (C7025)	490/523	4 µM	30	Cytoplasm, only metabolically active cells
DAPI (D1306)	405/450-520	300 µM	20	Nucleic acids
$DiOC_3$(3)	488(1P), 950 (2P)/ 500-650	13.6 µM, 4.5 µM	20-25	Membranes
Er-Tracker Blue-White DPX (E12353)	374 (1P), 790(2P)/ 430-640	2 µM	120	Endoplasmic reticulum
FITC (46952)	490/523	1 mM	20	General staining, aminogroups
Hoechst (H21486)	405/430-490	1.8 mM	30	Nucleic acids
LysoTracker Red DND-99 (L7528)	577/590	200 nM	120	Lysosomes
MitoTracker (M22426)	644/655	1 µM	120	Mitochondria
AlexaFluor 633 phalloidin (A22284)	633/647	130 nM	120	Actin
Propidium Iodide (70335)	532/600-670	7.5 µM	25	Nucleic acids
SYTO 16 (S7578]	488/513-530	10 µM	90	Nucleic acids
Texas Red C_2-imde	532/600-650	14 nM	40	General staining
TMRE (T-699)	532/560-590	1 µM	20	Mitochondria

Table 2: Excitation and emission wavelengths, final concentrations, staining times and targets of applied fluorescent probes.

Fluorescent probe	Targets of fluorescent probes					
	nucleolus, nucleus	cytoplasm	membranes	shell	spec. organelles	symbionts
Acid Fuchsine	-	+++	-	+++	-	-
Anilin Blue	-	-	-	+	-	-
BCECF-AM	-	++	+	+	-	-
CellTracker CMFDA	-	+	-	-	+++	-
$DiOC_3(3)$	-	-	+++	+	-	-
Er-Tracker	-	-	-	-	++	-
FITC	-	+++	-	+	-	-
MitoTracker	-	-	-	-	++	+++
Propidium Iodide	+	-	-	-	-	-
TMRE	-	-	-	-	+++	-

Table 3: Suitability of fluorescent probes for visualization various compartments and endosymbionts of testate amoebae (- unsuccessful, + poor, ++ successful, +++ excellent labeling).

Sample	Dye	Length / µm	Width / µm	Biovolume / µm³
Euglypha sp.	BCECF-AM	64.6	34.1	3.04×10^4
Cyphoderia ampulla	BCECF-AM	112	50.5	3.90×10^4
Difflugia oblonga	BCECF-AM	164	57.3	2.41×10^5
Euglypha sp. (cyst)	Acid fuchsine	53	25	9.74×10^3

Table 4: Biovolume of testate amoeba inside their shells evaluated by the stereological fakir method.

Figures:

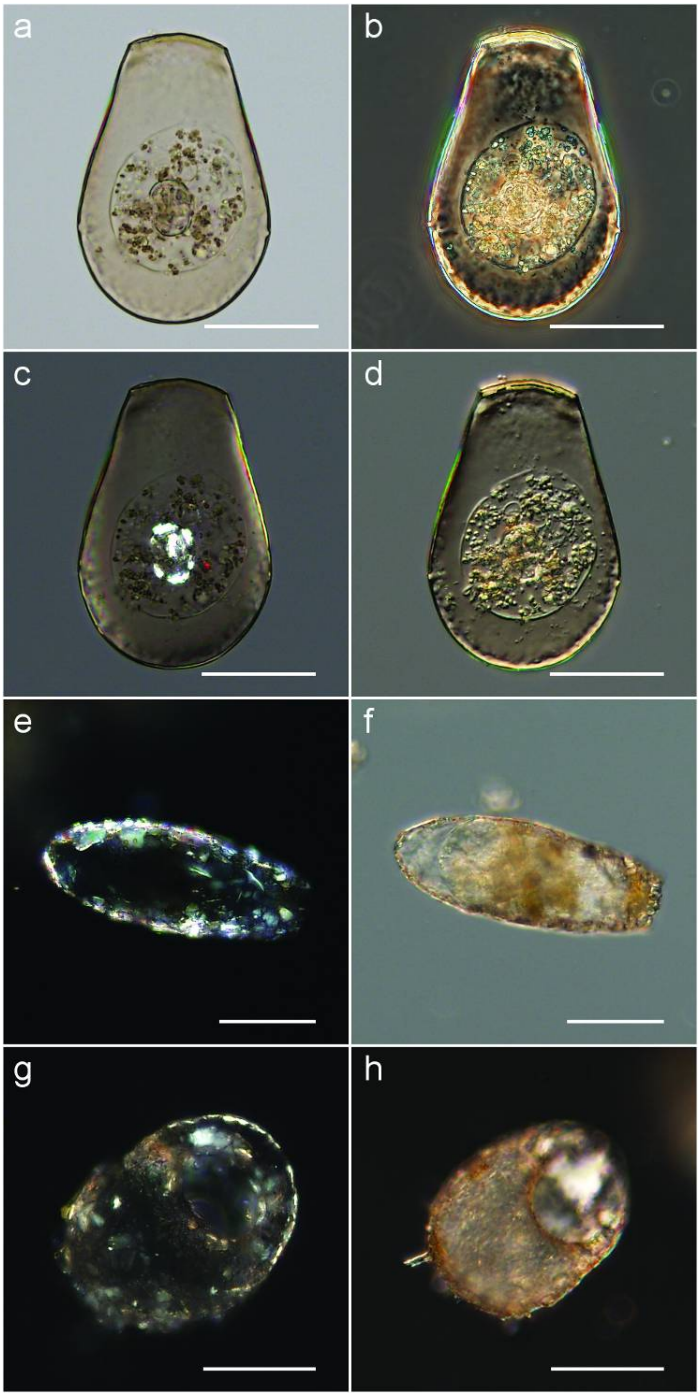

Fig. 1.

Optical contrasting of three testate amoeba species: (a-d) *Hyalosphenia papilio* (cyst), (e,f) *Difflugia oblonga* (living cell), and (g,h) *Centropyxis sp*. (two similar but different cells). Note the complementary nature of (a) bright-field, (b) phase-contrast, (c,e,g) polarization and (d,f,h) DIC Nomarski imaging. Scale bar in all images, 50 µm.

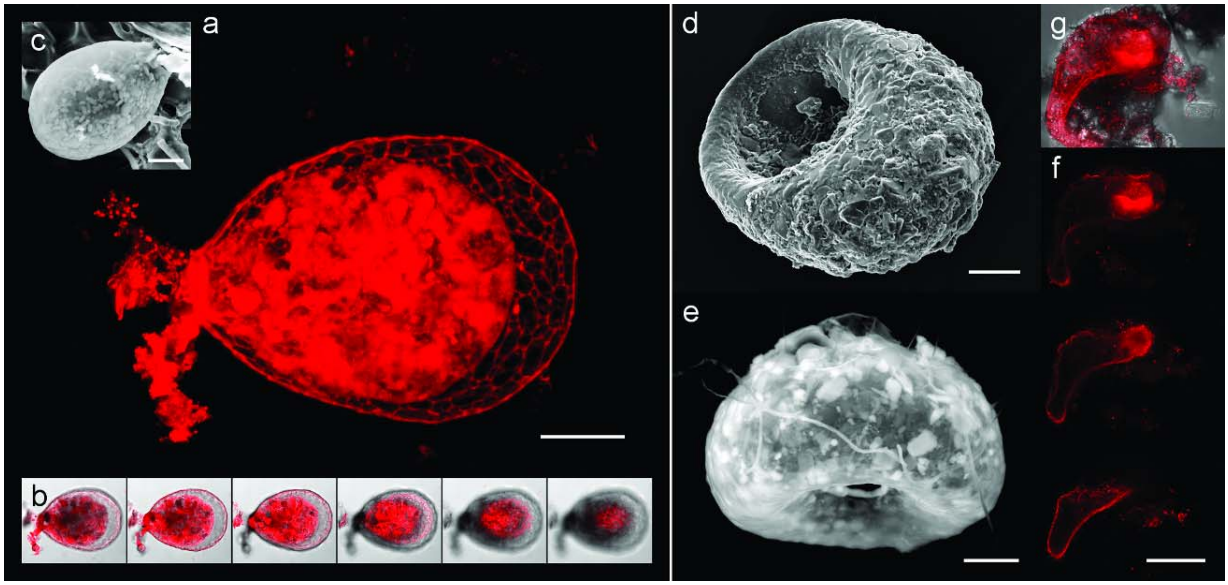

Fig. 2.

Shell (test) shapes and surface structures visualized by CLSM, SEM and ESEM.

(a,b) *Nebela tincta* in CLSM (acid fuchsine staining); (a) max. intensity projection, scalebar 20 µm, (b) serial optical sections.

(c) *Nebela tincta* in ESEM, scalebar 20 µm.

(d) *Centropyxis aculeata* in SEM, details of aperture, scalebar 20 µm.

(e) *Trigonopyxis arcula* in ESEM, scalebar 20 µm.

(f,g) *Centropyxis aculeata* in CLSM (acid fuchsine staining), cyst inside the test, scalebar 50 µm; (f) serial optical sections, (g) overlay of transmission channel and max. intensity projection of image *f*.

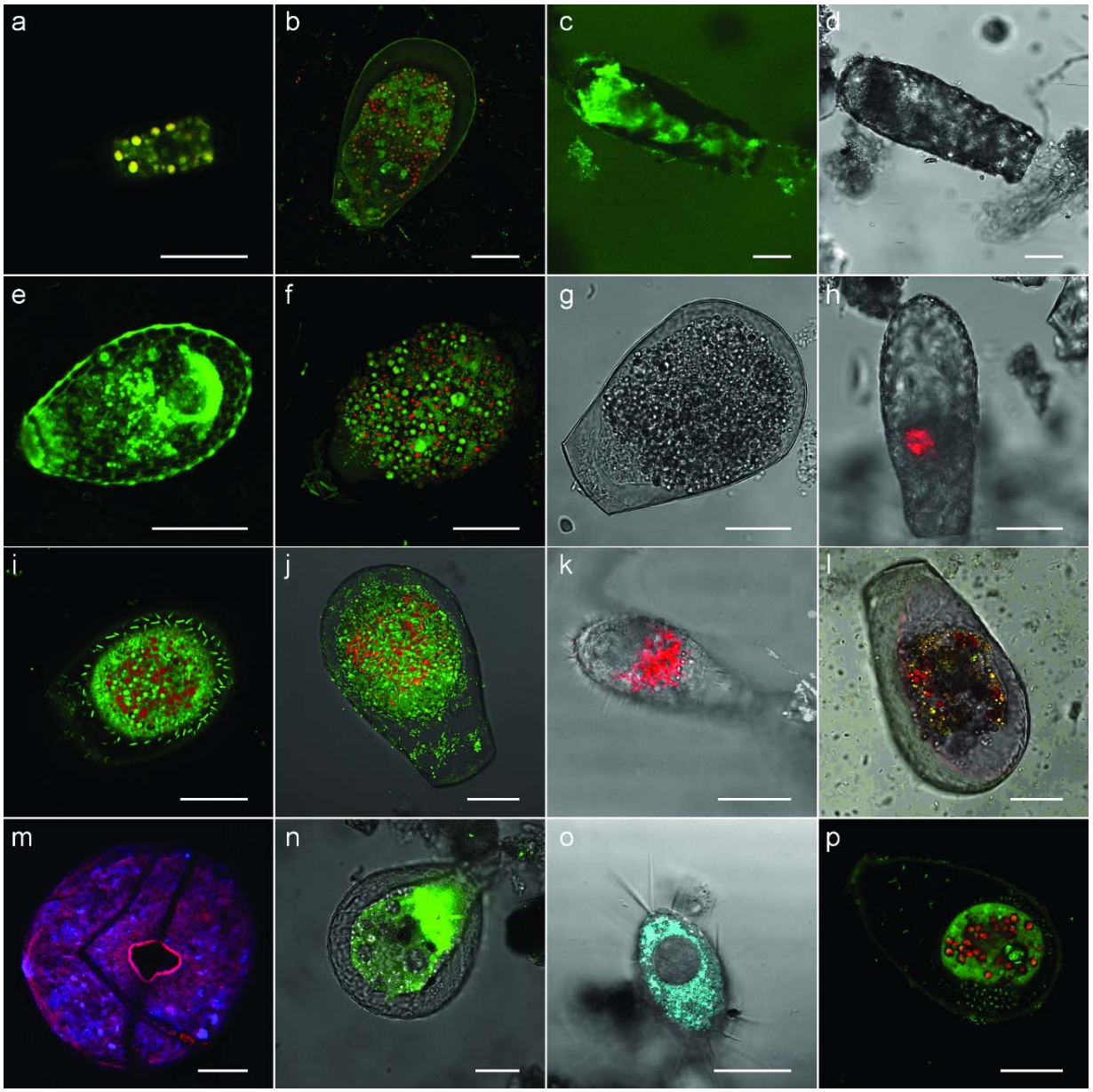

Fig. 3.

Testate amoebae in CLSM as stained by various fluorescent probes.

(a) *Archerella flavum*, cytoplasm and nucleolus (green, acid fuchsine) and endosymbionts' chlorophyll-a (red, autofluorescence), max. intensity projection; yellow color is due to overlaying red and green channels.

(b) *Hyalosphenia papilio*, cytoplasm (green, acid fuchsine) and endosymbionts' chlorophyll-a (red, autofluorescence), optical section.

(c) *Difflugia oblonga*, cytoplasm of living TA (green, BCECF-AM, optical section).

(d) *Difflugia oblonga*, transmission channel of image *c*.

(e) *Euglypha sp.*, cytoplasm and test (green, BCECF-AM), max. intensity projection; uneven cytoplasm staining may be attributed to a varying esterase activity across cellular compartments.

(f) *Hyalosphenia papilio*, generic staining, preferentially of amine and sulfhydryl groups on protein molecules (green, FITC) and symbionts' chlorophyll-a (red, autofluorescence), max. intensity projection.

(g) *Hyalosphenia papilio*, transmission channel of image *f*.

(h) *Difflugia oblonga*, nucleus (nucleic acids) in dead TA (red, propidium iodide), overlay with a transmission channel.

(i,j) *Hyalosphenia papilio*, membranes of living TA (green, $DiOC_3(3)$) and endosymbionts' chlorophyll-a (red, autofluorescence); (i) optical section, (j) overlay of max. intensity projection and transmission channel.

(k) *Euglypha sp.,* mitochondria (red, MitoTracker), overlay of max. intensity projection (three optical sections) and transmission channel.

(l) *Hyalosphenia papilio*, mitochondria (yellow, TMRE), endosymbionts' chlorophyll-a (red, autofluorescence), overlay with a transmission channel.

(m) *Trigonopyxis arcula*, test (blue, aniline blue; red, acid fuchsine), max. intensity projection.

(n) *Nebela bohemica*, generic staining (green, CMFDA), overlay with a transmission channel.

(o) *Euglypha sp.*, endoplasmatic reticulum (cyan, Er-Tracker), optical section, CLSM, transmission channel.

(p) *Hyalosphenia papilio*, cyst, generic staining (green, FITC) and endosymbionts' chlorophyll-a (red, autofluorescence).

Scalebar in all images 30 µm.

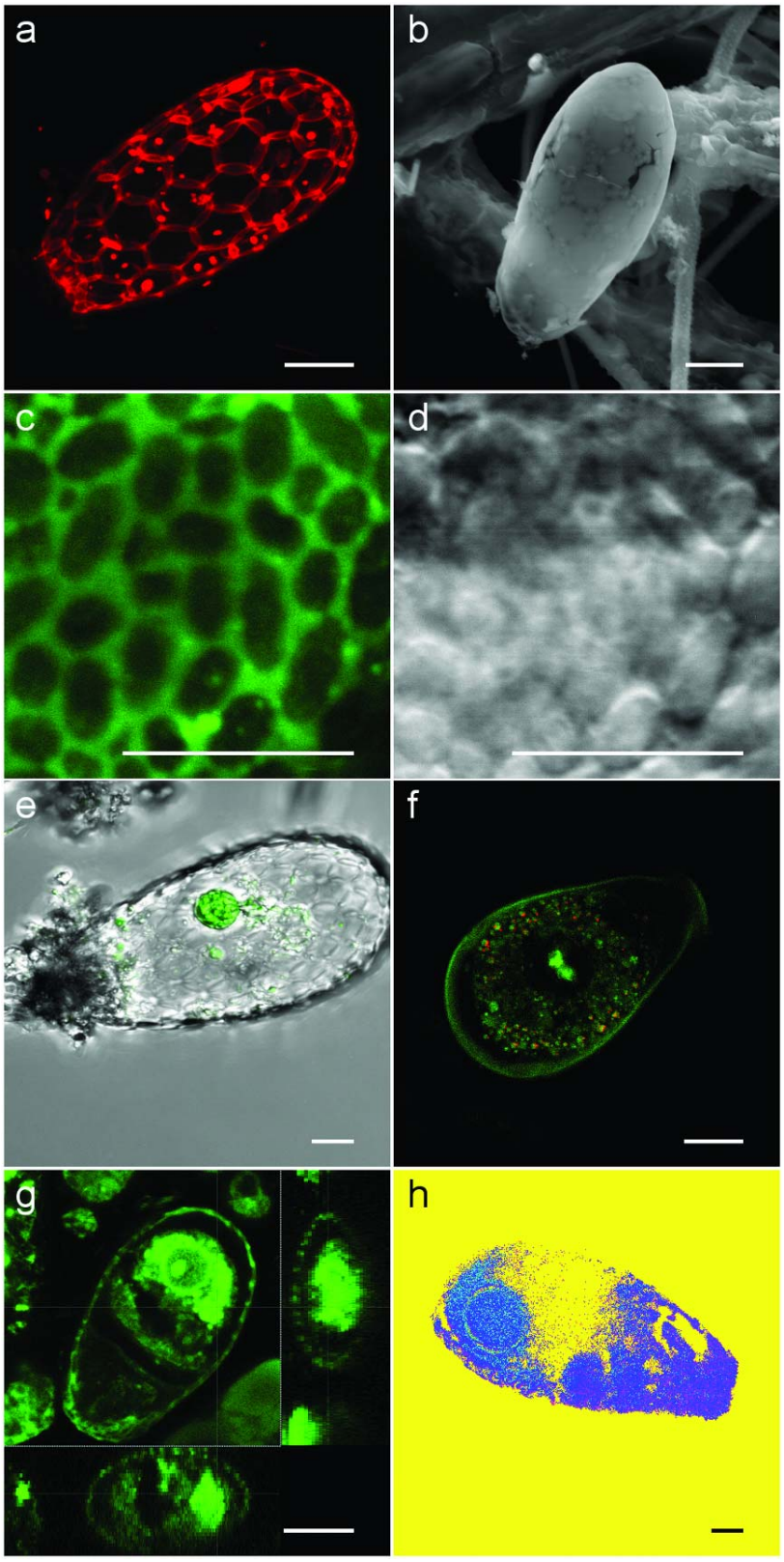
a
b
c
d
e
f
g
h

Fig. 4.

Advantages of CLSM imaging of testate amoebae.

(a) *Tracheleuphyta dentata* in CLSM, empty test (red, acid fuchsine), max. intensity projection, scalebar 10 µm.

(b) *Trinema sp.* in ESEM, test surface, scalebar 10 µm.

(c,d) *Nebela bohemica* in CLSM, detail of the test structure (green, BCECF-AM); (c) max. intensity projection, (d) transmission channel, scalebar 10 µm.

(e) *Euglypha sp.* in CLSM, protoplast inside the test (green, BCECF-AM), overlay with a transmission channel, scalebar 10 µm.

(f) *Hyalosphenia papilio* in CLSM, cell nucleus in mitosis and cytoplasm (green, BCECF-AM) and endosymbionts' chlorophyll-a (red, autofluorescence), scalebar 30 µm.

(g) *Corythion dubium* in CLSM, cytoplasm and test (green, BCECF-AM) with lateral views, scalebar 10 µm.

(h) *Euglypha sp.*, pH distribution determined by BCECF-AM (radiometric probe, pH-to-color not assigned), scalebar 10 µm.

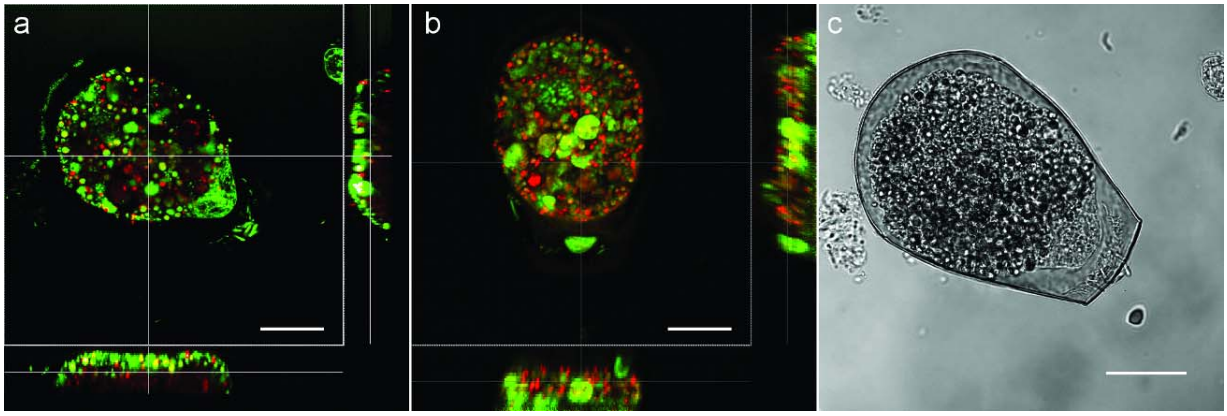

Fig.5.

Comparison of CLSM and TPEM in terms of penetrating depth (shown in lateral views) in *Hyalosphenia papilio.* Organic components (green, FITC) and endosymbionts' chlorophyll-a (red, autofluorescence); (a) CLSM, (b) TPEM, (c) transmission channel of image *a*.

Scalebar in all images 30 µm.

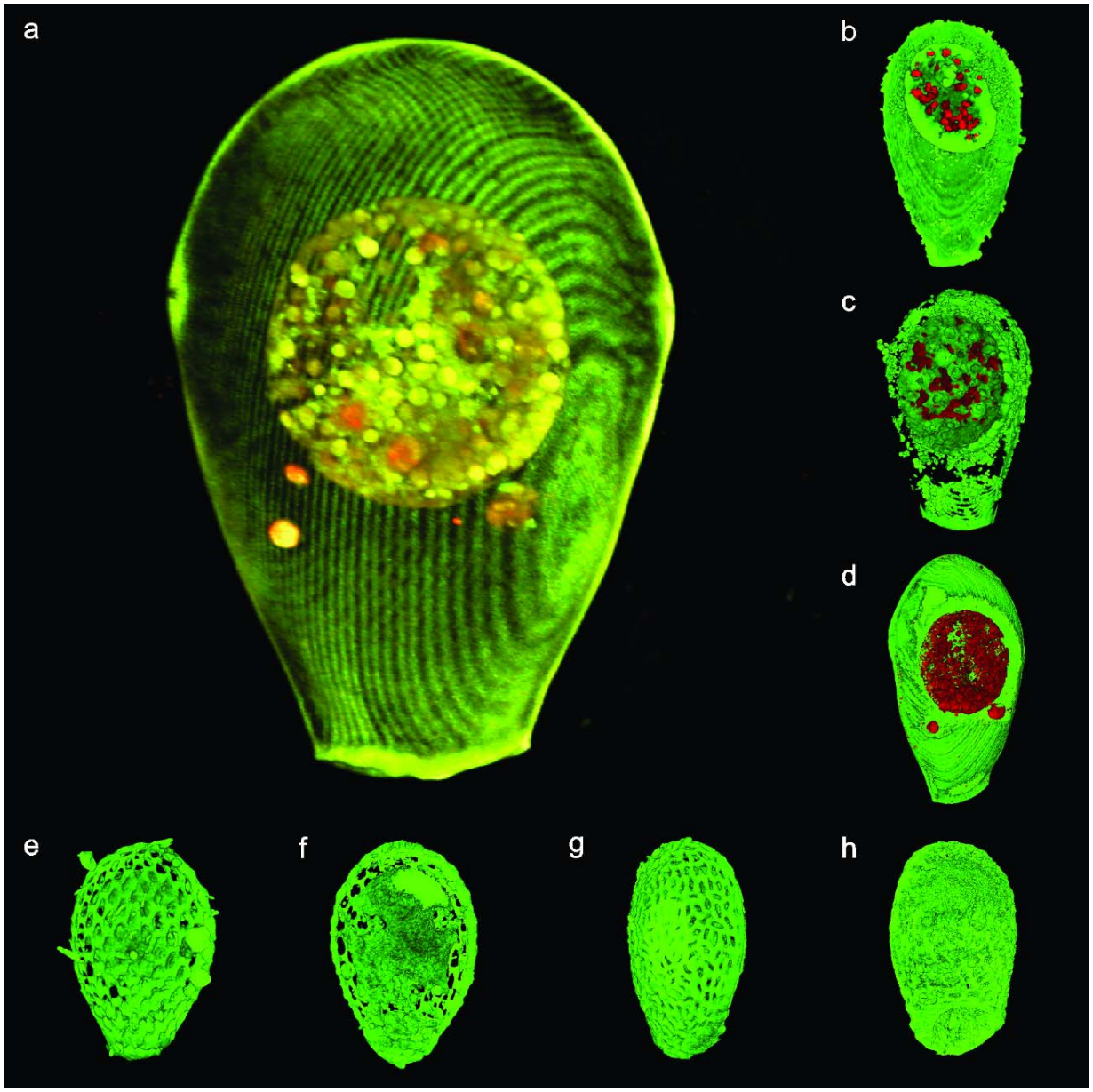

Fig. 6.

3D reconstructions of testate amoebae.

(a-d) *Hyalosphenia papilio* test (150 µm in length), membranes of TA (green, $DiOC_3(3)$) and endosymbionts' chlorophyll-a (red, autofluorescence) in CLSM; (a) VolumePro 1000 rendering board, (b-d) OpenGL-based volume rendering; the same cell is shown in *a* and *d*.

(e,f) *Euglypha sp.* test (75 µm in length, original image in Fig. 3e), enzymatic activity of cytoplasm (green, BCECF-AM) in CLSM, max. intensity projection; (e) front view, (f) back view.

(g,h) *Corythion dubium* test (40 µm in length, original image in Fig. 4g), enzymatic activity in cytoplasm (green, BCECF-AM) in CLSM, max. intensity projection; (g) back view, (h) front view.

4. AKTUOEKOLOGIE KRYTÉNEK SLADKOVODNÍHO PROSTŘEDÍ

4.1. Význam krytének v sladkovodním prostředí

Kryténky jsou rozšířeny kosmopolitně ve sladkovodním prostředí, částečně se vyskytují i v prostředí brakickém. Kryténky mají krátkou generační dobu (2-11 dní) (Medioli a Scott 1988) a mohou tudíž rychle reagovat na změny environmentálních parametrů, které mohou být ve vodním prostředí rychlejší a významnější než v prostředí terestrickém. Na druhou stranu je jejich druhově specifická citlivost ke změnám určitých environmentálních parametrů činí zajímavými bioindikátory kvality sladkovodních prostředí. Hodnocení výskytu druhů, jejich početnosti a morfologické variability v korelaci s limnologickými parametry je tak předmětem četných ekologických studií. Výzkumy v Kanadě a Itálii demonstrovaly efektivní využití krytének jako excelentních bioindikátorů úrovně znečištění (Collins et al., 1990; Asioli et al., 1996; Patterson 1996).

Mezi nejčastější druhy sladkovodního prostředí patří *Difflugia protaeiformis*, *Difflugia oblonga*, *Pontigulasia compressa*, *Centropyxis aculeata* a *Centropyxis constricta* (Patterson et al. 1985, Patterson et al. 1996). Ogden (1983) popisuje výskyt jednotlivých druhů rodu *Difflugia*, jehož zástupci se převážně vyskytují v jezerním sedimentu. Bartoš (1954) uvádí druh *Difflugia viscidula* jako zástupce krytének, jež se vyskytuje v jezerním a rybničním sedimentu, jeho pozorování potvrzuje Lorencová (2009). Mezi další druhy hojně nalézané v jezerních sedimentech patří *Difflugia corona* (Bartoš, 1954), *Difflugia tricuspis* (Medioli a Scott, 1983) a *Difflugia urceolata* (Bartoš, 1954). Předpokládá se, že četnost krytének se v tomto prostředí pohybuje okolo 500 jedinců na cm^3 (Patterson a Kumar, 2000a). Někteří zástupci jako rod *Trinema* a *Euglypha* jsou euryhalinní, jiné jako např. *Centropyxis aculeata* dominují brakickému prostředí (Patterson, 2002). Poznatky o ekologických valencích vodních krytének shrnuje Patterson 2002. Rod *Centropyxis* je popsán jako oportunistický generalista se schopností přežít v nepříznivých podmínkách, lépe než jiné druhy krytének (Patterson et al., 1996). Reindhard (1998) popisuje společenstva krytének s vysokou diverzitou, kde dominuje *Cucurbitella tricuspis* jako indikátor bentického prostředí a přítomnost druhu *Difflugia protaeiformis* indikuje zvyšující se environmentální stres. Tolonen (1986) revidoval použití krytének jako jezerních bioindikátorů; předpokládal, že hlavní kontrolu nad rozložením druhů má poměr C:N, velikost zrn, koncentrace

kyslíku a okolní vegetace. Pozdější studie ukazují, že odpověď společenstva krytének na environmentální podmínky je mnohem komplexnější (Escobar, 2008).

Patterson (1996) se věnoval přítomnosti krytének v substrátu kontaminovaném těžkými kovy (arsen, rtuť). Zjistil, že v kontaminovaném substrátu jsou přítomny *Centropyxis aculeata*, *Centropyxis constricta* a překvapivě *Arcela vulgaris*. *Difflugia protaeiformis* dobře indikuje znečištěné a acidofilní sedimenty (pH 3,9-4,5). Lorencová (2009) studovala rozdíly ve společenstvech z různých vodních prostředí Šumavy. Popisuje výskyt druhu *Difflugia globulus* z jezer s vyšší nadmořskou výškou (nad 1000 m.n.m.); stejně tak Collins et al. (1990) označuje druh *Difflugia globulus* jako dobrý indikátor chladného klimatu. *Difflugia oblonga* je typicky jezerní zástupce, který je popisován jako druh vyžadující vyšší obsah organického materiálu (Colins et al., 1990).

V menších a mělčích sladkovodních prostředích jako jsou např. rybníky, tůňky či kaluže, kde dochází k periodickému vysychání, se objevují také druhy půdní. Mísí se zde jak čistě vodní druhy (např. *Difflugia*) s druhy vyskytujícími se ve vodním i půdním prostředí, tak s druhy vyskytujícími se převážně v půdním prostředí (např. *Trinema*).

V rámci disertační práce na tomto tématu jsem monitorovala a zachytila změny v druhovém složení krytének v mělkých tůních. Tyto data jsem korelovala s celoročně měřenými limnologickými parametry. Ekologické nároky rodu *Arcella* a rodu *Difflugia* se zdají být v opozici. Z analýz vyplývá závislost druhového složení krytének na teplotě, koncentraci fosforu, NH_4^+, NO_3^-, As, Pb, Cd, Mn, Ni, PAH a Fe. Výsledky budou publikovány v níže uvedeném článku.

ČLÁNEK 2: Actuoecology of Testate Amoebae in the Komořany Pools of the Vltava Basin (v tisku v časopise Microbial Ecology)

Ecology of Testate Amoebae in the Komořany Ponds in the Vltava Basin

Running head: Ecology of Testate Amoebae

Zuzana Burdíková[1,2], Martin Čapek[1,3], Zdeněk Švindrych[1,4], Milan Gryndler[5], Lucie Kubínová[1], Katarína Holcová[2]

1. Institute of Physiology, Academy of Sciences of the Czech Republic, v.v.i., Vídeňská 1083, 14220 Prague, Czech Republic
2. Institute of Geology and Palaeontology, Faculty of Science, Charles University, Albertov 6, 128 43 Prague, Czech Republic
3. Faculty of Biomedical Engineering, Czech Technical University in Prague, nám. Sítná 3105, 272 01 Kladno, Czech Republic
4. Faculty of Mathematics and Physics, Charles University, Ke Karlovu 3, Prague 2, 121 16 Czech Republic
5. Faculty of Sciences, J.E. Purkinje University, České mládeže 8, Ústí nad Labem, 400 96, Czech Republic

Corresponding author: Zuzana Burdíková, tel.: +420 296 443 769, fax: +420 241 062 488, e-mail: burdikova@biomed.cas.cz

Keywords: ecology, freshwater ecosystem, testate amoebae, seasonal variability

ABSTRACT

Testate amoeba (TA) assemblages were collected in 2005 from four ponds in Komořany (Prague, Czech Republic). An analysis of seasonal taxonomic variability of TA populations and its correlation with the limnological characteristics of the area (temperature, pH, total organic carbon, nitrogen, phosphorus, heavy metals, etc.) was performed. The predominant genera were *Difflugia*, *Arcella* and *Centropyxis*. The most significant changes in the TA community occurred between March and July. *Arcella* genus dominated in March and April; in May, *Arcella* and *Centropyxis* genera were present in the same amount; in June, *Arcella* genus disappeared and *Difflugia* genus started to dominate the community. A multivariate redundancy analysis showed statistically significant correlations between the environmental parameters and the composition of the TA community. The results indicate a negative correlation between TA quantities and Ni, Cd, PAH, Mn, As and Pb. TA were also affected by concentrations of NH_4^+, NO_3^- and P, as well as by temperature variations. The observed correlations between the species composition and environmental parameters can be used in paleoecological interpretations of fossil TA communities. Our results also prove the suitability of TA as water-quality indicators in urban areas.

INTRODUCTION

Testate amoebae (TA), Amoebozoa:Arcellinida, are a group of amoebae (10-400 μm) protected by a solid test (shell). The test encloses the cell plasma, and usually has a single aperture for pseudopodia. TA play an important role in most aquatic and terrestrial ecosystems, and have thus been an essential subject of numerous scientific environmental studies [11**,** 42, 43, 53, 56]. TA belong to the small number of limnic species that can fossilize [27]. They are commonly used as model organisms in population ecology, ecotoxicology and paleoecology owing to their cosmopolitan dispersion and species-specific ecological preferences and capability to adapt to environmental changes [5, 12, 31, 32]. Ellison [16] described a relationship between TA distribution and physical and chemical parameters of tarn waters; he found that genus *Difflugia*

seems to prefer acidic environment with pH under 6.2. Other genera such as *Centropyxis*, *Lesquereusia* and some species of *Cyclopyxis* and *Difflugia* are common in lakes with pH above that value. Qin [45] showed that increasing eutrophication of the lake Zhangdu in China resulted in dramatic changes in the composition of lacustrine TA communities.

We suggest that TA can be used as indicator species for monitoring the environmental conditions in ponds. The following considerations make them particularly useful [12, 19]. First, various species respond differently to environmental conditions. Second, their small size enables them to rapidly colonize a suitable site [15]. Third, due to their abundant presence in late Quaternary lacustrine sediments TA can be used in paleoecological studies [14].

The taxonomy and ecology of freshwater TA (mainly from lakes) have been well documented [1, 2, 3, 7, 8, 10, 14, 21, 22, 27, 30, 34, 39, 41, 0, 51, 54, 55]. In lakes, TA assemblages can be correlated with a number of environmental parameters, e.g., eutrophication [50], water temperature changes [10], salinity [47], and pH [18]. The TA assemblages showed a strong correlation with phosphorus, reflecting the euthrophic status of the lakes and also substrate characteristics, total organic carbon and metal contaminants (particularly Cu^{2+} and Mg^{2+}) [48]. Only few articles have been published by now about environmental preferences or ecological factors such as heavy metal concentrations [e.g., 29, 35, 39, 43, 18]. Fossil TA datasets collected from kettle lakes indicated that TA appear to be sensitive to the past episodes of anthropogenic disturbances, including land clearance and changes in the trophic status of lakes, as associated with widespread application of fertilizers from the mid-twentieth century [41].

Further, Heal [23] described the seasonality in composition of testate amoeba assemblages. Warner [58] elucidated the relationships between TA and seasonal fluctuations of soil moisture in *Sphagnum* habitats and sensitivity of these organisms if they are to be used as reliable bioindicators of human pollution and environmental disturbance.

We chose the Komořany ponds, since it is an important test area for examining the relationship between TA and disturbances in water quality. Previous studies have focused mainly on bogs, sphagnum and large lakes, with minimum attention paid to ponds and their

limnological parameters. The aim of the present study is to fill this gap by answering these research questions:

1. How do populations of TA vary through the year?
2. How do populations of TA correlate with basic environmental factors (e.g., water chemistry)?

METHODS

The Komořany ponds biotope locality

The Komořany ponds chosen here as model habitat are a system of four ponds on the right bank of the Vltava in Prague, Czech Republic, Europe. They are located in the southern part of Prague, close to the confluence of Berounka and Vltava river (Fig. 1). They were built as a part of the flood protection system in the 19th century. Once a cascade of dams was constructed on the Vltava river, the ponds lost their importance in flood protection, and successive vegetation evolved in a secondary flood-plain ecosystem. The locality is now a refuge for original Prague fauna, and is the last functional fragment of the alluvial system in Prague. Despite its gradual deterioration due to numerous disturbances, it remains an important stabilizer of the Prague ecosystem (Kerouš K., 2002, Locality biological processing – the right bank of the Vltava at the confluence with the Berounka, report in Czech).

Geological and geomorphological characteristics

The Komořany pond complex is a territory with alluvial soils located in the southern part of the Prague plateau at an altitude of 190 m a.s.l. The Prague plateau is influenced by a continental climate with cold winters (average temperature around 0°C), warm and sunny summers (average temperature 20°C) and an average annual temperature of about 10ºC. The climate is also markedly influenced by the microclimate of the Prague metropolis. The annual precipitation is

about 530 millimeters. The base of the Komořany ponds is lined with shales of *Letná* formation (Ordovician), overlaid by sandy gravel of alluvial terraces, which are overlapped by alluvial loams [13]. The relief of the area consists of the flat floodplain of the Vltava river and a few shallow ponds. The hydrology of the Komořany area has been constantly monitored by "Povodí Vltavy" (Vltava River Basin), a state public enterprise (http://pvl.cz/laboratore-povodi-vltavy).

Biota

The freshwater area of the Komořany ponds, periodically inundated by water from the nearby Vltava river, is a significant ecosystem with high biodiversity. Most of the species are associated with the water pond habitat, see also their brief list in supplementary data. Strong anthropogenic influences predominantly affected the aquatic ecosystems of the four-hectare area. These influences have led, for example, to a marked reduction in the populations of amphibians in the last ten years. The decrease in the quality of the aquatic environment of the Komořany ponds has been caused by the elimination of flooding. Flooding, which used to sustain the quality of the environment by washing out sediments, is now much less frequent and much less extensive than before the cascade of dams was constructed.

Nowadays, the ponds are covered by a growing layer of sediments, especially of organic origin, resulting in oxygen deficit, eutrophication and changes in the chemistry of the environment and in the overall balance of nitrogen compounds. The only remaining water supply for the ponds is the permeable bedrock, which is homogeneous with the river bed. Another factor that has affected the aquatic environment is the increase in car traffic in the area, which causes pollution.

Characteristics of the Komořany ponds

All four ponds are shallow, euthrophic, and between 20 - 40 meters in diameter; the water is 0.1 - 0.8 m in depth. The coordinates, the area, the distance from the Vltava, and the composition of

the sediments of the ponds are described in Tab. 1. Snapshots of all ponds can be seen in supplementary Fig. S5 - S10.

The Komořany ponds form a dynamic ecosystem with periodic climatic cycles. Between December and March, the ponds may freeze repeatedly for periods of 1 - 4 weeks. Due to intense snowmelt and rainfalls, the ponds are periodically partially flooded by river water in March and April. In summer, the ponds dry out and anoxic zones appear. Due to this dynamics, most of TA tests from the previous years are washed away in the local spring floods. In summer and autumn, the locality becomes overgrown with vegetation, and the tests are deposited into the sediment in relatively large amounts.

Pond No. 1 is closest to the Vltava river, being localized near its confluence with the Berounka river (Fig. 1). It thus communicates with the Vltava river more strongly than the other three ponds. For this reason, it has the most stable environmental conditions throughout the year (e.g., a shorter period of oxygen deficiency during the summer months than the other ponds). This pond is about 0.2 - 0.8 m deep, and has a flat bottom. Pond No. 2 is similar to the first one and is second in the direction of river flow. The sedimentary composition is similar to that of the first pond. Pond No. 3 is third in the direction of river flow. Its sediment contains a higher percentage of sand than the sediment in the other ponds. The pond No. 4 is the last one. Its sediment is similar to sediments in ponds No. 1 and No. 2.

Sampling

TA were sampled in the period of November 2004 - September 2005. Ten sets of samples were collected per pond, with a sampling interval of approximately one month (Tab. 2). Samples were not collected in December 2004 and in February 2005, when the ponds were frozen, and in March 2005, when they were completely flooded. The upper unconsolidated sediment layer was sampled by inserting a tube (15 cm in diameter) into the layer and sliding a plate beneath the bottom of the tube. The volume of the sampled sediments depended on the thickness of the

unconsolidated layer, and varied from 20 to 70 cm^3. Though the sampled layer may contain also TA from previous time intervals, clear differences between subsequent/consecutive samples were recorded, which reflects seasonal changes in composition of assemblages.

The samples were gently centrifuged, and the resulting supernatant was replaced by 4% formaldehyde or 70% ethanol as fixatives. A subsample of 20 cm^3 was wet sieved, and 36 - 500 µm fractions were used for the TA study. Similar studies analyze fractions >63 µm [e.g., 1, 14, 22, 29, 39, 40, 0, 51]. However, since many TA species are smaller than 63 µm [18], an appropriate sieve size was chosen, see also [57].

The 36 - 500 µm residues were air-dried at 20 - 30°C prior to identification and quantification. Use of the dry residuum selectively eliminated most autogenous tests. A reduction in autogenous tests in dried residues corresponds to reduction during fossilization [18] and, therefore, results are well applicable in paleoecology.

TA tests were picked from the dried residuum, identified and enumerated using a stereomicroscope. When TA were too abundant in the sample, the dried residuum was split into parts using a dry microsplitter. The parts were repeatedly split until they consisted of ~30 - 300 tests, which is suitable for calculating the percentage occurrences. Typically, one to three levels of splitting were applied.

Biochemical water analysis

The analysis report was provided by “Povodí Vltavy”, a state public enterprise. The samples for biochemical analysis were taken from the Vltava river near the Komořany ponds. The parameters of the analysis were monitored in 2004 - 2005, according to the ISO/IEC 17025 certified quality control system and Annex 5 of Decree No. 252/2004 Coll., amended by Decree 187/2005 Coll. (Ministry of Health of the Czech Republic, in Czech), which stipulate the health requirements for drinking water.

The analysis involved basic chemical and physical parameters (including air temperature, water temperature, pH, electrolytic conductivity, a number of mineral anions and kations, dissolved oxygen, oxygen saturation, total organic carbon, total nitrogen, inorganic nitrogen), as well as organic parameters (PAH - polyaromatic hydrocarbons and other regulated substances). Among all these parameters, we selected environmental variables with a potential influence on the species composition of TA assemblages for further analyses. The values of the selected parameters are shown in supplementary data (Tab. S1).

Statistical analysis

Shannon index

At the assemblage level, the relative health of an aquatic environment can generally be indicated by the diversity, usually measured by the Shannon diversity index (SDI) [49], and by the total abundance of the specimens. In unfavorable environments, the SDI is generally low (<1.5). These environments are typically dominated by only one or two species and/or strains, with other forms being rare. By contrast, healthy TA fauna usually have SDI values >2.5 and abundance of over 500 specimens/cm^3 [12]. This rule applies to entire communities.

When processing the sample from dry residual relics, it is necessary to take into account that data on species with fragile tests is missing, since the tests of these species are mechanically destroyed, which prevents the detection (Burdíková, unpublished data).

Redundancy analysis

We applied redundancy analysis (RDA) for an evaluation of the effect of various factors and substances on the TA populations. RDA is a canonical form of principal component analysis that enables us to identify relationships between two sets of variables (species and environmental variables). It assumes linear relations both among species and between species and

environmental variables [24]. The significance of the species-environment relationship (the effect of environmental parameters on TA assemblages during the year) was assessed using the Monte Carlo permutation test. The computations were carried out using *Canoco* software, version 4.5 [6].

Image acquisition

To study test morphology in detail, TA were imaged using JEOL-6380LV scanning electron microscope (SEM). The fixed tests were critical point dried or partially dried, mounted on metal stubs with a double-sided adhesive conductive tape (carbon tape) and coated with gold (4 min at 20 mA in a vacuum of about 10 Pa, with argon present) using a sputter coater. The stubs were then affixed by the carbon tape to a microscope stage. The gold-coated TA shells were observed at 20 - 30 kV in high vacuum mode, using an Everhart-Thornley secondary electron detector.

TA Systematics

The TA classification is based on a detailed morphological study of tests [4, 9, 17, 26, 37, 38] (Fig. 2 and Fig. 3). The taxonomic status is often complicated by the fact that holotypes and lectotypes of species were not clearly determined.

In Tab. 2 we determined the following variants of *Difflugia* (*D.*) *oblonga*: *D. oblonga acuminata* Ehrenberg, 1838; *D. oblonga brevicolla* Cash, 1909; *D. oblonga claviformis* Penard, 1899, *D. oblonga cylindrus* Thomas, 1953; *D. oblonga inflata* Penard 1899, *D. oblonga longicollis* Gassowsky, 1936; *D. oblonga venusta* Penard, 1902; *D. oblonga schizocaulis* Stepanek, 1952; *D. oblonga oblonga* Ehrenberg, 1838 [4]. Since there is no consensus book or publication for TA identification and, concurrently, the taxonomy has a strong impact on the results, we also put *D. oblonga* Ehrenberg, 1838 in Tab. 2, which summarizes all variants of *D. oblonga* together [38].

RESULTS

Characteristics of TA assemblages

Forty-nine species of TA were identified in the studied material, see Tab. 2 and supplementary Fig. S2. With a few exceptions, all detected individuals belonged to one of three genera - *Arcella*, *Centropyxis* or *Difflugia*. Their relative abundances in the individual samples during the observed period in each pond are depicted in Fig. S3 of the supplementary data, and are summarized for all ponds in Fig. 4. The number of species found in each assemblage sampled at the same time varied from zero to twenty-four. The most abundant species in total were (top 10%): *D. oblonga oblonga* Ehrenberg, 1838; *Centropyxis* (*C.*) *minuta* Deflandre, 1929; *C. aculeata* var. *discoides* Ehrenberg, 1830; *Arcella* (*A.*) *gibbosa* Penard, 1890; *A. arenaria* Greeff, 1866.

Seasonal changes in TA assemblages in the Komořany ponds in the course of the year

Generally, the species composition of the assemblages changes gradually in the course of the year. In November, the most abundant genus present was *Arcella*, namely species *A. gibbosa* and *A. vulgaris*. The second highest occurrence, just slightly lower than that of *Arcella*, was observed for *Difflugia* genus, with the most frequent species *D. oblonga oblonga* and *D. lacustris*. The least abundant was genus *Centropyxis – C. aculeata*, *C. cassis*, *C. minuta*.

In January, the *Arcella* genus was represented by *A. gibbosa*, *A. vulgaris*, and the *Centropyxis* genus was represented by *C. aculeata*, *C. discoides*, *C. minuta*. The dominant genus was *Difflugia – D. corona*, *D. gramen*, *D. lacustris*, *D. oblonga acuminata*, *D. oblonga brevicolla*, *D. oblonga oblonga*.

In February 2005 the ponds were frozen and, after a rise in temperature in March, inundated by the river. During spring (March, April), *Arcella* genus and small *Centropyxis* species, e.g., *C. minuta*, were the most frequent in the samples from all the ponds. In April, *Arcella* became less prevalent while the numbers of *Centropyxis* specimens increased (e.g., *C. aculeata*

var. *discoides*). In May, *Arcella* and *Centropyxis* genera were present in approximately the same numbers while the number of *Difflugia* individuals increased slowly. By June, *Arcella* was in regress. Although the relative abundances of *Centropyxis* genus remained steady, small species such as *C. minuta* decreased in favor of bigger species, namely *C. discoides* and *C. ecormis*. In June, there was an increase not only in the total number of individuals of *Difflugia* genus, but also in the number of species; the most frequent ones being *D. avellana*, *D. corona* and *D. oblonga claviformis*.

At the beginning of July, we observed the disappearance of *Arcella* genus. At the same time, *C. aculeata* dominated in *Centropyxis* genus, *C. minuta* increased noticeably and the abundance of *C. ecornis* decreased. *Difflugia* was the dominant genus in the assemblages in these months; the abundance of species and individuals of *D. compressa*, *D. lacustris*, *D. oblonga claviformis*, *D. oblonga curvicaulis*, *D. oblonga oblonga*, *D. urceolata* increased. At the end of July, genus *Arcella* – *A. vulgaris*, genus *Centropyxis* – *C. aculeata*, *C. aerophila*, *C. constricta*, *C. ecornis*, *C. minuta* and genus *Difflugia* – *D. corona*, *D. lacustris*, *D. viscidula* were present. In August, we encountered *Arcella* genus – *A. arenaria*, genus *Centropyxis* – *C. aculeata* and *Difflugia* – *D. corona, D. lacustris*, *D. oblonga oblonga*. In September, genus *Arcella* was present only sporadically while genus *Centropysis* – *C. aculeata*, *C. aerophila*, *C. minuta* – dominated. The presence of *Difflugia* genus in the assemblage decreased, and the most abundant species were *D. corona*, *D. oblonga oblonga*, *D. oviformis*.

The diversity of TA assemblages in the course of the year, as characterized by the Shannon index of diversity, is documented in supplementary Fig. S4 as a summarization for all ponds. Fig. 5 demonstrates the results for each sampling date and pond. The highest abundances of both species and individuals were observed in the pond No. 1. The ponds No. 1 and No. 2 were comparable in this respect while the number of individuals in the pond No. 4 was noticeably lower than in any of the other ponds.

Correlation of environmental variables and TA assemblages

Graphic presentations (biplots) of RDA results (Fig. 6 - 10) illustrate dependency on various environmental parameters for the most abundant TA. The arrows or small triangle tips represent the scores of environmental parameters or TA species, respectively. An opposite or similar orientation of the scores indicates a negative or positive correlation of the environmental factors/species, respectively. The results of a Monte-Carlo permutation analysis are shown in Tab. 3.

We observed following interactions of environmental factors with TA species:

Temperature: Temperature is not an important factor for most TA species, since the Monte-Carlo test result is insignificant if no co-variable is introduced into the analysis (Tab. 3). The result becomes significant only after pond identification is introduced as a co-variable, i.e. when the variability caused by the location of the pond is subtracted from the model. From the results of RDA (with pond identification included as a co-variable), see Fig. 6, it seems that *Arcella* genus and also a few *Difflugia* species show a weak tendency to prefer low temperatures. However, there is almost no correlation, or only a very weak positive correlation, with temperature for *Centropyxis*.

Phosphorus: Most TA species show weak negative correlation of marginal significance with the concentration of phosphorus ions (Fig. 7). Thus, we can conclude that a high concentration of phosphorus ions tends weakly to decrease the numbers of TA in the environment. These results are independent of the location of the ponds, since they are similar with or without using pond identification as a co-variable (data not shown).

NH_4^+, NO_3^- ions: A part of *Difflugia* species appears to be positively correlated with NH_4^+, the other part showing the negative correlation. All the species seems to be independent of the presence of NO_3^- (Fig. 8).

Toxic substances (Fig. 9): Almost all species show a negative correlation with Pb (lead), PAH (polycyclic aromatic hydrocarbons), Cd (cadmium) and Mn (manganese). *Arcella* has the strongest correlation with Ni (nickel) and a significant negative correlation with As (arsenic). *Difflugia* seems to be less affected by arsenic concentrations than other genera. *C. discoides* shows obvious positive correlation with As.

Fe (iron): *Arcella* prefers a higher concentration of iron, *Centropyxis* appears to be independent of iron while *Difflugia* shows a mild negative correlation, see Fig. 10.

Macrobiogenic elements: Sulphate, calcium and magnesium failed to exhibit any dependence (data not shown).

DISCUSSION

In this paper we report our findings on changes in TA assemblages in the course of the year, and our study on the use of TA as water-quality indicators in actuoecology. To the best of our knowledge, no exhaustive study of this kind on the development of TA communities in the course of the year has previously been reported.

The TA assemblages in the Komořany ponds undergo significant changes in composition in the course of the year. At the beginning of the year, *Arcella* and *Centropyxis* genera predominated. Other authors [48] have explained similar observations by the stress caused by low oxygen availability. During the summer months, the genus *Difflugia* was predominant, probably as a result of the pond eutrophication. From our other results, see Fig. 4, we can conclude that the genera *Arcella* and *Difflugia* have opposite occurrence trends, life strategies and ecological preferences. *Centropyxis* seems to be a genus capable of withstanding hostile conditions better than most TA species.

To evaluate the limnological significance of TA assemblages, it is important to understand their ecology and distribution [14]. Our results show that *Arcella* prefers clean waters with low

concentrations of organic materials and lower temperatures (Fig. 6). These requirements are fulfilled in running waters or, in our case, in the ponds in spring. It is supposed that the organic compounds are used up in winter. Given their slightly psychrophilic nature, it was not surprising that populations of TA grow first in the freshwater ecosystem, starting in late winter.

Difflugia seems to have different ecological requirements. It starts to grow later than *Arcella*, but it cannot be distinguished whether this is caused mainly by temperature or by a lack of organic material in the ponds, since these two factors are highly correlated. Our results confirm the assumption that the species of *D. oblonga* are excellent indicators of eutrophication [45]. Generally, the genus *Centropyxis* seems to be very tolerant to different environmental conditions in the Komořany ponds in the course of the year, which is in accordance with the results of other authors, e.g. [48, 18]. Also, Reinhardt [46] described that *Centropyxis*, sampled from contaminated shallows and rich organic substrates, is a genus that tolerates significant levels of environmental stress.

Our data indicate that the distribution of TA is commonly explained by abiotic factors. This corresponds to the findings of others [33] who report that TA assemblages respond dynamically to environmental changes. These organisms are therefore regarded as important bioindicators of environmental changes [28].

Fig. 6 shows that neither *Difflugia* nor *Centropyxis* genus correlates with specific temperatures. On the other hand, *Arcella* genus weakly correlates with low temperatures. However, as mentioned above, it cannot be distinguished whether this correlation is a direct result of temperature or of some other factors dependent on temperature, e.g. water eutrophication.

The TA assemblages showed weak negative correlation dependence on phosphorus (Fig. 7) and, at the same time, phosphorus has the greatest influence on TA assemblage distributions in some ecological studies [48]. The phosphorus concentrations in a given locality correspond to a hypertrophic environment (concentration of P in water >100 µg/l) or a euthrophic environment (in our case, March, August: concentration of P in water <100 µg/l).

Unfavorable conditions in the ponds were the reason for the dominance of the genus *Difflugia.* This is in accordance with the results of Collins et al. [10], who described the species *D. oblonga* as the major indicator taxa of high organic contents.

Published reports, e.g. [20], show that nitrogen (N) is an important ecological factor severely affecting TA assemblages. Krashevska et al. [25] show that N strongly increased the density of TA individuals, and the concentration of N has specific effects on different species in the community. This is in accordance with our results.

C. constricta is known to be the first pioneering form that inhabits clean environments [52]. This is in accordance with the results presented in Fig. 8 which indicate that *C. constricta* prefers a freshwater system with a low concentration of NH_4^+, NO_3^-, Fe and P. *C. aculeata* did not show any considerable preference in terms of water eutrophication in our study.

Heavy metals are extensively monitored pollutants due to their high toxicity for organisms. Many studies [e.g., 35] have focused on the use of microorganisms (other than TA) for monitoring of this type of pollution. Previous studies have also shown the negative effect of road traffic pollution on TA communities [2], and a negative correlation between TA assemblages in mosses and atmospheric pollution by heavy metals, in particular by lead [36].

The results in our study, see Fig. 9, are in accordance with the results of the authors mentioned above, and show that TA assemblages correlate negatively with heavy metal concentrations in the environment. Our observations further suggest that *Centropyxis* is sensitive to arsenic contamination, but that it is relatively insensitive to nickel concentrations. This is in agreement with the result of Davis and Wilkinson [15] who suggest that *Centropyxis* is tolerant to metal pollutants.

Arsenic combines readily with other substances, and the resultant chemical compounds produce changes in pH and in biological activity. In particular, lower forms of aquatic life, such as TA, accumulate arsenic. Since they are near the bottom of the food chain, TA are excellent indicators of arsenic contamination [41]. In our case, the most sensitive genus is *Arcella*.

Patterson, et al. [39] describe the tolerance of *A. vulgaris* to arsenic. In our study we found an opposite trend for the whole *Arcella* genus, including *A. vulgaris*, see Fig. 9. *C. discoides, D. oblonga, D. bartosi and D. oviformis* have positive tolerances to arsenic. Other recent studies carried out in lakes have also identified a positive relationship between specific strains of *Arcella* and heavy metal pollution [1, 14, 39, 0].

Nguyen-Viet et al. [36] show that the richness and the total density of the TA species correlate negatively with the concentrations of lead accumulated in the moss. Our study of the ponds indicates the same trend (Fig. 9).

Iron is an essential nutrient and a component of the test of some TA species, possibly contributing to its structural rigidity. Extracellular iron deposition may be also connected with a detoxification mechanism that keeps metals (including iron) outside the cell membrane [44].

In urban mosses, Nguyen-Viet et al. [35] recorded no significant correlation between total abundance TA and concentration of iron. This agrees with our results for genus *Centropyxis*, see Fig. 10. However, we found a slight positive correlation between *Arcella* genus and higher iron concentrations. Both of these genera have been supposed to accumulate iron. By contrast, *Difflugia* showed a slightly negative correlation with iron.

CONCLUSION

The TA assemblages present in the ponds under study, composed mainly of *Arcella*, *Centropyxis* and *Difflugia* genera, showed the variability in species composition in the course of the year. In these four ponds, the most prominent changes in community composition were observed between January and June, when *Arcella* individuals were gradually replaced by *Difflugia* individuals. These changes are mainly due to different conditions of the environmental parameters in the course of the year. It is possible that the differences between the community compositions of the ponds are caused by distance from the river. Anoxic conditions may appear in more distant ponds.

The statistical analysis shows clearly that TA correlate with temperature, concentration of phosphorus, NH_4^+, NO_3^-, As, Pb, Cd, Mn, Ni, PAH and iron.

ACKNOWLEDGEMENTS

This study was supported by the Academy of Sciences of the Czech Republic (grant No. AV0Z50110509 and grant No. AV0Z50200510), Ministry of Education, Youth and Sports of the Czech Republic (research programs LC06063, MSM6840770012, MSM0021620855) and the Czech Science Foundation (P108/11/0794).

We also wish to express many thanks to David M. Wilkinson, Radek Pelc and reviewers for their fruitful comments on earlier version of the manuscript.

REFERENCES

1. Asioli A, Medioli FS, Patterson T (1996) Thecamoebians as a tool for reconstruction of paleoenvironments in some Italian lakes in the foothills of the southern Alps (Orta,Varese and Candia). J Foramin Res 26:248-263
2. Balík V (1991) The effect of the road traffic pollution on the communities of testate amoebae (rhizopoda, testacea) in Warsaw (Poland). Acta Protozool 30:5-11
3. Balík V, Song B (2000) Benthic freshwater testate amoebae assemblages (Protozoa: Rhizopoda) from Lake Dongting, People's Republic of China, with description of a new species from the Genus Collaripyxidia. Acta Protozool 39:149-156
4. Bartoš E (1954) Koreňonožce radu testacea. Vydavatelstvo Slovenskej akadémie vied, Bratislava
5. Booth RK (2002) Testate amoebae as paleoindicators of surface-moisture changes on Michigan peatlands: modern ecology and hydrological calibration. J Paleolimnol 28:329-348

6. Braak CJF ter, Šmilauer P (1998) Canoco reference manual and users guide to Canoco for Windows. Ithaca, NY:Microcomputer Power
7. Burbidge SM, Schröder-Adams CJ (1998) Thecamoebians in Lake Winnipeg: a tool for Holocene paleolimnology. J Paleolimnol 19:309-328
8. Burdíková Z, Čapek M, Ostašov P, Machač J, Pelc R, Mitchell EAD, Kubínová L (2010) Testate amoebae examined by confocal and two-photon microscopy: implications for taxonomy and ecophysiology. Microsc Microanal 16:735-746
9. Clarke KJ (2003) Guide to the identification of soil protozoa - testate amoebae. Freshwater Biological Assn.
10. Collins ES, McCarthy FMG, Medioli FS, Scott DB, Hönig CA (1990) Biogeographic distribution of modern thecamoebians in a transect along the eastern north American coast. In: Hembleden C, Kaminski M, Kuhnt W, Scott DB (eds) Paleoecology, biostratigraphy, paleoceanography and taxonomy of agglutinated foraminifera. Kluwer Academic Publishers, Dordrecht, pp 783-792
11. Charman DJ (1997) Modeling hydrological relationships of testate amoebae (Protozoa: rhizopoda) on New Zealand peatlands. J Roy Soc New Zeal 27:465-483
12. Charman DJ (2001) Biostratigraphic and palaeoenvironmental applications of testate amoebae. Quaternary Sci Rev 20:1753-1764
13. Chlupáč I, Brzobohatý R, Kovanda J, Straník Z (2011) Geologická minulost České republiky. Academia, Prague
14. Dalby AP, Kumar A, Moore JM, Patterson RT (2000) Preliminary survey of arcellaceans (thecamoebians) as limnological indicators in tropical lake Sentani, Irian Jaya, Indonesia. J Foramin Res 30:135-142
15. Davis SR, Wilkinson DM (2004) The conservation management value of testate amoebae as 'restoration' indicators: speculations based on two damaged raised mires in northwest England. Holocene 14:135-143
16. Ellison RL (1995) Paleolimnological analysis of Ullswater using testate amoebae. J Paleolimnol 13:51-63

17. Ellison RL, Ogden CG (1987) A guide to the study and identification of fossil testate amoebae in quaternary lake sediments. Int Revue ges Hydrobiol 72:639-652
18. Escobar J, Brenner M, Whitmore TJ, Kenny WF, Curtis JH (2008) Ecology of testate amoebae (thecamoebians) in subtropical Florida lakes. J Paleolim 40:715-731
19. Foissner, W (1997) Protozoa as bioindicators in agroecosystems, with emphasis on farming practices, biocides, and biodiversity. Agric Ecosyst Environ 62:93-103
20. Gilbert D, Amblard C, Boudier G, Francez AJ (1998) Short-term effect of nitrogen enrichment on the microbial communities of a peatland. Hydrobiologia 373/374:111-119
21. Golemansky V (1970) A list of testacea (Protozoa, Rhizopoda) from the Duszatynskie Lakes in Poland. Fragment faunistica 16:21-25
22. Haman D (1982) Modern thecamoebinids (Arcellinida) from the Balize Delta, Louisiana. Trans GCAGS 32:353-376
23. Heal OW (1964) Observations on the seasonal and spatial distribution of testacea (Protozoa: Rhizopoda) in Sphagnum. J Anim Ecol 33:395-412
24. Jongman RHG, Braak CJF ter, van Tongeren OFR (1995) Data analysis in community and landscape ecology. Cambridge University Press
25. Krashevska V, Maraun M, Ruess L, Scheu S (2010) Carbon and nutrient limitation of soil microorganisms and microbial grazers in a tropical montane rain forest. Oikos 119:1020-1028
26. Kumar A, Dalby AP (1998) Identification key for Holocene lacustrine arcellacean (thecamoebian) taxa. Paleontological Society. http://www.uic.edu/orgs/paleo/homepage.html. Accessed 10 March 2010
27. Lorencová M (2009) Thecamoebians from recent lake sediments from the Šumava Mts, Czech Republic. B Geosci 84:359-376
28. Lamentowicz Ł, Gąbka M, Lamentowicz M (2007) Testate amoebae (Protists) of peatland: species composition and environmental parameters. Polish Journal of Ecology 55:749-759
29. Medioli FS, Scott DB (1983) Holocene Arcellacea (Thecamoebians) from eastern Canada. Cushman Foundation, Washington D.C.

30. Medioli FS, Scott DB (1988) Lacustrine thecamoebians (mainly Arcellaceans) as potential tools for palaeolimnological interpretations. *Palaeogeogr Palaeoclimatol Palaeoecol* 62:361-386
31. Medioli FS, Scott DB, Collins ES, McCarthy FMG (1990) Fossil thecamoebians: present status and prospects for the future. In: Hemleben C, Kaminski MA, Kuhnt W, Scott DB (Eds.) Paleoecology, Biostratigraphy, Paleoceanography and Taxonomy of Agglutinated Foraminifera. NATO Advanced Study Institute Series, Series C, Mathematical and Physical Science 327, pp 813-840
32. Mitchell EAD, Buttler AJ, Warner BG, Gobat JM (1999) Ecology of testate amoebae (Protozoa: Rhizopoda) in Sphagnum peatlands in the Jura Mountains, Switzerland and France. Ecoscience 6:565-576
33. Mitchell EAD, Gilbert D (2004) Vertical micro-distribution and response to nitrogen deposition of testate amoebae in Sphagnum. J Eukaryot Microbiol 51:480-490
34. Morcazewski J (1961) Testacea du littoral peu profond du lac Kisajno (Region des lacs de mazurie). Pol Arch Hydrobiol 9:175-194
35. Nguyen-Viet H, Bernard N, Mitchell EAD, Cortet J, Badot PM, Gilbert D (2007) Relationship between testate amoeba (Protist) communities and atmospheric heavy metals accumulated in Barbula indica (Bryophyta) in Vietnam. Microb Ecol 53:53-65
36. Nguyen-Viet H, Bernard N, Mitchell EAD, Badot PM, Gilbert D (2008) Effect of lead pollution on testate amoebae communities living in Sphagnum fallax: An experimental study. Ecotox Environ Safe 69:130-138
37. Ogden CG (1983) Observations on the systematics of the genus Difflugia in Britain (Rhizopoda, Protozoa). Bull Br Mus nat Hist (Zool) 44:1-73
38. Ogden CG, Hedley RH (1980) An atlas of freshwater testate amoebae. Oxford University Press, Publication No 814
39. Patterson RT, Barker T, Burbidge SM (1996) Arcellaceans (Thecamoebians) as proxies of arsenic and mercury contamination in northeastern Ontario lakes. J Foramin Res 26:172-183

40. Patterson RT, Kumar A (2000) Assessment of arcellacean (thecamoebian) assemblages, species, and strains as contaminant indicators in James Lake, northeastern Ontario, Canada. J Foramin Res 30:310-320
41. Patterson RT, Kumar A (2002) A review of current testate rhizopod (thecamoebian) research in Canada. *Palaeogeogr Palaeoclimatol Palaeoecol* 180:225-251
42. Patterson RT, MacKinnon KD, Scott DB, Medioli FS (1985) Arcellaceans (Thecamoebians) in small Lakes of New Brunswick and Nova Scotia: Modern distribution and Holocene stratigraphic changes. J Foraminifer Res 15:114-137
43. Payne R, Mitchell E (2007) Ecology of testate amoebae from mires in the Central Rhodope Mountains, Greece and development of a transfer function for paleohydrological reconstruction. Protist 158:159-171
44. Payne JP (2011) Can testate amoeba-based palaeohydrology be extended to fens? J Quaternary Sci 26:15-27
45. Qin Y, Booth RKK, Gu Y, Wang Y, Xie S (2009) Testate amoebae as indicators of 20th century environmental change of Lake Zhangdu, China. Fund Appl Limnol 175:29-38
46. Reinhardt ED, Daldy AP, Kumar A, Patterson RT (1998) Arcellaceans as pollution indicators in mine tailing contaminated lakes near Cobalt, Ontario, Canada. Micropaleontology 44:131-148
47. Roe HM, Patterson RT (2006) Distribution of thecamoebians (testate amoebae) in small lakes and ponds, Barbados, West Indies. J Foram Res 36:116-134
48. Roe HM, Patterson RT, Swindles GT (2010) Controls on the contemporary distribution of lake thecamoebians (testate amoebae) within the Greater Toronto Area and their potential as water quality indicators. J Paleolimnol 43:955-975
49. Sageman BB, Bina CR (1997) Diversity and species abundance patterns in Late Cenomanian black shale biofacies, Western Interior, US. Palaios 12:449-466
50. Schönborn W (1990) Shell polymorphism and habitat structure in testacea (Rhizopoda). J Protozool 37:62A

51. Scott DB, Medioli FS (1983) Agglutinated rhizopods in Lake Erie: modern distribution and stratigraphic implication. J Paleontol 57:809-820
52. Scott DB, Medioli FS, Schafer CT (2001) Monitoring in coastal environments using foraminifera and thecamoebian indicators. Cambridge University Press, Cambridge
53. Swindles GT, Roe HM (2007) Examining the dissolution characteristics of testate amoebae (Protozoa:Rhizopoda) in low pH conditions: Implications for peatland palaeoclimate studies. Palaeogeogr Palaeocl 252:486-496
54. Štěpánek M, Veselý J, Majer V (1992) The major importance of nitrate increase for the acidification of two lakes in Bohemia. Documenta Dell'Istituto Italiano Di Idrobiologia 32:83-92
55. Vohník M, Burdíková Z, Albrechtová J, Vosátka M (2009) Testate amoebae (Arcellinida and Euglyphida) vs. Ericoid mycorrhizal and DSE fungi: A possible novel interaction in the mycorrhizosphere of ericaceous plants? Microb Ecol 57:203-214
56. Vohník M, Burdíkova Z, Vyhnal A, Koukol O (2011) Interactions between testate amoebae and saprotrophic microfungi in a Scots pine litter microcosm. Microb Ecol 61:660-668
57. Wall AAJ, Magny M, Mitchell EAD, Vanniere B, Gilbert D (2010) Response of testate amoeba assemblages to environmental and climatic changes during the Lateglacial–Holocene transition at Lake Lautrey (Jura Mountains, eastern France). J Quaternary Sci 25:945-956
58. Warner BG, Asada T, Quinn NP (2007) Seasonal influences on the ecology of testate amoebae (Protozoa) in a small sphagnum peatland in Southern Ontario, Canada. Microb Ecol 54:91-100

TABLES

Table 1: Coordinates and basic parameters of the Komořany ponds.

Pond No.	Coordinates (pond centers)	Area [m^2]	Distance from the river Vltava [m]	Sediment composition: organic material / sand / clay
1	49°59'16.923"N, 14°24'4.860"E	1122	8	50% / 25% / 25%
2	49°59'18.823"N, 14°24'6.042"E	1350	36	50% / 25% / 25%
3	49°59'21.039"N, 14°24'5.663"E	1677	25	70% / 25% / 5%
4	49°59'22.836"N, 14°24'5.565"E	1404	32	50% / 25% / 25%

Table 2: Abundances of TA species in samples of 20 cm^3 taken from the four Komořany ponds in 2004 - 5.

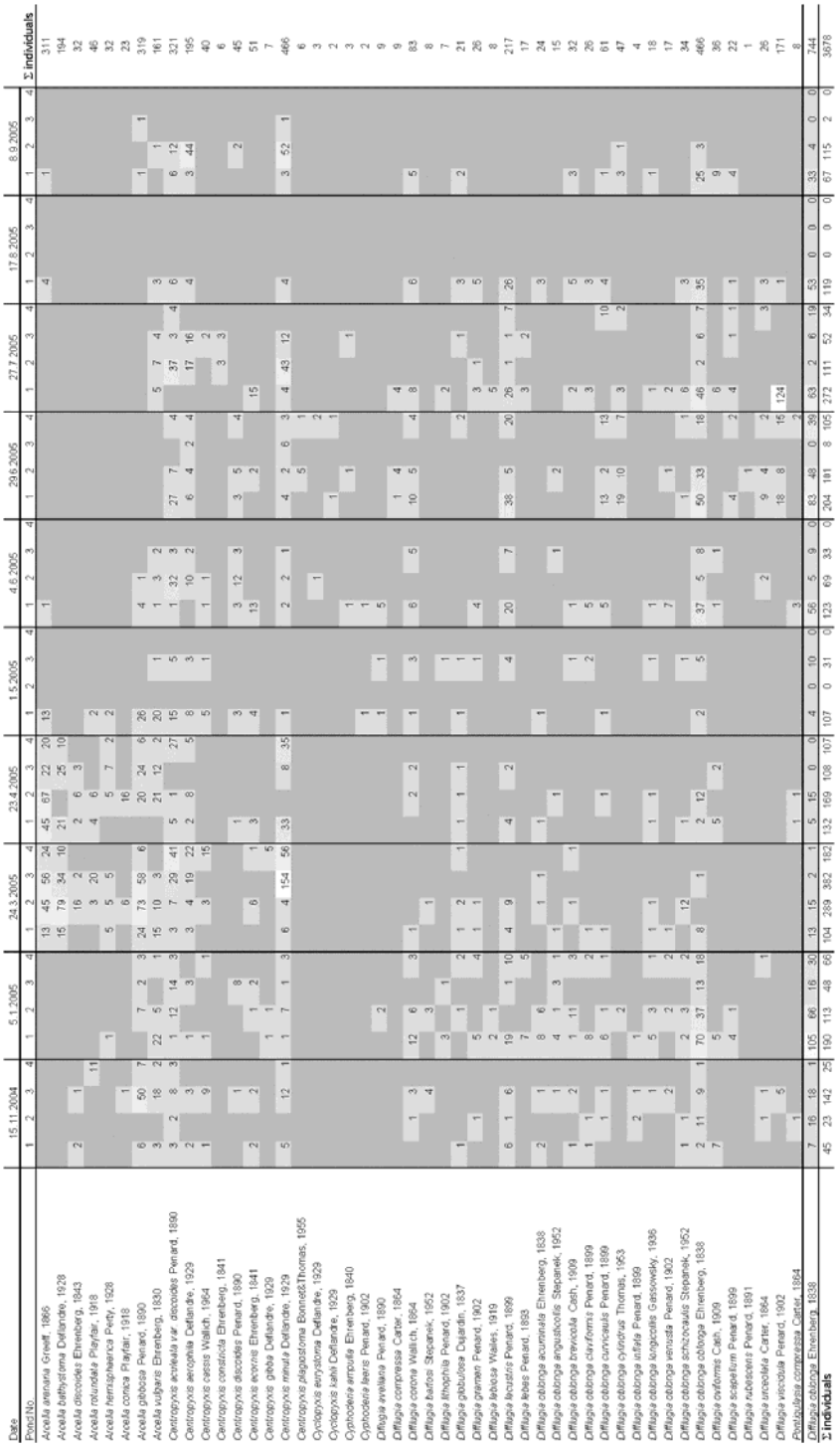

Date	15.11.2004				5.1.2005				24.3.2005				23.4.2005				1.5.2005				4.6.2005				29.6.2005				27.7.2005				17.8.2005				8.9.2005				Σ individuals
Pond No.	1	2	3	4	1	2	3	4	1	2	3	4	1	2	3	4	1	2	3	4	1	2	3	4	1	2	3	4	1	2	3	4	1	2	3	4	1	2	3	4	
Arcella arenaria Greeff, 1866									13	45	56	24	45	67	22	20	13				1												4				1				311
Arcella bathystoma Deflandre, 1928									15	79	34	10	21		25	10																									194
Arcella discoides Ehrenberg, 1843		2		1						16	2		2	6	3																									32
Arcella rotundata Playfair, 1918								11			3	20	4	6			2																							46
Arcella hemisphaerica Perty, 1928					1				5	5	5			5	7	2	2																							32
Arcella conica Playfair, 1918				1						6			16																											23
Arcella gibbosa Penard, 1890	6		50	7		7	2	3	24	73	58	6		20	24	6	26				4	1														1			1	319
Arcella vulgaris Ehrenberg, 1830	3		18	2	22	5		1	15	10	3		21	12	2	20		1			1	3	2						5	7	4		3						161
Centropyxis aculeata var. discoides Penard, 1890	3	2	8	3	1	12	14	3	3	7	29	41	5	1		27	15				1	32	3		27	7		4		37	3	4	6				6	12		321
Centropyxis aerophila Deflandre, 1929	2		3			3			3	4	19	22	2	8		5	8	3				10	2		6	4	2	4		17	16		4				3	44		195
Centropyxis cassis Wallich, 1864	1		9		1		3			3		15					5	1			1	1								3	3									40
Centropyxis constricta Ehrenberg, 1841																															2									6
Centropyxis discoides Penard, 1890			1				8						1				3				3	12	3		3	5		4								2				45
Centropyxis ecornis Ehrenberg, 1841	2		2			1	2			6		1	3				4				13					2			15										51
Centropyxis globa Deflandre, 1929					1	1						5																											7
Centropyxis minuta Deflandre, 1929	5		12	1	1	7	1	3	6	4	154	56	33		8	35	1				2	2	1		4	2	6	3	4	43	12		4				3	52	1	466
Centropyxis plagiostoma Bonnet&Thomas, 1955																									4	5		1												6
Cyclopyxis eurystoma Deflandre, 1929																					1							2												3
Cyclopyxis kahli Deflandre, 1929																												1												2
Cyphoderia ampulla Ehrenberg, 1840																					1				1															3
Cyphoderia lens Penard, 1902																	1				1										1									2
Difflugia avellana Penard, 1890						2											1				5																			9
Difflugia compressa Carter, 1864																	1								1	4			4											9
Difflugia corona Wallich, 1864		1	3		12	6			3		1			2	2		1		3		6		5		10	5		4	8			6				5				83
Difflugia flatosi Stepanek, 1952			4			3						1																											8
Difflugia khophlia Penard, 1902					3		1																						2										7
Difflugia globulosa Dujardin, 1837	1					1		2	1	2		1	1	1	1		1		1							2				1		3				2				21
Difflugia gramen Penard, 1902		1			5			4	1	1							1				4								3	1		5							26
Difflugia lebosa Wailes, 1919					2	1																							5										8
Difflugia lecudsta Penard, 1899	6	1	6		19		1	10	4	9			4	2			4				20	7			38	5			20	26	1	1	7	26						217
Difflugia lebes Penard, 1893					7			5																						3	2									17
Difflugia oblonga acuminata Ehrenberg, 1838	2		1		8	6			1	1			1				1																3							24
Difflugia oblonga angustiostis Stepanek, 1952			1		4	1	3	1	1					1						1					2														15
Difflugia oblonga brevicolla Cash, 1909	1		2		1	11		3	1			1						1			1							2				5			3				32
Difflugia oblonga claviformis Penard, 1899	1	1			8			2	1									2			5							3				3							26
Difflugia oblonga curvicaulis Penard, 1899		1	1		6	1		1	1						1		1				5				13	2					10	4			1				61
Difflugia oblonga cylindrus Thomas, 1953						2																			19	10			7	3		2				3	1		47
Difflugia oblonga ulkifa Penard, 1899		2	1		1																																		4
Difflugia oblonga longicollis Gassowsky, 1936			1		5	3		1	1	1			1	1			1				1					1			1							1				18
Difflugia oblonga venusta Penard, 1902			2			2			1												7					1			2										17
Difflugia oblonga schizocaulis Stepanek, 1952	1	1			2	3		2	1	2			1				1								1				6				3						34
Difflugia oblonga oblonga Ehrenberg, 1838	2	11	9	1	70	37	13	18	8		1		2	12			2		5		37	5	8		50	33			18	46	2	6	7	35			25	3		466
Difflugia oviformis Cash, 1909	7				5								5		2						1		1						6							9				35
Difflugia scapetum Penard, 1899					4	1																			4				2	4		1	1	1		4				22
Difflugia rubescens Penard, 1891																										1														1
Difflugia urceolata Carter, 1864		1	1								1										2				9	4			2			3	3							26
Difflugia viscidula Penard, 1902			5																						18	8			15	124			1							171
Pontigulasia compressa Carter, 1864		1																			3								2											8
Difflugia oblonga Ehrenberg, 1838	7	16	18	1	105	66	16	30	13	15	2	1	5	15	0	0	4	0	10	0	56	5	9	0	83	48	0	39	63	2	6	19	53	0	0	0	33	4	0	0	744
Σ individuals	45	23	142	25	190	113	48	66	104	269	382	182	132	169	108	107	107	0	31	0	123	69	33	0	204	181	8	105	272	111	52	34	119	0	0	0	67	115	2	0	3678

Table 3: Parameters and results of a redundancy analysis of the TA data showing co-variables, eigenvalues/traces, F values and significances of Monte-Carlo permutation test results (P), determined using Canoco software.

No	Explanatory variables	Co-variables	Monte-Carlo test of first canonical axis			Monte-Carlo test of all canonical axes		
			Eigenvalue	F	P	Trace	F	P
1	Temperature	Ponds	-	-	-	0.080	3.294	0.002
2	Temperature	None	-	-	-	0.051	1.834	0.090
3	Phosphorus	None	-	-	-	0.061	2.199	0.046
4	NH_4^+, NO_3^-	None	0.084	3.03	0.020	0.094	1.707	0.046
5	As, Pb, Cd, Mn, Ni, PAH	None	0.154	5.26	0.016	0.265	1.741	0.004
6	Iron	None	-	-	-	0.067	2.423	0.020

FIGURES

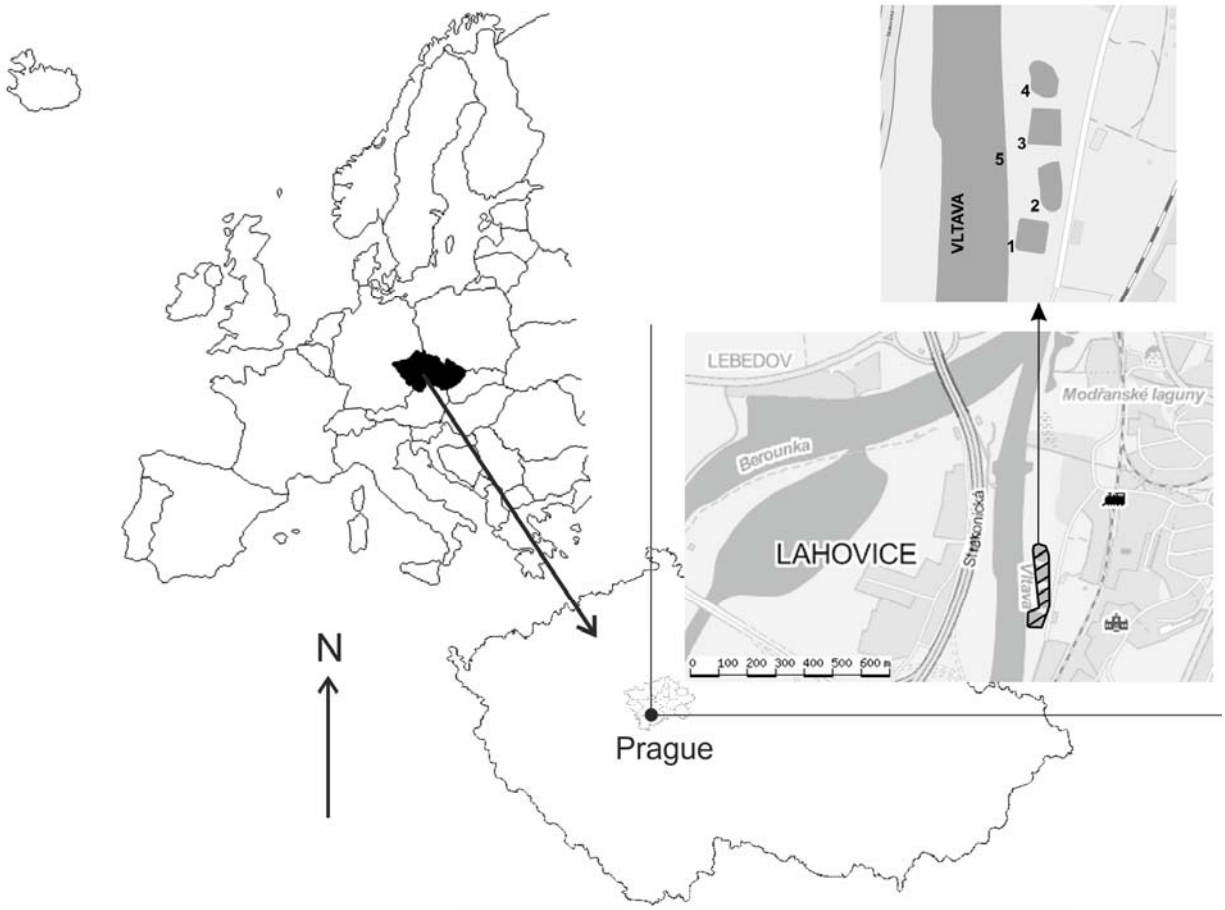

Figure 1: The Komořany ponds in Prague, Czech Republic. The five sampling places – four ponds and the Vltava – are numbered in the image on the upper right.

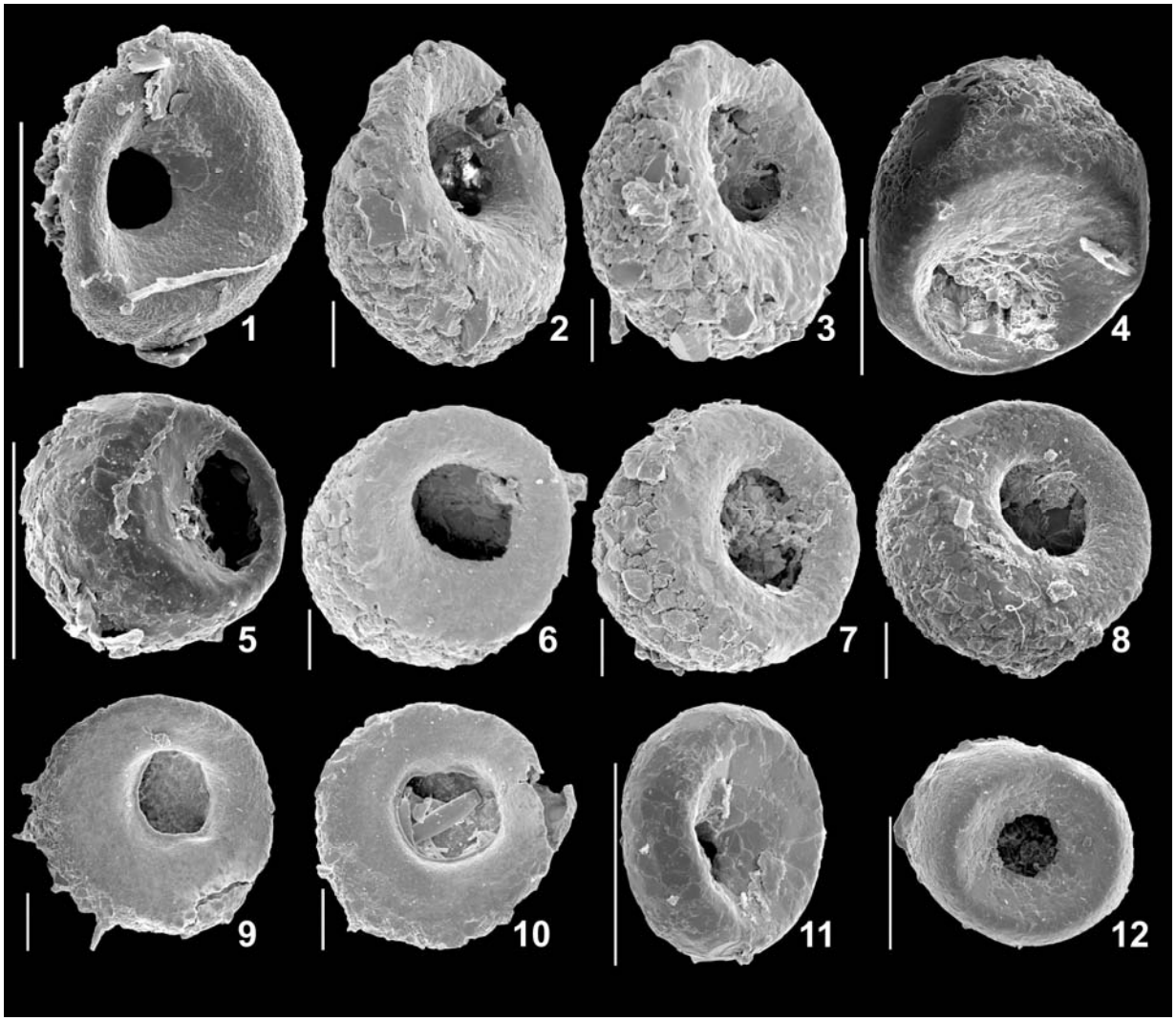

Figure 2: Testate amoebae found and identified in the samples from the Komořany ponds; acquired by SEM; the bars correspond to 50 µm: (1) *Arcella discoides*, (2) *Centropyxis* (*C.*) *constricta*, (3) *C. constricta*, (4) *C. constricta*, (5) *C. cassis*, (6) *C. ecormis*, (7) *C. ecormis*, (8) *C. ecormis*, (9) *C. discoides*, (10) *C. discoides*, (11) *C. plagiostoma*, (12) *Cyclopyxis kahli*.

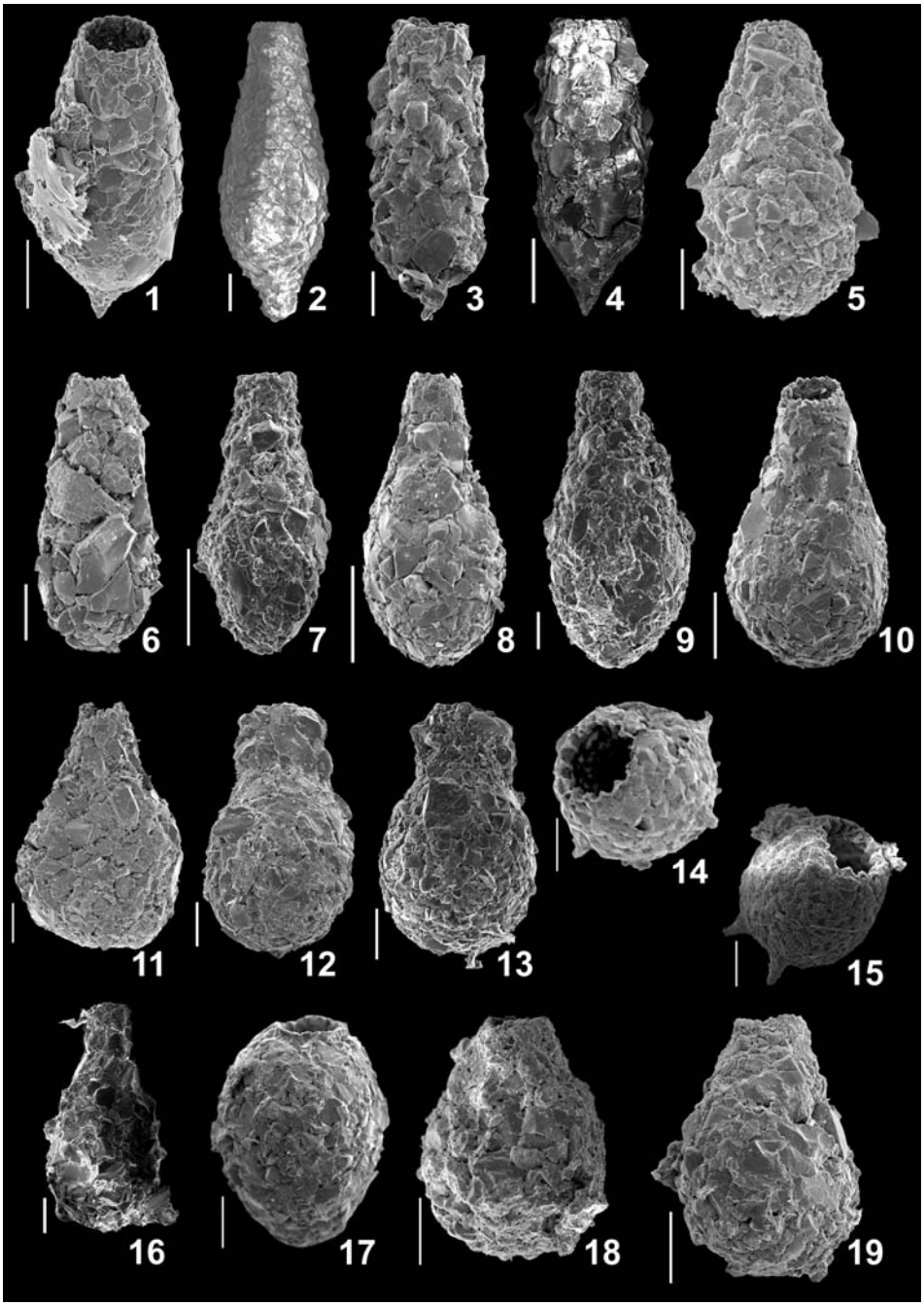

Figure 3: Testate amoebae found and identified in the samples from the Komořany ponds; acquired by SEM; the bars correspond to 50 µm: (1) *Difflugia* (*D.*) *oblonga acuminata*, (2) *D. oblonga claviformis*, (3) *D. oblonga acuminata*, (4) *D. scalpellum*, (5) *D. lacustris*, (6) *D. lacustris*, (7) *D. venusta*, (8) *D. oblonga*, (9) *D. oblonga*, (10) *D. oblonga*, (11) *D. oblonga*, (12) *D. oblonga*

var. *cylindrus*, (13) *D. oblonga* var. *cylindrus*, (14) *D. corona*, (15) *D. corona*, (16) *D. oblonga longicollis*, (17) *D. labiosa*, (18) *Pontigulasia compressa*, (19) *Pontigulasia compressa*.

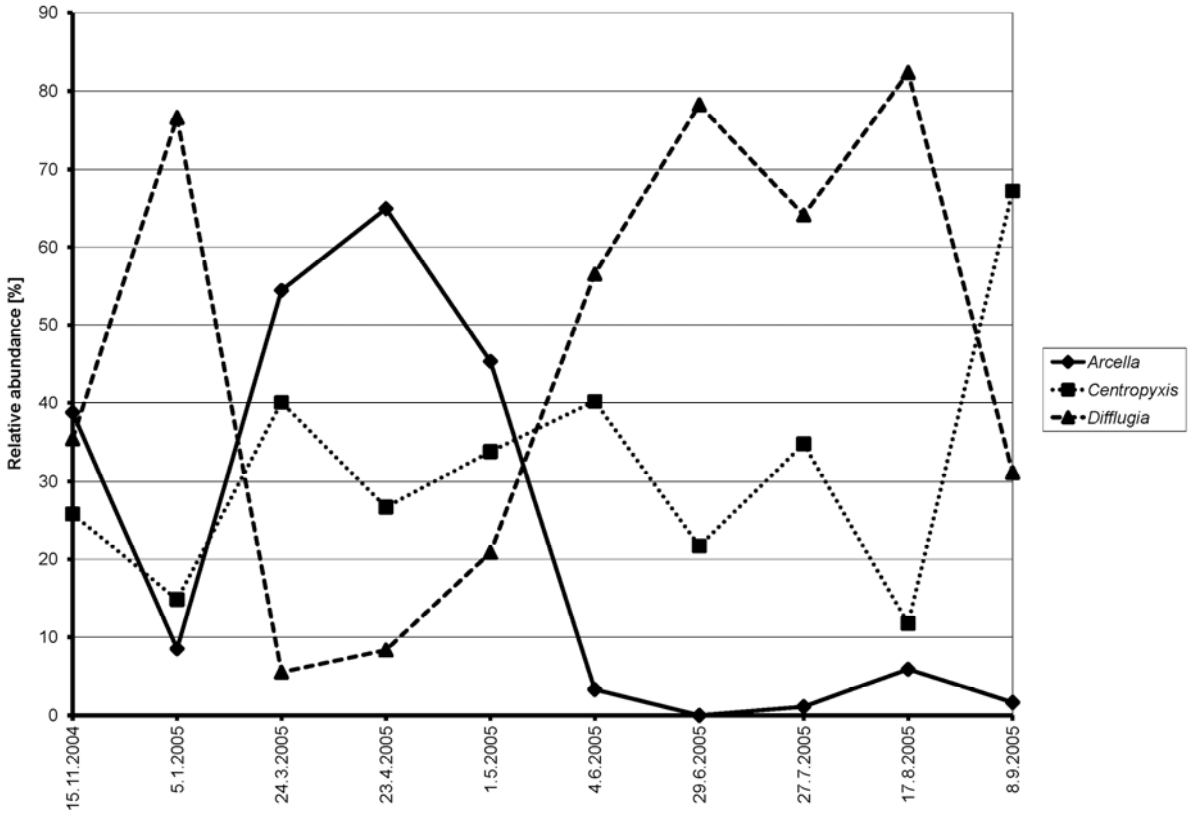

Figure 4: Relative abundances [%] of three main genera – *Arcella*, *Centropyxis* or *Difflugia* – found in samples, summarized for all ponds.

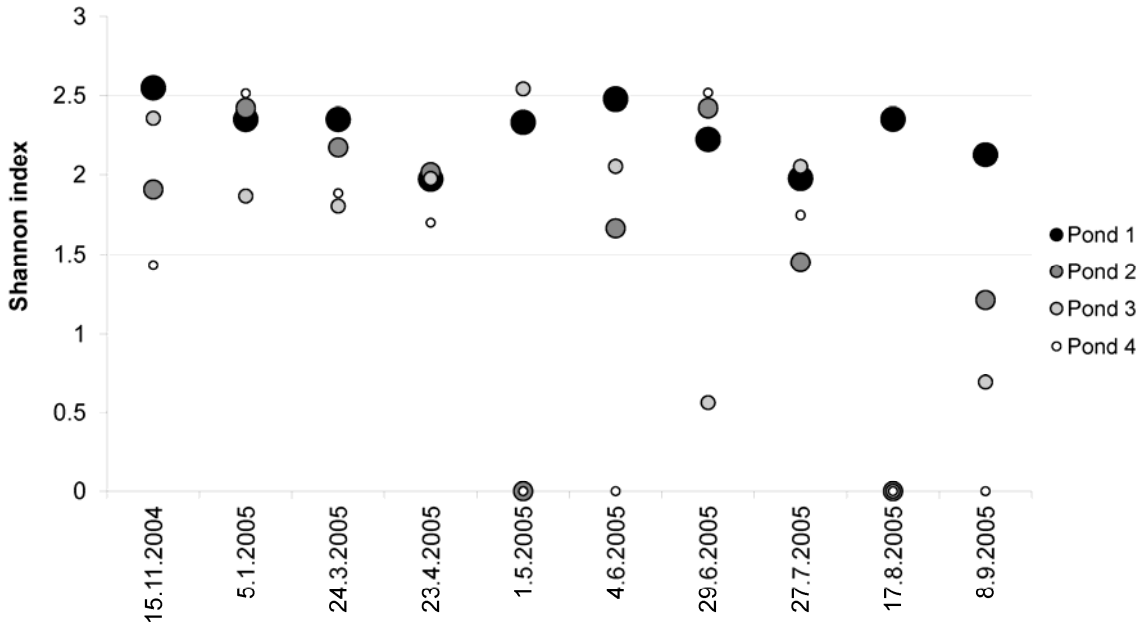

Figure 5: Shannon index of diversity for each sampling date and for each pond during the observation period.

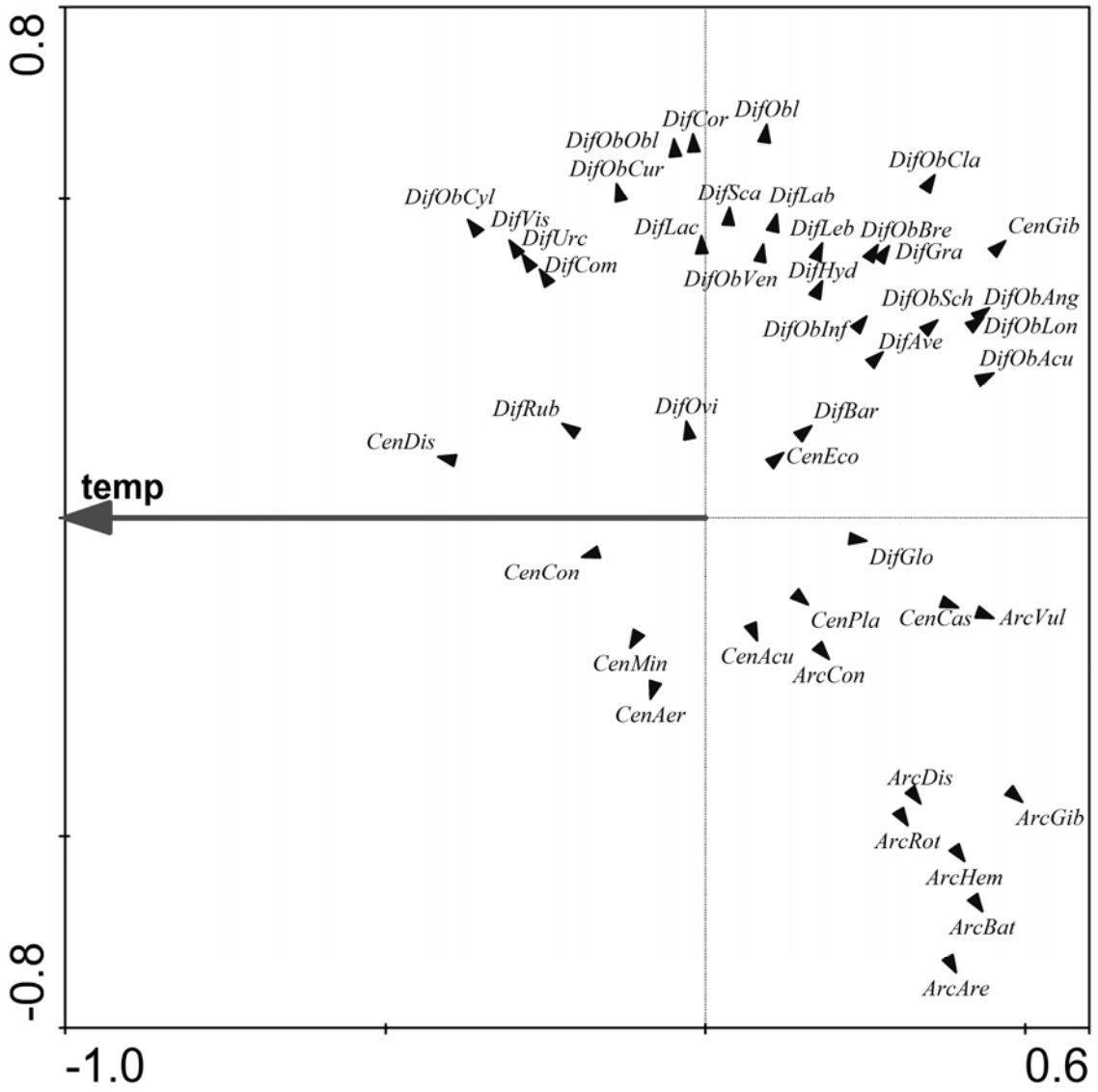

Figure 6: A graphic evaluation of the dependence of TA on temperature, using multivariate redundancy analysis. The length of the projections of arrows with TA names on the **temp** axis indicates the measure of their dependence on temperature. According to this plot, for example, *C. discoides* (CenDis) is the species that is most positively dependent on temperature, while *A. gibbosa* (ArcGib) is the species that is most negatively dependent. Abbreviations: ArcAre, *A. arenaria*; ArcBat, *A. bathystoma*; ArcDis, *A. discoides*; ArcRot, *A. rotundata*; ArcHem *A. hemisphaerica*; ArcCon, *A. conica*; ArcGib, *A. gibbosa*; ArcVul, *A. vulgaris*; CenAcu, *C. aculeata*

var. *discoides*; CenAer, *C. aerophila*; CenCas, *C. cassis*; CenCon, *C. constricta*; CenDis, *C. discoides*; CenEco, *C. ecornis*; CenGib, *C. gibba*; CenMin, *C. minuta*; CenPla, *C. plagiostoma*; DifAve, *D. avellana*; DifCom, *D. compressa*; DifCor, *D. corona*; DifBar, *D. bartosi*; DifHyd, *D. lithophila*; DifGlo, *D. globulosa*; DifGra, *D. gramen*; DifLab, *D. labiosa*; DifLac, *D. lacustris*; DifLeb, *D. lebes*; DifObAcu, *D. oblonga acuminata*; DifObAng, *D. oblonga angusticollis*; DifObBre, *D. oblonga brevicolla*; DifObCla, *D. oblonga claviformis*; DifObCur, *D. oblonga curvicaulis*; DifObCyl, *D. oblonga cylindrus*; DifObInf, *D. oblonga inflata*; DifObLon, *D. oblonga longicollis*; DifObVen, *D. oblonga venusta*; DifObSch, *D. oblonga schizocaulis*; DifObObl, *D. oblonga oblonga*; DifObl, *D. oblonga* (summarizes all variants of *D. oblonga* together); DifOvi, *D. oviformis*; DifSca, *D. scapellum*; DifRub, *D. rubescens*; DifUrc, *D. urceolata*; DifVis, *D. viscidula*.

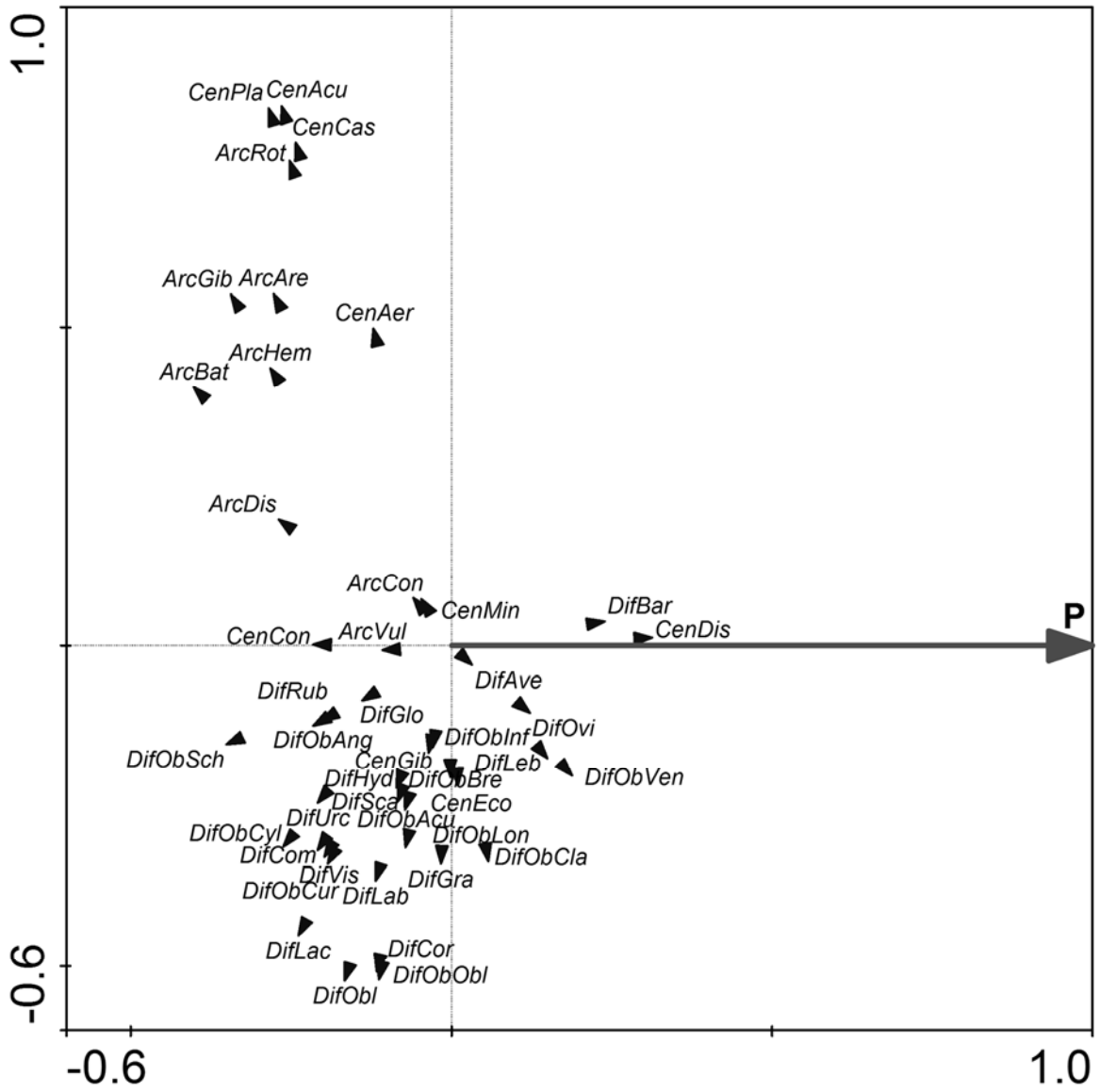

Figure 7: Plot of a multivariate redundancy analysis of the dependency of TA on phosphorus (P).

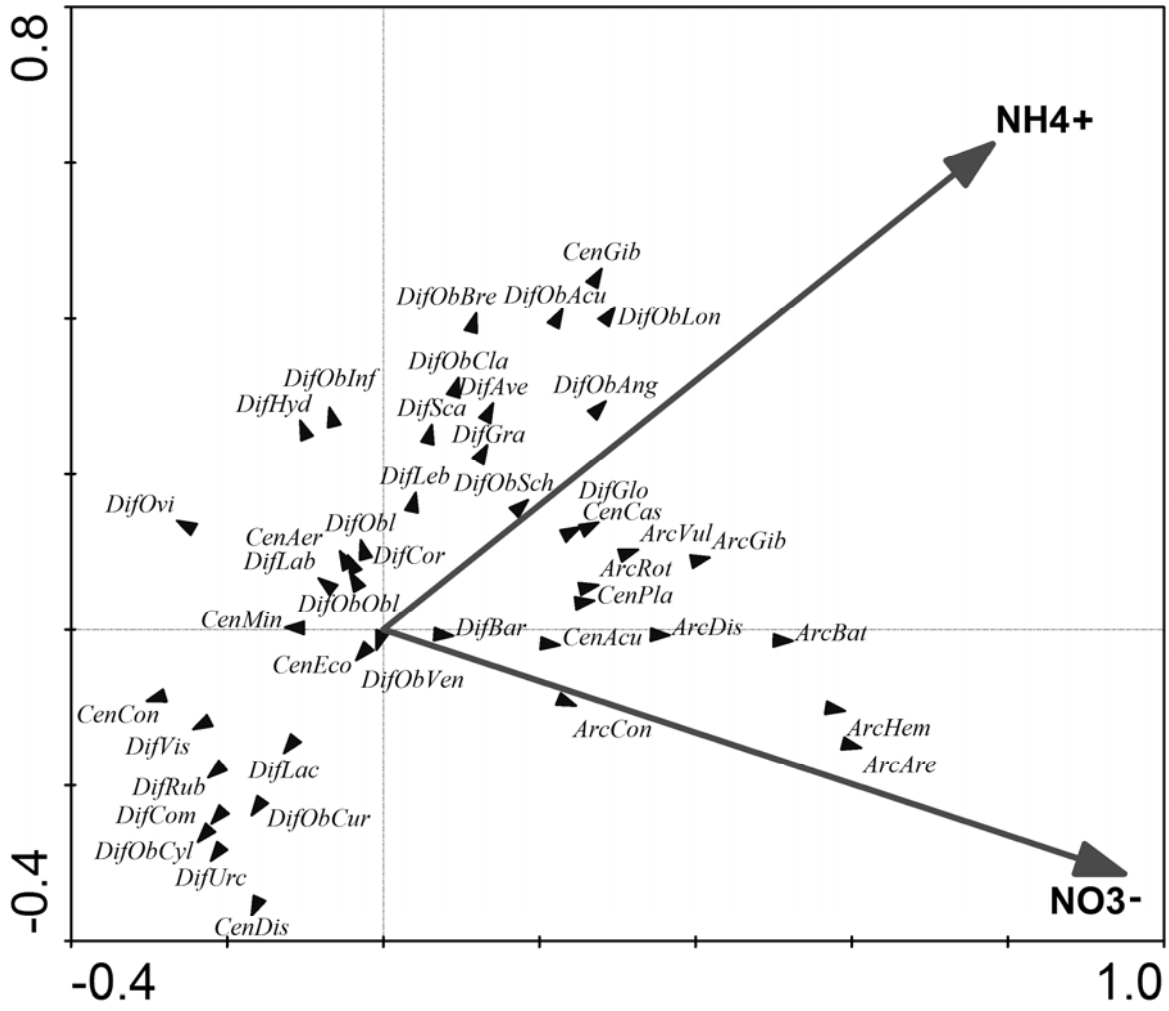

Figure 8: Plot of a multivariate redundancy analysis of the dependency of TA on nitrogen.

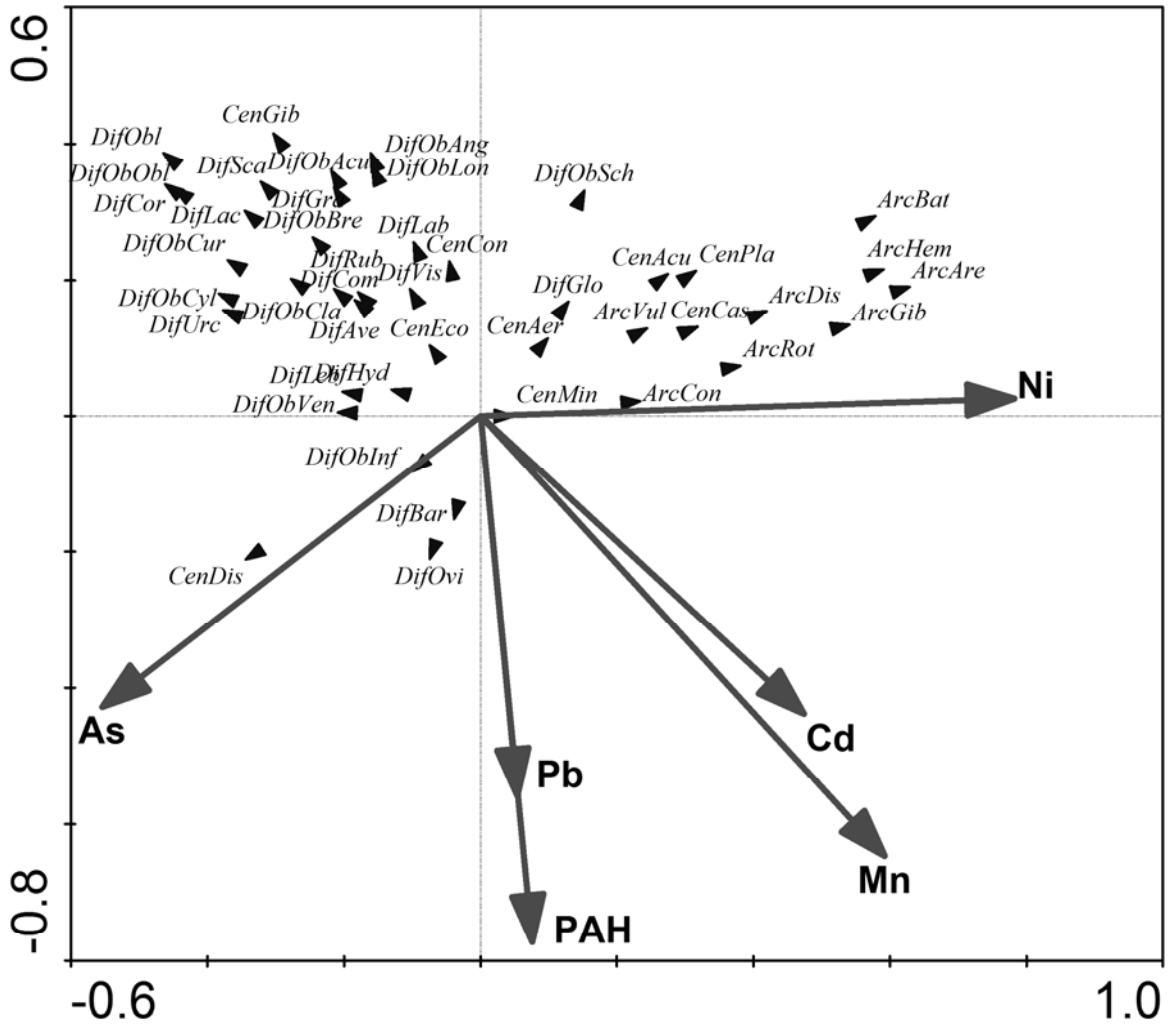

Figure 9: Plot of a multivariate redundancy analysis of the dependency of TA on pollutants and heavy metals.

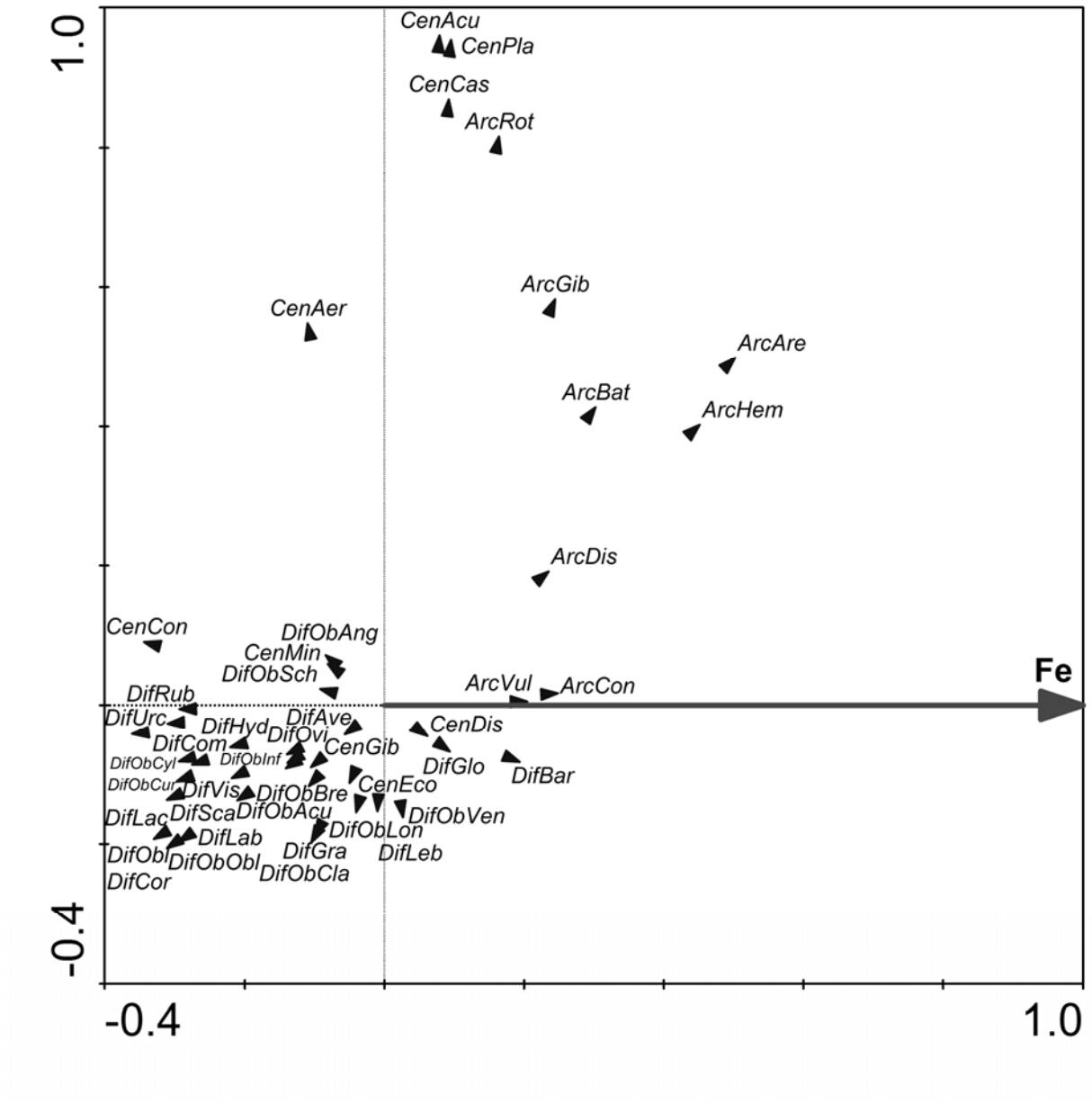

Figure 10: Plot of a multivariate redundancy analysis of the dependency of TA on iron (Fe).

date	temperature [°C]	pH	electrolytic conductivity [mS/m]	organic carbon [mg/l]	ammoniac nitrogen [mg/l]	nitrate nitrogen [mg/l]	total phosphorus [mg/l]	chlorides [mg/l]	sulphates [mg/l]	calcium [mg/l]
15.11.2004	8.2200	8.1272	34.2680	7.5272	0.0596	2.3600	0.1325	23.8720	44.0840	36.0000
5.1.2005	3.8682	7.4732	33.7832	6.3084	0.1107	3.6101	0.1264	23.9017	46.2017	34.1006
24.3.2005	5.3584	7.5614	30.5227	7.5908	0.0955	4.3908	0.0917	21.4068	42.4497	32.0000
23.4.2005	10.3110	7.6515	31.8011	8.1059	0.0663	4.1853	0.1439	25.3061	44.7756	35.7747
1.5.2005	11.6259	7.6764	32.3836	8.2058	0.0596	3.9356	0.1647	27.1038	45.4913	37.6057
4.6.2005	16.2201	8.1929	31.6876	8.7880	0.0364	3.2360	0.1846	28.0072	44.3234	37.5991
29.6.2005	17.1075	8.6545	26.4073	9.1615	0.0300	3.1384	0.1119	19.3227	37.9228	27.2381
27.7.2005	15.8466	7.5444	23.6588	8.3740	0.0347	2.4836	0.1078	16.8657	35.4645	26.1668
17.8.2005	15.9665	7.4609	25.4526	7.2792	0.0499	2.0977	0.0830	18.3688	33.6248	31.0000
8.9.2005	18.2268	7.3986	28.6483	8.6822	0.0577	2.2536	0.1477	20.4732	38.6911	31.0000

date	magnesium [mg/l]	PAH [ng/l]	chrome [µg/l]	total manganese [mg/l]	iron [mg/l]	nickel [µg/l]	copper [µg/l]	cadmium [µg/l]	lead [µg/l]	arsenic [µg/l]
15.11.2004	9.0160	41.9919	0.9872	0.0852	0.2604	2.1904	2.4848	0.1236	1.3008	4.1664
5.1.2005	9.4916	21.1212	0.8933	0.0502	0.3117	2.7916	2.6849	0.0885	1.5832	2.9849
24.3.2005	8.0000	16.7835	1.1749	0.1007	0.4488	5.2903	2.9749	0.0993	1.4546	1.5319
23.4.2005	8.3432	30.7135	1.4627	0.1234	0.5575	6.0303	3.8461	0.1177	2.2265	1.7461
1.5.2005	8.5096	36.5892	1.3962	0.1251	0.5708	5.4144	4.0625	0.1361	2.6759	1.9625
4.6.2005	8.2799	38.7054	0.9480	0.1120	0.4732	2.9519	3.9439	0.1216	3.0638	2.6720
29.6.2005	6.7922	13.5469	0.5000	0.0823	0.2208	1.9154	2.4153	0.0162	1.4231	2.6846
27.7.2005	6.0767	17.4416	0.4302	0.0807	0.1574	2.2069	1.8000	0.0537	1.1508	2.3233
17.8.2005	5.9769	9.8716	0.1942	0.0492	0.0466	1.9012	1.7931	-0.0007	-0.0278	2.3792
8.9.2005	7.5357	18.5233	0.5839	0.1038	0.2727	1.8232	2.2607	0.0461	1.8429	3.7822

Table S1: Environmental variables of water from the Vltava river on the sampling dates.

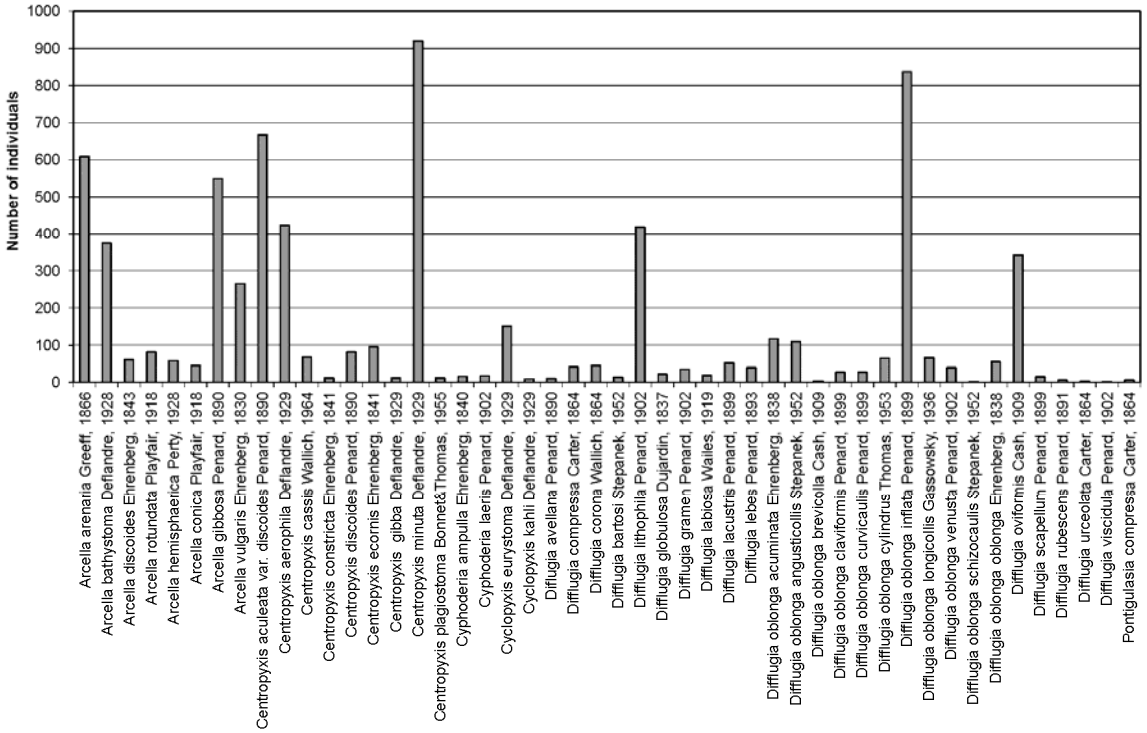

Figure S2: Total numbers of testate amoebae individuals found during the observed period, sorted by species.

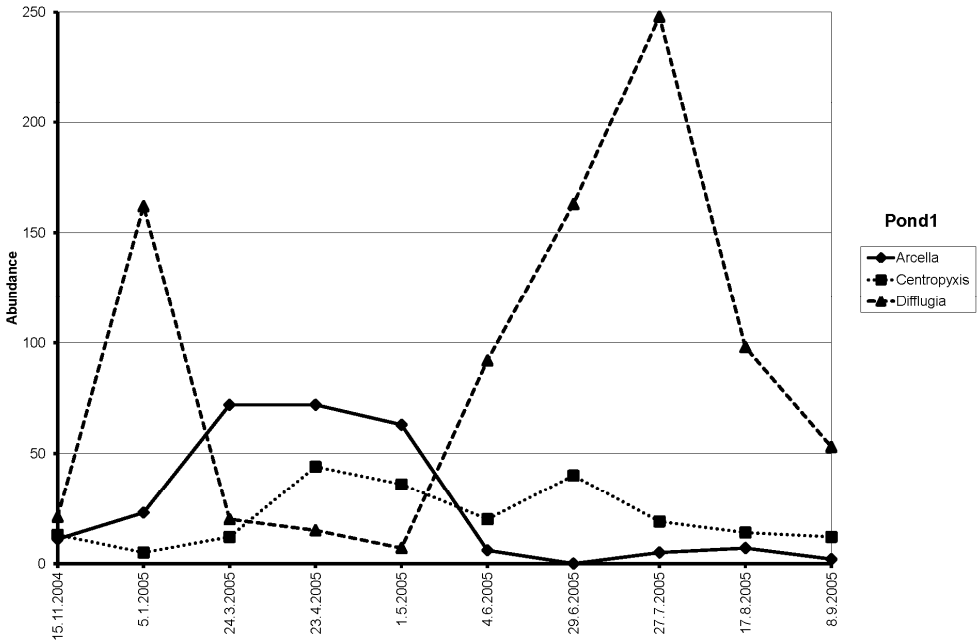
Pond1
Abundance
250
200
150
100
50
0
15.11.2004
5.1.2005
24.3.2005
23.4.2005
1.5.2005
4.6.2005
29.6.2005
27.7.2005
17.8.2005
8.9.2005
Arcella
Centropyxis
Difflugia

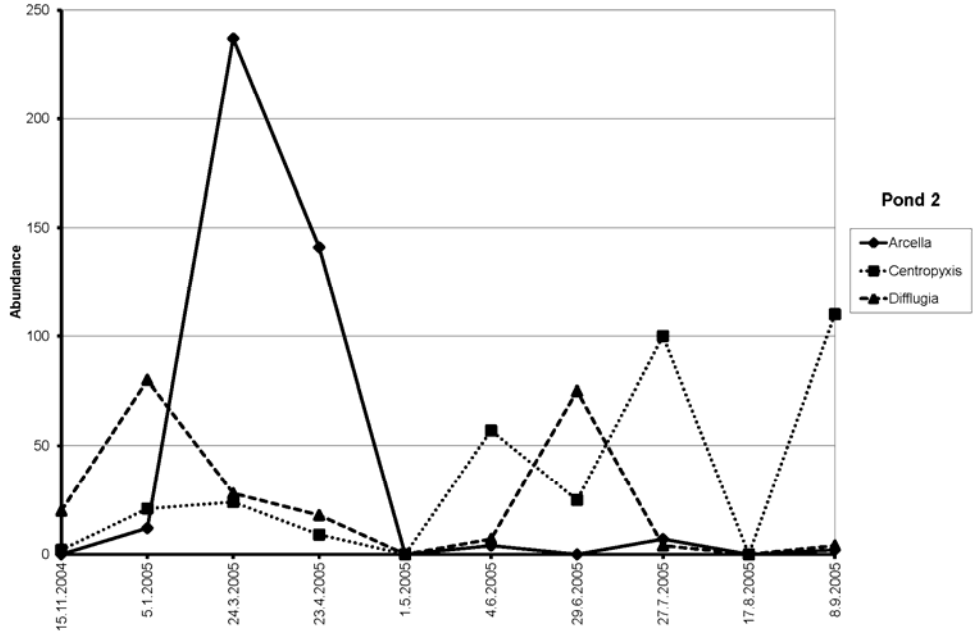
Pond 2
Abundance
250
200
150
100
50
0
15.11.2004
5.1.2005
24.3.2005
23.4.2005
1.5.2005
4.6.2005
29.6.2005
27.7.2005
17.8.2005
8.9.2005
Arcella
Centropyxis
Difflugia

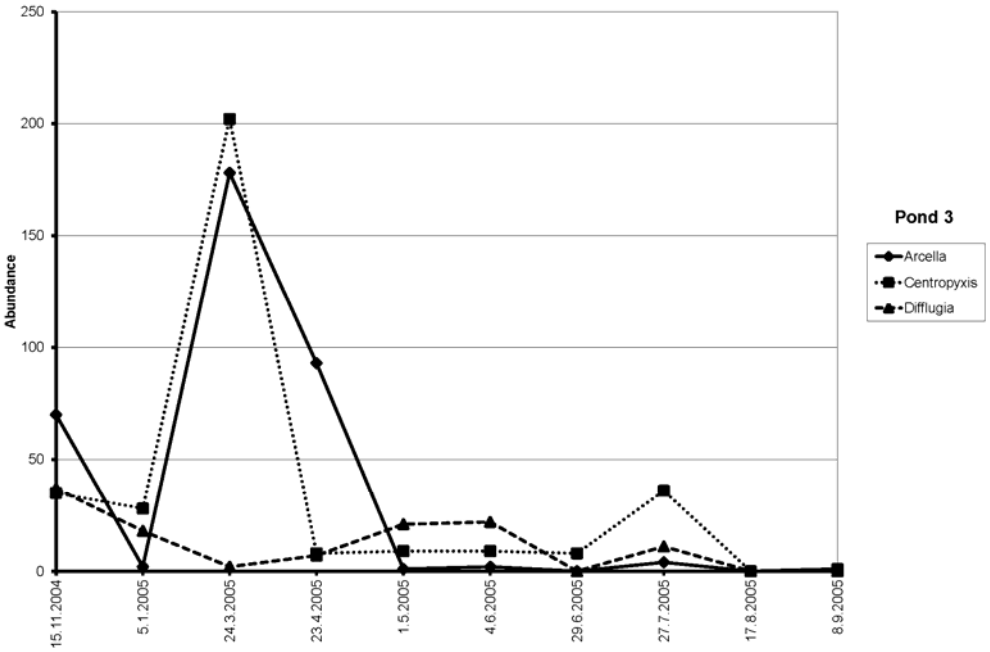
Pond 3
Abundance
250
200
150
100
50
0
15.11.2004
5.1.2005
24.3.2005
23.4.2005
1.5.2005
4.6.2005
29.6.2005
27.7.2005
17.8.2005
8.9.2005
Arcella
Centropyxis
Difflugia

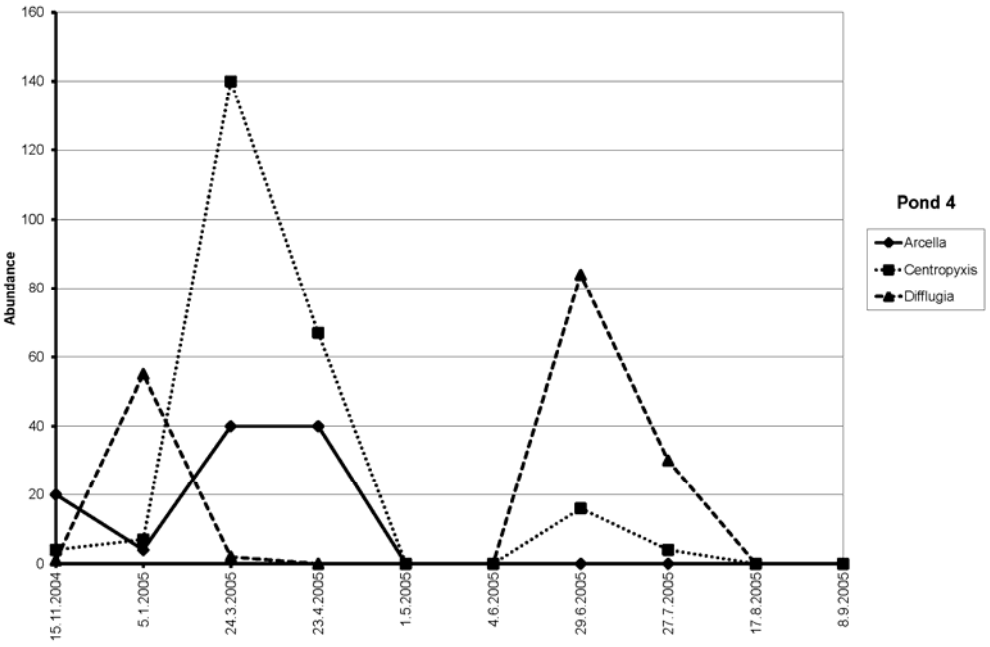
Pond 4
Abundance
160
140
120
100
80
60
40
20
0
15.11.2004
5.1.2005
24.3.2005
23.4.2005
1.5.2005
4.6.2005
29.6.2005
27.7.2005
17.8.2005
8.9.2005
Arcella
Centropyxis
Difflugia

Figure S3: Abundances and seasonal variability of genera *Arcella*, *Centropyxis* and *Difflugia* in the individual ponds during the observed period.

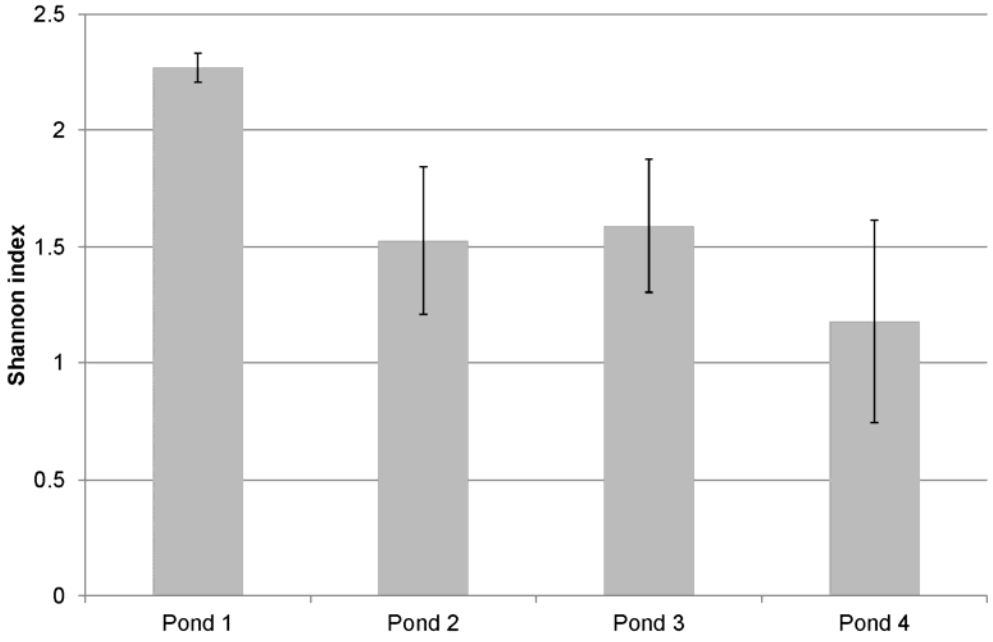

Figure S4: Shannon index of diversity with standard deviations for each pond, calculated for the whole observation period.

Figure S5: Pond No. 1, pictures of the ponds were taken in autumn 2011.

Figure S6: Pond No. 2.

Figure S7: Pond No. 3, the largest one.

Figure S8: Pond No. 3, the largest one; the river Vltava is seen in the upper left.

Figure S9: Pond No. 4.

Figure S10: Pond No. 4.

Fauna species and vegetation present in the area of the Komořany ponds

Invertebrates: Insecta: *Hymenoptera – Bombus terrestris, Bombus bombus, Odonata – Calopteryx splendens, Coenagrion puella, Aeschna grandis, Libellula depresa, Sympetrum sanquineum, Heteroptera – Hydrometra stagnorum,* Molusca: *Lymnaea stagnalis, Anodonta anatina.* Vertebrata: Amphibia: *Rana temporaria, Rana dalmatina, Rana ridibunda, Bufo bufo, Triturus vulgaris*. Reptilia: *Anguis fragilis, Coronella austriaca, Natrix natrix.* Aves: *Accipiter nisus, Bucephala clangula, Dendrocopos mediu, Lanius collurio, Mergus merganser, Micropus apus, Oenanthe oenanthe, Phalacrocorax carbo, Podiceps cristatus, Perdix perdix, Sterna hirundo, Tachybaptus ruficollis. Mammalia – Mustela nivalis, Neomys fodiens, Sciurus vulgaris, Vulpes vulpes*.

The vegetation includes: Ponds – *Alisma plantago-aquatica, Butomus umbellatus,Ceratophyllum demersum, Hydrocharis morsus-ranae, Iris pseudacorus, Lemna minor, Nymphoides peltata, Potamogeton trichoides, Sagittaria sagittifolia, Spirodela polyrhiza, Utricularia australis. Edge of ponds – Alnus glutinosa, Juncus effuses, Lysimachia vulgaris, Phalaris arundinacea, Robinia pseudacacia, Salix alba, Salix fragilis, Salix pentandra, Salix viminalis, Typha angustifolia, Typha latifolia.* All species of the vegetation community are described by Hrčka D. (2009, Modřany and Komořany ponds, Prague, report in Czech).

5. ČÁST III: INTERAKCE MEZI KRYTÉNKAMI A MYKORHIZNÍMI A SAPROTROFNÍMI HOUBAMI

5.1. Význam mykorhizních a saprotrofních hub a jejich interakcí s půdní mikrobiotou

Mykorhizní symbióza je mutualistické soužití specializované skupiny půdních hub s kořeny vyšších rostlin. Jedná se o jednu z evolučně nejstarších a nejrozšířenějších rostlinných symbióz, v současné době žije v symbióze s mykorhizními houbami cca. 70-90% dosud zkoumaných vyšších rostlin. Základním principem fungování mykorhizní symbiózy je transport asimilátů (uhlíkatých produktů fotosyntézy) z hostitelské rostliny do symbiotické houby a minerálních živin z houby do rostliny, přičemž vztah mezi oběma symbionty je v ideálním případě vyvážený a oboustranně prospěšný. Pokud pronikají houbové vlákna do kořenových buněk primární kůry, jedná se o endomykorhizní symbiózy. Zvláštní druh představuje erikoidní mykorhizní symbióza, mutualistické soužití mezi specializovanými půdními houbami a kořeny rostlin z čeledi vřesovcovité (Ericaceae). Erikoidní mykorhiza je zásadní pro přežití vřesovcovitých rostlin v půdních podmínkách s nízkým obsahem minerálních látek, ale vysokým obsahem těžko dostupných organických látek, vysokým poměrem uhlík:dusík či nízkým pH (rašeliniště, vřesoviště). Erikoidně mykorhizní houby jsou velmi dobrými saprotrofy a jako takové tvoří široké spektrum enzymů (např. chitinázy), které jim umožňují čerpat látky z odumřelých hyf hub či živočichů.

Zvláštním typem asociace kořenů vyšších rostlin a vláknitých půdních hub je DSE-asociace, pojmenovaná podle hub, které ji tvoří (*Dark Septate Endophytes*) (Jumpponen a Trappe, 1998). DSE houby mohou mít symbiotický charakter (kolonizují přímo kořeny) nebo asymbioticky ovlivňují společenstva mykorhizních hub a jiných mikroorganizmů v půdě okolo kořenů (mineralizují organický substrát a zpřístupňují ho tak rostlinám, což může vést k jejich zlepšenému růstu) (Mandyam a Jumponen, 2005). DSE houby se vyskytují téměř u všech rostlinných čeledí včetně vřesovcovitých. U vřesovcovitých rostlin se erikoidní mykorhizy a DSE-asociace mohou vyskytovat jednotlivě nebo paralelně (Cázares et al., 2005).

Jak již bylo uvedeno výše, erikoidně mykorhizní houby tvoří enzym chitinázu, jež hydrolyticky rozkládá aminopolysacharid chitin a tím umožňuje využívat chitin jako zdroj živin (Gortari a Hours 2008). Erikoidně mykorhizní houby by tedy mohly být schopny rozkládat

chitinózní schránky krytének a následně je využívat jako zdroj živin/energie. Tento ekologický aspekt dosud nebyl zkoumán, avšak z dostupné literatury vyplývá, že biomasa krytének představuje kvantitativně významnou součást biomasy půdních organismů, zejména v jinak na živiny chudých stanovištích (rašeliniště, lesní půdy) (Gilbert, 1998a). Tyto habitaty bývají nezřídka osídleny vřesovitými rostlinami, které zde přirozeně tvoří erikoidní mykorrhizy a/nebo asociace s DSE houbami (Cairney, 2003; Read 1996). Mykorhizní houby mohou obecně využívat dusík uložený např. v rostlinném opadu, ale i odumřelých tělech živočichů (Klironomos, 2001), na druhou stranu představují půdní houby nezanedbatelný zdroj potravy pro půdní kryténky (Gilbert, 2003).

Mezi substráty chudé na živiny patří také půdy jehličnatých a opadavých lesů. Ty jsou kolonizovány velmi rozmanitým spektrem nejrůznějších hub, jež se výraznou měrou podílejí na dekompozičních procesech a samy představují významný zdroj živin pro edafon a mikroorganismy. Je prokázáno, že houbové mycelium může ovlivňovat složení populace půdních protistů (Ingham a Mastigotte, 1994), např. Timoten (2004) popsal významné rozdíly ve složení společenstev protistů vyskytujících se v mykorhizosféře rostlin žijících v symbióze s různými ektomykorhizními houbami. Napolitano a Flanagan (1981) zavedli analogicky k efektu rhizosféry termín *efekt karposféry* – pozorovali, že hustota améb se snižovala s rostoucí vzdáleností od houbových plodnic a klesala s klesající hustotou mycelia v půdě. Na druhou stranu mohou půdní protisti redukovat ektomykorhizní kolonizaci kořenů rostlin nebo snižovat hustotu mykorhizních hyf v mykorhizosféře (Bonkowski, 2001). Existuje nicméně pouze malá hrst prací, zabývajících se přímými interakcemi krytének a půdních/mykorhizních hub. Např. na rozpadajících se jehlicích borovice lesní, rozkládaných saprotrofními houbami, se v asociaci s těmito houbami často vyskytuje kryténka *Phryganela acropodia* (Ogden, 1990). *P. acropodia* se živí selektivně fragmenty hyf různých druhů hub, hyfovými exudáty a s nimi asociovanými bakteriemi.

V rámci své disertační práce jsem se v této oblasti zaměřila na dvě témata, přičemž jsem výsledky svého snažení v obou případech opublikovala ve vědeckém článku. V prvním článku (Microbial Ecology 2009, ČLÁNEK 3 této DP) jsem s kolegy z Botanického ústavu AVČR v.v.i. v Průhonicích zkoumala interakce mezi erikoidně mykorhizními a DSE houbami a kryténkami v mykorhizosféře evropských rododendronů. Druhý článek (Microbial Ecology

2011, ČLÁNEK 4 této DP) se zabývá vlivem mycelia saprotrofních hub obývajících opad borovice lesní na distribuci a druhové složení komunit půdních krytének.

5.2. *ČLÁNEK 3: Testate amoebae (Arcellinida and Euglyphida) vs. ericoid mycorrhizal and DSE fungi: A possible novel interaction in the mycorrhizosphere of ericaceous plants? (Microbial Ecology 57: 203–214, 2009)*

Testate Amoebae (Arcellinida & Euglyphida) vs. Ericoid Mycorrhizal and DSE Fungi: A Possible Novel Interaction in The Mycorrhizosphere of Ericaceous Plants?

M. Vohník[1,2], Z. Burdíková[3,4], J. Albrechtová[2,1], M. Vosátka[1]

(1) Department of Mycorrhizal Symbioses, Institute of Botany, Academy of Sciences of the Czech Republic, Lesní 323, 252 43 Průhonice, Czech Republic

(2) Department of Plant Physiology, Faculty of Science, Charles University in Prague, Viničná 5, 128 44 Prague, Czech Republic

(3) Department of Paleontology, Faculty of Science, Charles University in Prague, Albertov 6, 128 44 Prague, Czech Republic

(4) Department of Biomathematics, Institute of Physiology, Academy of Sciences of the Czech Republic, Vídeňská 1083, 142 20 Prague, Czech Republic

Abstract

Common occurrence of testate amoebae (TA) in the rhizosphere of mycorrhizal plants indicates existence of yet undocumented ecological interactions, involving three distinct groups of organisms: soil protists, mycorrhizal fungi, and their host plants. This tripartite relationship was to date investigated only to a limited extent, despite its probable importance for processes taking place in the mycorhizosphere. In this study, we i) explored spectra of different TA genera naturally associated with the rhizoplane of three autochthonous European *Rhododendron* species, ii) screened natural fungal colonization of the TA shells occupying the rhizoplane of selected rhododendrons, and iii) carried out two *in vitro* experiments addressing the question, whether TA shells may serve as a source of nutrients for ericoid mycorrhizal fungi (ErMF) and dark septate endophytes (DSE). Our field observations indicated that TA regularly associated with the rhizoplane of all screened rhododendrons and that ErMF and/or DSE associated with their roots possibly exploited the TA shells as a nutrient source. In general, the TA spectra were qualitatively and quantitatively similar among rhizoplanes of all three *Rhododendron* species, being dominated by *Diplochlamys*, *Centropyxis*, *Cyclopyxis*, *Euglypha*, *Trinema* and *Assulina*. The highest fungal colonization was observed in *Centropyxidae* and *Trigonopyxidae*, reaching up to 45% of the shells in the case of *Trigonopyxis*. In the *in vitro* experiments, both ErMF *Rhizoscyphus ericae* and DSE *Phialocephala fortinii* regularly colonized TA shells, utilizing them as a source of nutrients. We hypothesize a complex relationship between ErMF/DSE and TA. If corroborated, it would represent an interesting nutrient loop in the mycorhizosphere of ericaceous plants.

Introduction

Protists (protozoans) represent an important part of soil biota, playing a crucial role in decomposition of organic matter and thus in nutrient cycling (14, 18, 49). Testate amoebae (TA),

also known as thecamoebae, testaceans, thecamoebians or arcellaceans (38), are a polyphyletic group of aquatic or terrestrial protists, whose cytoplasm is enclosed within a discrete shell/testa, which normally consists of one chamber with a single aperture (40). Most TA belong to one of two major groups: Arcellinida (Amoebozoa) and Euglyphida (Cercozoa) (38).

The diagnostic character of most TA is the architecture and composition of the shell. Several reports were published with respect to the latter; for instance, Bartoš (11) mentioned that the TA shell was formed by a protein-chitinaceous matrix produced by the TA cytoplasm; Joyon and Charret (30) stated that the shell wall of *Hyalosphenia papilio* was composed of a mucoprotein; Moraczewski (39) reported that the shell wall of *Arcella discoides* contained several amino acids, similar to those found in the organic cement of agglutinate marine foraminifera (28); Ogden and Hedley (40) distinguished proteinaceous, agglutinate, siliceous, and calcareous TA shells. The shells of most TA species are additionally strengthened with organic and/or inorganic particles (xenosomes), e.g. sand grains, diatoms etc. (11, 40).

TA occupy various habitats, including heathlands and peat bogs (38), and in these environments, they represent an important part of the community of soil protists. For instance, Gilbert et al. (23) found that TA represented 48% of the total microbial biomass (excluding fungi) in a Sphagnum peatland, and Gilbert et al. (24) stated, that TA contributed with nearly 14% to the total microbial biomass (including fungi) in a *Sphagnum fallax – Carex rostrata* fen. Hence, dead TA constitute a considerable pool of nutrients in such nutrient-impoverished habitats, however in an organic form, which is directly unavailable to plants.

The presence of soil protists in the rhizosphere significantly affects plant growth (12) and this effect can be mediated by interactions with mycorrhizal fungi (13). Similarly to protists, mycorrhizal fungi are also considered as drivers of nutrient exchange in the rhizosphere, with fundamental effects on plant fitness (44, 45). Important role of mycorrhizal fungi is pronounced in nutrient-poor habitats where they access organically bound nutrients and make them available to host plants. Members of *Ericaceae* and ericoid mycorrhizal fungi (ErMF) are an excellent example of this phenomenon. Ericaceous plants typically inhabit soils poor in available nitrogen (N) and often dominate vegetation in heathlands and peat bogs (16, 43). They regularly

form ericoid mycorrhiza (ErM) with ErMF, which provide N supply to their hosts (48). ErMF are able to utilize such complex substrates as peptides (2), proteins (3), chitin (33), fungal mycelium (34) or plant/mycorrhizal necromass (35). The last study (35) showed that the typical ErMF *Rhizoscyphus ericae* (Read) Zhuang & Korf produced extracellular protease and chitinase when grown on mycorrhizal root biomass and used fungal chitin as a source of N, transporting it into host plant tissues. Analogically to plant/mycorrhizal necromass, *R. ericae* could use TA necromass, a cocktail of organic nutrients containing chitin and proteins, which is abundantly available in peatlands (23, 24), as a substrate for its growth and transport obtained N to host plants in exchange for photosynthetic carbon.

Interactions between soil protists and mycorrhizal fungi comprise dynamic and complex processes that may influence all partners entering the interaction: spore germination, root colonization, growth of fungal mycelium or sporulation can be affected on the fungal side (21), production of biomass on the plant side (13) and composition of the community (29) on the protist side. Even though investigations of interactions between TA and soil fungi are scarce, they reveal consequences important for ecophysiology of the rhizosphere. Mycophagy is accepted as one of the TA's nutrition strategies (18). Couteaux (17) used malt extract to stimulate the growth of fungi in a non-sterile soil and screened the response of the TA community to this manipulation. The biomass of the fungal mycelium remained unaltered, but the incidence of the most abundant TA, *Phryganella acropodia*, increased with time. This led the author to hypothesize *P. acropodia* mycophagy, which was further supported by frequent observations of its shells attached to fungal hyphae. Gilbert et al. (25) reported that spores and mycelium of soil fungi represented 36% of the identified prey of the members of the TA complex *Nebela tincta major-bohemica-collaris*. This suggested that soil fungi, possibly including mycorrhizal, represented an important part of the diet for this species. Ingham and Massicotte (29) found that TA regularly inhabited the mycorhizosphere of ectomycorrhizal (EcM) roots of five conifers and that their communities quantitatively and qualitatively differed depending on host plants and EcM fungi colonizing their roots. This indicated that the composition of an EcM community might determine the composition of a TA community in the mycorrhizosphere. However,

mechanisms of this relationship were unknown. Ingham and Massicotte suggested that mycorrhizal fungi could influence the protist community by controlling/altering the bacterial community in the rhizosphere.

Although reports describing direct interactions between TA and mycorrhizal fungi are lacking, several interesting facts can be inferred from the literature focused on related topics. To summarize, i) TA represent a quantitatively important part of soil biota in nutrient-poor peatland habitats (23); ii) such habitats are often dominated by ericaceous plants, which regularly form ErM and/or DSE-association (16, 31, 32, 43); iii) in such habitats, ErMF, and possibly also dark septate endophytes (DSE), help plants to access organic nutrients, namely N (37, 45); iv) mycorrhizal fungi can access animal N (36); v) soil fungi represent an important part of TAs' feed (25). In addition, our previous observations indicate that vi) shells of probably dead TA are regularly associated with mycelium emerging from ericoid mycorrhizal roots (Vohník, unpublished data). These facts together indicate a possible complex relationship between mycorrhizal fungi and TA, which might also influence physiology and ecology of mycorrhizal plants.

In the present study, we investigated several aspects of this relationship, focusing mainly on phenomena related to the hypothesis that mycorrhizal fungi can use TA shells as a nutrient source. We describe the composition and similarity of the TA communities found in the rhizoplane of three native European *Rhododendron* species, and quantify fungal colonization of their shells. Additionally, we report observations of the association between TA shells and fungal mycelium emerging from *Rhododendron* mycorrhizal roots. In two *in vitro* experiments, we address the question whether TA shells could serve as a source of nutrients and/or propagule carriers for ErMF *R. ericae* and DSE *Phialocephala fortinii* Wang & Wilcox.

Materials and Methods

Occurrence of TA in the rhizoplane of three Rhododendron species

Three European *Rhododendron* species (*Rhododendron hirsutum* L., *Rhododendron kotschyi* Simk. and *Rhododendron luteum* Sweet) were screened for TA occurring in their rhizoplane. The roots of *R. hirsutum* were collected in June 2005 at Velika Planina plateau, Slovenia (~1400 m a. s. l.), the roots of *R. kotschyi* were collected in September 2005 in the Carpathian Mts., Romania (1724 - 2505 m a. s. l.) and the roots of *R. luteum* were collected in September 2005 in a deciduous forest (tree dominants *Fagus sylvatica* L., *Quercus petraea* (Mattusch.) Liebl., *Carpinus betulus* L. and *Castanea sativa* Mill.) near the municipality of Boštanj, Slovenia (~220 m a. s. l.). For each species, four to seven individuals were screened. From each individual, three root samples (each containing approx. 15 cm of roots) were taken from the upper soil layer (depth 5 – 15 cm), inserted in plastic bags and stored in a fridge (8 °C) until screened.

Roots with adhering rhizospheric soil were gently washed under running tap water on a sieve (Ø 1 mm) to remove excessive substrate. Washed roots with adhering rhizoplanic substrate were divided into three parts. The first part was placed into 250-ml flasks with lactoglycerol and stored in the fridge for one month. After this period, the rhizoplanic material, which separated from the roots of *R. hirsutum* (n = 6), *R. kotschyi* (n = 7) and *R. luteum* (n = 4) due to gravity, was collected from the bottom of the flasks with plastic pipettes and was screened for TA shells. In each sample, at least 100 shells were collected, determined to the genus level according to Alekperov and Snegovaya (1), Balík (5, 6, 7, 8, 9, 10), Bartoš (11), Deflandre (19, 20), Foissner and Korganova (22), Ogden and Hedley (40) and Patterson et al. (41), and % frequency of each genera was counted. Qualitative and quantitative similarity of the TA spectra among all *Rhododendron* individuals was assessed by the cluster analysis using the Jaccard index and the Morisita index. PAST 1.4 (Hammer et al. 2001) was used for statistical analyses.

Natural colonization of TA shells by fungal hyphae

The TA shells from separated rhizoplanic material were additionally screened for colonization by fungal hyphae. To accomplish this, one individual was randomly chosen per each Rhododendron species. At least 300 shells from its rhizoplane were collected, immersed in 0.05% trypan blue in lactoglycerol (lactic acid : glycerol : de-ionized water = 1 : 1 : 3) to stain fungal mycelium and observed with an Olympus SZX12 inverted microscope equipped with the Olympus Relief Contrast (max. magnification 400x) and an Olympus BX60 microscope equipped with DIC (max. magnification 1000x). A shell was considered as being colonized when fungal hyphae either grew on its surface or inside its lumen. Percentual frequency of the colonized shells was counted for each TA genera.

Association between TA shells and Rhododendron roots

The remaining two parts of the roots were subjected to direct observation of associated TA shells using light microscopy and scanning electron microscopy (SEM). Prior to observation, one part was treated according to the methods commonly used for screening mycorrhizal colonization (15), i.e., autoclaved in 10% KOH for 20 min at 121 ºC, rinsed in 3% HCl, washed with running tap water and autoclaved in 0.05% trypan blue in lactoglycerol for 20 min at 121 ºC and left overnight at room temperature (= the common treatment). The other part of the roots was directly immersed in a solution of 0.05% trypan blue in lactoglycerol and left overnight at room temperature (= the alternative treatment). Roots were de-stained by immersing in de-ionized water and screened for the presence of associated shells of TA and mycorrhizal structures using a dissecting microscope. Because there were no TA shells associated with the roots in the common treatment, we further focused only on the roots from the alternative treatment. Here, mycorrhizal roots associated with TA shells via fungal mycelium were cut into 1-cm pieces and mounted onto non-permanent slides for light microscopy or were directly

examined using SEM. Slides were observed at high magnification (400x or 1000x) using an Olympus BX60 microscope equipped with DIC. SEM photographs were taken in the Olympus ESEMTM mode at low temperatures (-6 ºC to -3 ºC) using a FEI Quanta 200 microscope. The Olympus ESEMTM mode enables screening of non-collapsed roots without previous treatment (e.g. coating or critical-point drying).

Additionally to native *Rhododendrons*, roots of four rooted stem cuttings (size approx. 10 cm) of *Rhododendron* cv. Azurro, cultivated four months in a growth chamber (16/8 h day/night, average temperature 20°C, 150 µmol m^{-2} s^{-1}) in a non-sterile peat-based substrate (peat : zeolite : perlite = 1 : 1 : 1) were treated in the same manner and screened for association between TA shells and their roots.

Experiment 1 – colonization of TA shells by Phialocephala fortinii and Rhizoscyphus ericae

Cyclopyxis and *Trigonopyxis* shells were extracted with fine forceps from a water suspension of a peat-based substrate, collected from the rhizosphere of *Vaccinium myrtillus* L. in Modrava, Šumava National Park, Czech Republic in September 2005. These two TA genera were used because of their abundance in the suspension and shell size suitable for manipulation. Moreover, we found that *Cyclopyxis* and especially *Trigonopyxis* shells were frequently naturally colonized by fungal hyphae in the rhizoplanic samples from *Rhododendron* roots (see Results), which indicated their suitability for inoculation experiments. Grains of serially washed quartz sand (Provodínské písky Inc., CZ; fraction <1 mm) were used as a negative control and were treated in the same manner as the TA shells.

Extracted shells/sand grains were transferred onto moistened PRAGOPOR 6 nitrocellulose membranes (Ø adjusted to 1 cm, pore size 0.4 µm; Pragochema Ltd., CZ) placed in glass Petri dishes, five shells/grains per membrane, and autoclaved for 20 min at 121 °C. Autoclaved membranes with adhering shells/grains were aseptically placed into plastic Petri dishes with water agar (WA).

P. fortinii and *R. ericae* axenic cultures were pre-cultivated in plastic Petri dishes on WA for one month at room temperature in the dark. Small pieces of their mycelium (approx. 1 mm^3) were obtained from margins of their actively growing colonies and were transferred approx. 3 mm from each membrane. *P. fortinii* was the strain PFO-F (GenBank EF446149), which is deposited in the Culture Collection of Fungi (Department of Botany, Faculty of Science, Charles University in Prague, CZ) under the accession number CCF 3586. It corresponds to the *P. fortinii* cryptic species CSP7 (= *P. fortinii* s. s.) sensu Grünig et al. (26) and forms DSE-association with ericaceous host plants (50). *R. ericae* was a culture derived from the strain UAMH 6735 (GenBank AJ319078), isolated by Pearson and Read (41). It forms ErM with ericaceous host plants (51, 52).

There were three treatments (*P. fortinii*-inoculated, *R. ericae*-inoculated and non-inoculated), each containing in total 60 autoclaved TA shells on 12 membranes in four Petri dishes (three membranes in one dish, each membrane with five TA shells) and 60 autoclaved sand grains organized in the same manner as the shells. The dishes were sealed and incubated at room temperature in the dark for two months. After this period, the shells/grains were extracted with forceps and divided into three parts for each variant, each part containing 20 shells/grains on four membranes. The first part was screened for colonization with *P. fortinii* or *R. ericae* mycelium using light and/or scanning electron microscopy. The sand grains were observed by SEM only.

Experiment 2 – TA shells as a source of nutrients for Phialocephala fortinii and Rhizoscyphus ericae

The second part of the shells/grains was aseptically transferred onto new autoclaved moistened nitrocellulose membranes, placed on WA in plastic Petri dishes (Ø 9 cm), sealed and incubated at room temperature in the dark for two months. The third part of the shells/grains was transferred onto new autoclaved moistened nitrocellulose membranes, placed on serially washed quartz sand (the same provenience as the grains) in glass Petri dishes (Ø 5 cm), sealed and incubated at room temperature in the dark for two months. The mycelium emerging from the shells/grains

was observed and documented periodically each week. After two months, the shells were screened using light and scanning electron microscopy. The grains were observed by SEM only.

Results

Occurrence of TA in the rhizoplane of three Rhododendron species

In total, we found 13 genera of TA to be associated with the rhizoplane of *R. hirsutum*, R. luteum and R. kotschyi. They were (alphabetically): *Arcella*, *Assulina*, *Centropyxis*, *Corythion*, *Cyclopyxis*, *Diplochlamys*, *Euglypha*, *Heleopera*, *Nebela*, *Pseudodifflugia*, *Tracheleuglypha*, *Trigonopyxis* and *Trinema*. Shells of *Pseudodifflugia* were found only in the *R. hirsutum* samples, all other TA genera were found in the rhizoplane of all three *Rhododendron* species (Table 1). On average, we were unable to identify to genus level approx. 5 - 6% of the collected TA shells. The average value of the Jaccard index for all *Rhododendron* individuals was 0.777, with minimum 0.583 (*R. hirsutum* #1 vs. *R. luteum* #4 and #5) and maximum 1 (*R. hirsutum* #1 vs. *R. kotschyi* #3, *R. hirsutum* #3 vs. *R. luteum* #3, *R. kotschyi* #4 vs. *R. luteum* #7 and *R. luteum* #4 vs. *R. luteum* #5). The average value of the Morisita index was 0.697, with minimum 0.276 (*R. hirsutum* #4 vs. *R. luteum* #4) and maximum 0.969 (*R. hirsutum* #1 vs. *R. luteum* #3).

Natural colonization of TA shells by fungal hyphae

The highest natural fungal colonization was found in shells of relatively scarce *Trigonopyxis* (approx. 45%, 42% and 44% of the shells in the rhizoplane of *R. hirsutum*, *R. luteum* and *R. kotschyi*, respectively), followed by *Cyclopyxis* (34%, 32% and 36%), *Centropyxis* (34%, 29% and 32%), *Diplochlamys* (29%, 25% and 44%), *Arcella* (20%, 0% and 38%), *Trinema* (13%, 0% and 6%), *Nebela* (0%, 10%, 13%), *Euglypha* (8%, 7%, 10%), *Assulina* (0%, 4%, 7%), *Tracheleuglypha* (0, 6, 0) and *Corythion* (0%, 0%, 3%). As can be seen, the shells of some TA genera differed in the fungal colonization with respect to *Rhododendron* species, whereas the colonization of others was similar in all *Rhododendron* rhizoplanes (Table 1).

Association between TA shells and Rhododendron roots

We documented the association between TA shells and roots via the mycelium of putative mycorrhizal fungi in all samples of all three *Rhododendron* species and *Rhododendron* cv. Azurro in the alternative treatment. We estimated that there was at least one TA shell associated with the mycorrhizal root by means of the fungal mycelium per 5cm of the total root length. We found no associated TA shells in the samples from the common treatment. In some cases, TA shells appeared to be only loosely attached to the root surface by means of the fungal mycelium (Fig. 1), in other cases however, the association between TA shells and the root appeared to be very intimate (Fig. 2). TA shells were frequently embedded in the fungal mycelium, often being partially decomposed (Fig. 3), which substantially hampered their identification. Some of the objects with the TA shells' appearance were filled with darkly pigmented thick-walled cells (Fig. 4), which resembled the colonization pattern of the DSE *P. fortinii* (see below). All screened ericaceous plants developed ErM colonization and also possessed DSE-association.

Experiment 1 – colonization of TA shells by Phialocephala fortinii and Rhizoscyphus ericae

Both *Cyclopyxis* and *Trigonopyxis* shells were colonized by the mycelium of both ErMF *R. ericae* and DSE *P. fortinii*. Commonly, *R. ericae* mycelium almost completely covered the surface of the colonized shells (Fig. 5). *P. fortinii* was slower in colonization and its mycelium usually did not cover the whole surface of the shells (Fig. 6). *P. fortinii* hyphae often entered the shell via its aperture (Fig. 6). The intracellular colonization of such shells consisted of short, thick, darkly colored and thick cell-walled hyphae, which usually occupied the whole lumen of the shell (Fig. 7). This was connected with notable color change – the shells colonized intracellularly by *P. fortinii* were dark brown to black, which contrasted with the yellowish to light brownish color of the shells, which were colonized only superficially. Such intracellular colonization resembled microsclerotia, formed by DSE in the roots of higher plants (Fig. 11). The surface of the sand grains was only poorly colonized by either single hyphae or a very loose weft of the mycelium of *P. fortinii* or *R. ericae*.

Experiment 2 – TA shells as a source of nutrients for Phialocephala fortinii and Rhizoscyphus ericae

After transferring the *P. fortinii*- and *R. ericae*- pre-colonized shells/grains onto new membranes and during their two-month cultivation on WA, both fungi were able to utilize the TA shells as a source of nutrients. This was indicated by vigorous growth of their hyphae, which radiated from the pre-colonized shells and lack of such growth from the pre-colonized sand grains. Vigorous growth was notable especially for the hyphae of *P. fortinii*, which expanded from the dark-colored pre-colonized shells in all directions, covering the whole surface of the shells and completely disorganizing their shape with progressing time (Fig. 8). Also the mycelium of *R. ericae* completely covered the surface of the pre-colonized shells and partially disorganized their shape with progressing time (Fig. 9).

When the membranes with the pre-colonized shells/grains were transferred into the dishes with serially washed quartz sand, a similar situation occurred: the pre-colonized shells gave rise to new abundant *P. fortinii* or *R. ericae* mycelium (Fig. 10), which was not the case of the pre-colonized sand grains. The dark brown to black colored shells, which were intracellularly colonized by *P. fortinii* as described above, gave rise to more abundant mycelium than the yellow- to light-brown-colored shells, which lacked significant intracellular colonization.

Discussion

To date, the relationship between soil protists and fungi has not been frequently investigated. One direction of the research was focused on investigations of communities of protists in the rhizosphere. For instance, Ingham and Massicotte (29) explored ectomycorrhizospheres of *Pinus ponderosa*, *Pseudotsuga menziesii*, *Picea sitchensis*, *Tsuga heterophylla* and *Abies grandis*, and identified six types of protist communities, which always included ciliates, TA, naked amoebae and flagellates, but differed qualitatively and quantitatively with respect to different host plants and different symbiotic fungi. Protists generally tended to be more abundant and diverse in

roots colonized by fungi from the EcM genera *Rhizopogon* than in roots symbiotic with EcM fungus *Thelephora terrestris* or DSE fungi from the *Mycelium radicis atrovirens* complex (formed predominantly by *P. fortinii* cryptic species), or in non-mycorrhizal roots. TA were relatively poor in species number and abundance, especially when compared with flagellates, and included *Nebela*, *Euglypha*, *Valkanovia*, *Difflugia*, *Trinema*, *Corythionopsis* and *Arcella*, the first genera being the most abundant across all combinations of host species and mycorrhizal fungi.

Contrary to Ingham and Massicote, we found no clear differences in the average frequencies of TA among the rhizoplanes of the three *Rhododendron* species. Additionally, these frequencies differed qualitatively and quantitatively from those found in the coniferous ectomycorrhizospheres. This discrepancy might be caused by several factors, because designs of both studies varied in many ways. We focused on environmental samples, whereas the results of Ingham and Massicote were derived from a greenhouse inoculation experiment. We examined ErM- and DSE-colonized hair roots of mature ericaceous plants, whereas the other study targeted EcM roots of young coniferous seedlings. Not least, ericaceous plants associate with unique spectrum of fungi, which does not include EcM fungi from the *Rhizopogon* genera. Moreover, in contrast to EcM fungi, ErMF or DSE do not coat root tips with a compact fungal sheath – it is very likely that in our study, TA had direct access to the root surface and its products whereas in the other study, TA interacted mostly with the fungal mantle. On one hand, these facts seriously hamper comparison of the results; on the other, they emphasize the need for further screening of preferably environmental root samples of plants from various ecosystems and with different mycotrophy, to make future comparisons possible.

Our root samples originated from different *Rhododendron* species and were collected in different environments. Then, why were the average frequencies of different TA genera relatively similar? The answer could be in the conclusion that similar protist communities could be on roots of different host plants, but with the same mycorrhizal fungi (29). We have not identified the respective fungi colonizing the screened roots; on the other hand, it is assumed that ErM and DSE-association are formed by only limited number of symbiotic fungi and that most ErM

and DSE-associations are formed by *R. ericae* and *P. fortinii*, respectively (48). As a consequence, relatively uniform spectrum of ErM/DSE fungi could attract a relatively uniform spectrum of TA.

Alternatively, and possibly more accurately, the similarity of the TA spectra in the *Rhododendron* rhizoplanes could be the result of general uniformity of ericaceous roots (43) and environments they inhabit (16). Apparently, further investigations are needed on the relative importance of micro-environment versus host plant and root-inhabiting fungi identity as a determinant of TA community structure.

The other direction of the protists vs. soil fungi research examined trophic relationships between both groups of organisms. Couteaux (17) investigated the relationship between TA community and soil fungi by addition of malt extract (ME) into experimental microcosms. She concluded that one of the TA species monitored in her study, *Phryganella acropodia*, was mycophagic, i.e. consumed mycelium of soil fungi, growth of which was stimulated by introduction of ME. Gilbert et al. (25) drew additional attention to the nutritional importance of fungal mycelium for soil protists by showing that it could represent a considerable part (up to 36%) of the diet of some TA species. In contrast, we had focused on the trophic relationship from the fungal perspective and showed that TA shells collected from environmental root samples were regularly colonized by fungal mycelium, and the colonization in some genera reached considerable frequency.

These findings point at frequent interactions between TA and soil fungi. From the fungal point of view, interactions with TA may have two different modes of functioning: passive and active. In the former mode, fungal hyphae (dead or alive) are only mechanically glued to alive TA shells and are de facto organic xenosomes. Slowly moving TA could serve as carriers for vital fungal propagules, which, attached to the surface, wait for their chance to rapidly colonize the shell after its death. In the latter mode, there is an indication of active fungal growth towards/from the shell and we can expect that the fungus immediately explores the shell (or its parts) as a nutrient source. From the TA (or rather the TA-researcher) point of view, frequent and genera-specific fungal colonization might hamper proper assessment of TA community composition. Identified *Trigonopyxis* shells were represented relatively poorly in our rhizospheric samples; this

could reflect either their genuine scarcity, or the possibility that they were decomposed or deformed by fungi more frequently/rapidly than other genera. Future investigations of TA communities from mycorhizospheres should consider the fact that fungal colonization could rapidly and totally alter shape of TA shells (see further text).

Nutrients obtained by soil fungi from TA shells could be transported directly to the host plant in exchange for photosynthetic carbon if the fungi were mycorrhizal and associated with roots. We showed that direct connections between presumably dead TA and ericaceous roots by means of symbiotic fungi, which is a prerequisite for the hypothetical nutrient flow, were relatively common in the ericaceous rhizoplane. Magnitude, if any, of such nutrient exchange remains to be established. However, relatively high incidence of such connections and high fungal colonization of some TA shells in the mycorrhizosphere indicate that the 'TA-root symbiotic fungi-host plants' association is not an exceptional curiosity. Subsequently, a question arose: Why this association had not been reported earlier? We see two probable reasons: i) the common treatment (see Materials and Methods) prevents observation of fragile TA shells and their more fragile association with the fungal mycelium emerging from the root, and ii) colonization by ErMF and DSE notably changes shape of the colonized shells. To date, TA species are identified mostly using the morphology of their shells (38, 40); very likely, those colonized by soil fungi, especially in later stages of decomposition, would not be recognized as TA at all (cf. Figs 3, 8 and 9).

The proposed nutrient flow between TA and plants by means of mycorrhizal fungi has two steps: nutrient uptake by the fungus followed by transport to the plant. We had focused on the first step and demonstrated in vitro that TA shells represented an acceptable nutrient source for ErMF and DSE. It could be argued that WA or the membranes (see Materials and Methods) served as an additional source of nutrients for the mycelium expanding from the shells. However, it was shown that the nitrocellulose membranes used in the experiments were resistant to microbial degradation (4) and the results from WA were repeated on serially washed quartz sand. Moreover, the differences between the growth of the mycelium from the pre-inoculated shells and the sand grains indicated that both fungi did utilize the shells as a source of

nutrients. Certainly, it would be interesting to determine which parts of the TA shell serve as the actual source of nutrients for the colonizing fungus. It could be a wide range of organic compounds forming the shell, or even the cytoplasm of the amoeba. With this respect, it appeared that ErMF and DSE had favored different colonization strategies: the former group of fungi had readily colonized all available shells, suggesting ErMF utilized whole TA necromass, but the latter had appeared to ignore empty shells, indicating DSE preferred organic matter hidden in the lumen to the organic substances forming the shell itself. Primarily triggered by organic compounds, P. fortinii later developed multicellular structures consisting of short, thick-walled hyphae inside the lumen of some shells. Such structures notably resembled intracellular microsclerotia formed by DSE in roots of higher plants (31). Thus, a dead TA shell could represent a shelter for fungal reproductive structures, similarly to root cells for microsclerotia or cavities of dead seeds for spores of arbuscular mycorrhizal fungi (46, 47).

Our observations and findings together with the published papers on related topics (see Introduction) indirectly favor existence of the second step – transport of nutrients derived from TA shells to host plants. However, its corroboration will depend on a direct demonstration, probably with the help of isotopically labeled compounds. Likewise, it remains to be established whether such highly probable interaction has any significant effect on the host plant. With this respect, we might parallel our deductions to a nutrient cycle demonstrated by Klironomos and Hart (36), who investigated a tripartite relationship between *Pinus strobus*, an EcM fungus *Laccaria bicolor* and a springtail *Folsomia candida* in a microcosms experiment. The authors reported that *P. strobus* was able to derive up to 25% of its N from either dead or live soil-dwelling arthropods via its fungal partner. Interestingly, *L. bicolor* was able to immobilize the animals before infecting them - do ErMF or DSE have similar capabilities towards TA? As the authors concluded, “EcM plants could indirectly depredate soil arthropods for a significant source of nitrogen through their fungal partners” – could ErM plants derive a part of their nitrogen from TA in a similar way? According to Klironomos and Hart, their results revealed “a nitrogen cycle of far greater flexibility and efficiency than was previously assumed, where the fungal partner uses animal-origin nitrogen to ´barter´ for the carbon from the host tree”.

However, it remained unclear whether the observed phenomenon was widespread or functional under natural conditions. In contrast, our observations and results suggest that the interaction between TA and root-symbiotic fungi is both widespread and functional under natural conditions. This might have profound impacts on all partners entering this interaction, as mentioned throughout the discussion. Hopefully, our report will encourage further investigations to elucidate ecological significance of the proposed 'TA - mycorrhizal fungi - host plants' bi-directional nutrient loop.

Acknowledgments

This study was supported by the Academy of Sciences of the Czech Republic (AV0Z60050516 and AV0Z50110509), and Ministry of Education, Youth and Sports of the Czech Republic (research program LC06063). M. Vohník was financially supported by the Grant Agency of the Czech Republic (GACR 206/03/H137). The authors thank to D. Vodnik, S. Lukančič and M. Fendrych for help with collection of the environmental samples.

References

1. Alekperov I, Snegovaya N (2000) The fauna of testate amoebae (Rhizopoda, Testacea) in freshwater basins of Apsheron peninsula. Protistology 1: 135-147
2. Bajwa R, Read DJ (1985) The biology of mycorrhiza in the Ericaceae: IX. Peptides as nitrogen sources for mycorrhizal and non-mycorrhizal plants. New Phytol 101: 459-467
3. Bajwa R, Abuarghub S, Read DJ (1985) The biology of mycorrhiza in the Ericaceae. X. The utilization of proteins and the production of proteolytic enzymes by mycorrhizal plants. New Phytol 101: 469-486
4. Baláž M, Vosátka M (2001) A novel inserted membrane technique for studies of mycorrhizal extraradical mycelium. Mycorrhiza 11: 291-296

5. Balík V (1990) Zur Kenntnis der Bodentestaceen (*Rhizopoda: Testacea*) Südböhmens. Act Mus Boh Meridion in Č. Budějovice 30: 1-12 [in Czech with German summary]
6. Balík V (1992a) Krytenky (Rhizopoda, Testacea) z několika lokalit z chráněné krajinné oblasti Beskydy (Severní Morava, ČSFR). Čas Slez Muz Opava 41: 31-40 [in Czech with English summary]
7. Balík V (1992b) Testate amoebae fauna (*Protozoa*, *Rhizopoda*, *Testacea*) from the marsh habitats in the Krkonoše Mountains National Park (Czechoslovakia). Opera Corcontica 29: 139-154 [in Czech with English summary]
8. Balík (1992c) Die Testaceen (Rhizopoda, Testacea) aus dem Naturschutzgebiet Trojmezná hora im Böhmerwald (Tschechoslowakei). Act Mus Boh Meridion in Č. Budějovice 32: 69-78 [in Czech with German summary]
9. Balík V (1994) Testaceenfauna (Protozoa, Rhizopoda, Testacea) aus dem Naturschutzgebiet Žofínský prales (Novohradské hory Gebirge) in Südböhmen (Tschechische Republik). Act Mus Boh Meridion in Č. Budějovice 34: 55-67 [in Czech with German summary]
10. Balík V (1997) Fauna krytenek (Protozoa, Testacea) západní části Tatranského Národního Parku (Slovenská republika). Štúdie o Tatranskom Národnom Parku 2: 103-122 [in Czech]
11. Bartoš E (1954) Koreňonožce radu Testacea. Vydavaťelstvo Slovenskej Akadémie Vied, Bratislava. 1-185 [in Slovak]
12. Bonkowski M, Cheng W, Griffiths BS, Alphei J, Scheu S (2000) Microbial-faunal interactions in the rhizosphere and effects on plant growth. Eur J Soil Biol 36: 135-147
13. Bonkowski M, Jentschke G, Scheu S (2001) Contrasting effects of microbial partners in the rhizosphere: interactions between Norway Spruce seedlings (*Picea abies* Karst.), mycorrhiza (*Paxillus involutus* (Batsch) Fr.) and naked amoebae (protozoa). Appl Soil Ecol 18: 193-204
14. Bonkowski M (2004) Protozoa and plant growth: the microbial loop in soil revisited. New Phytol 162: 617-631
15. Brundrett M, Bougher N, Dell B, Grove T, Malajczuk N (1996) Working with mycorrhizas in forestry and agriculture. ACIAR Monograph 32, Canberra, 374 pp

16. Cairney JWG, Meharg AA (2003) Ericoid mycorrhiza: a partnership that exploits harsh edaphic conditions. Eur J Soil Sci 54: 735-740
17. Coûteaux M-M (1985) Relationships between testate amoebae and fungi in humus microcosms. Soil Biol Biochem 17: 339-345
18. Coûteaux M-M, Darbyshire JF (1998) Functional diversity amongst soil protozoa. Appl Soil Ecol 10: 229-237
19. Deflandre G (1929) Le genre *Centropyxis* Stein. Archiv für Protistenkunde 67: 322-375
20. Deflandre G (1936) Etude monographique sur le genre *Nebela* Leidy. Annals de Protistologie 5: 201-286
21. Fitter AH, Garbaye J (1994) Interactions between mycorrhizal fungi and other soil organisms. Plant Soil 159: 123-132
22. Foissner W, Korganova GA (2000) The *Centropyxis aerophila* Complex (Protozoa: Testacea). Acta Protozool 39: 257-273
23. Gilbert D, Amblard C, Bourdier G, Francez A-J (1998a) The microbial loop at the surface of a peatland: structure, function, and impact of nutrient input. Microb Ecol 35: 83-93
24. Gilbert D, Amblard C, Bourdier G, Francez A-J (1998b) Short-term effect of nitrogen enrichment on the microbial communities of a peatland. Hydrobiologia 373/374: 111-119
25. Gilbert D, Mitchell EAD, Amblard C, Bourdier G, Francez A-J (2003) Population dynamics and food preferences of the testate amoeba *Nebela tincta major-bohemica-collaris* complex (Protozoa) in a Sphagnum peatland. Acta Protozool 42: 99-104
26. Grünig CR, McDonald BA, Sieber TN, Rogers SO, Holdenrieder O (2004) Evidence for subdivision of the root-endophyte *Phialocephala fortinii* into cryptic species and recombination within species. Fungal Genet Biol 41: 676-687
27. Hammer Ř, Harper DAT, Ryan PD (2001) PAST: Palaeontological Statistics software package for education and data analysis. Palaeontologia Electronica 4:9
28. Hedley RH (1963) Cement and iron in the arenaceous foraminifera. Micropaleontology 9: 433-441

29. Ingham ER, Massicotte HB (1994) Protozoan communities around conifer roots colonized by ectomycorrhizal fungi. Mycorrhiza 5: 53-61
30. Joyon L, Charret R (1962) Sur l'ultrastructure du Thécamoebien Hyalosphenia papilo (Leidy). C R Acad Sci 255: 2661-2663 [in French]
31. Jumpponen A, Trappe JM (1998) Dark septate endophytes: a review of facultative biotrophic root-colonizing fungi. New Phytol 140: 295-310
32. Jumpponen A (2001) Dark septate endophytes – are they mycorrhizal? Mycorrhiza 11: 207-211
33. Kerley SJ, Read DJ (1995) The biology of mycorrhiza in the Ericaceae. XVIII. Chitin degradation by *Hymenoscyphus ericae* and transfer of chitin-nitrogen to the host plant. New Phytol 131: 369-375
34. Kerley SJ, Read DJ (1997) The biology of mycorrhiza in the Ericaceae. XIX. Fungal mycelium as a nitrogen source for the ericoid mycorrhizal fungus *Hymenoscyphus ericae* and its host plant. New Phytol 136: 691-701
35. Kerley SJ, Read DJ (1998) The biology of mycorrhiza in the Ericaceae. XX. Plant and mycorrhizal necromass as nitrogenous substrates for ericoid mycorrhizal fungus *Hymenoscyphus ericae* and its host. New Phytol 139: 353-360
36. Klironomos JN, Hart MM (2001) Animal nitrogen swap for plant carbon. Nature 410: 651-652
37. Mandyam K, Jumpponen A (2005) Seeking the elusive function of the root-colonising dark septate endophytic fungi. Stud Mycol 53: 173-189
38. Mitchell EAD, Charman DJ, Warner BG (2007) Testate amoebae analysis in ecological and paleoecological studies of wetlands: past, present and future. Biodivers Conserv DOI 10.1007/s10531-007-9221-3
39. Moraczewski J (1961) Testacea du littoral peu profound du lac Kisajno (Region des lacs de Mazurie). Polskie Archiwum Hydrobiol 9: 175-194 [in Polish and French]
40. Ogden CG, Hedley RH (1980) An atlas of freshwater testate amoebae. Oxford University Press, Oxford. 222 pp

41. Patterson RT, Dalby A, Kumar A, Henderson LA, Boudreau EA (2002) Arcellaceans (thecamoebians) as indicators of land-use change: settlement history of the Swan Lake area, Ontario as a case study. J Paleolimn 28: 297-316
42. Pearson V, Read DJ (1973) The biology of mycorrhiza in the Ericaceae. I. The isolation of the endophyte and synthesis of mycorrhiza in aseptic culture. New Phytol 72: 371-379
43. Read DJ (1996) The structure and function of the ericoid mycorrhizal root. Ann Bot 77: 365-374
44. Read DJ, Perez-Moreno J (2003) Mycorrhizas and nutrient cycling in ecosystems – a journey towards relevance? New Phytol 157: 475-492
45. Read DJ, Leake JR, Perez-Moreno J (2004) Mycorrhizal fungi as drivers of ecosystem processes in heathland and boreal forest biomes. Can J Bot 82: 1243-1263
46. Rydlová J, Vosátka M (2000) Sporulation of symbiotic arbuscular mycorrhizal fungi inside dead seeds of a non-host plant. Symbiosis 29: 231-248
47. Rydlová J, Batkhuugyin E, Vosátka M (2004) Sporulation of four arbuscular mycorrhizal fungi isolates inside dead seed cavities and glass capillaries. Symbiosis 36: 269-284
48. Smith SE, Read DJ (1997) Mycorrhizal Symbiosis. Second Edition. Academic Press. London. 323-345 pp
49. Vargas R (1990) Avances en microbiologia de suelos: los protozoarios y su importancia en la mineralizacion del nitrogeno. Agronomía Costarricense 14(1): 121-134 [in Spanish]
50. Vohník M, Lukančič S, Bahor E, Regvar M, Vosátka M, Vodnik D (2003) Inoculation of *Rhododendron* cv. Belle-Heller with two strains of *Phialocephala fortinii* in two different substrates. Folia Geobotanica 38: 191-200
51. Vohník M, Albrechtová J, Vosátka M (2005) The inoculation with *Oidiodendron maius* and *Phialocephala fortinii* alters phosphorus and nitrogen uptake, foliar C:N ratio and root biomass distribution in *Rhododendron* cv. Azurro. Symbiosis 40: 87-96
52. Vohník M, Fendrych M, Albrechtová J, Vosátka M 2007 Intracellular colonization of *Rhododendron* and *Vaccinium* roots by *Cenococcum geophilum*, *Geomyces pannorum* and *Meliniomyces variabilis*. Folia Microbiologica 52: 407-414

TABLE 1: Percentual frequency of testate amoebae (TA) shells associated with the rhizoplane of three European *Rhododendron* species, and their colonization by fungal hyphae

Roots of six, seven and four individuals of *R. hirsutum*, *R. luteum* and *R. kotschyi* were screened for occurrence of TA shells. Additionally, one individual was randomly chosen per each *Rhododendron* species and its associated TA shells were screened for colonization by fungal hyphae. The values in the table are mean ± SD percentual frequencies of respective TA genera followed by (number of TA shells screened for fungal colonization/number of those actually colonized). n.e. = not estimated

	R. hirsutum n (% frequency): 747	***R. luteum*** n (% frequency): 1282	***R. kotschyi*** n (% frequency): 677
Diplochlamys	21.6 ± 7.8 (28/8)	14.5 ± 7.6 (8/2)	16.5 ± 9.4 (9/4)
Centropyxis	15.8 ± 6.4 (67/23)	12.5 ± 6.7 (63/18)	11.4 ± 2.8 (62/20)
Cyclopyxis	11.6 ± 7.6 (56/19)	9.0 ± 3.1 (53/17)	8.7 ± 7.6 (25/9)
Euglypha	9.0 ± 3.0 (36/3)	13.4 ± 6.7 (57/4)	10.0 ± 7.2 (63/6)
Trinema	7.7 ± 7.1 (38/5)	10.8 ± 7.6 (25/0)	11.4 ± 10.8 (52/3)
Assulina	10.4 ± 11.0 (16/0)	6.7 ± 5.1 (28/1)	11.0 ± 4.1 (45/3)
Corythion	4.7 ± 3.2 (11/0)	2.6 ± 3.3 (4/0)	8.3 ± 4.7 (32/1)
Arcella	5.6 ± 3.6 (10/2)	2.4 ± 3.1 (4/0)	4.7 ± 4.9 (8/3)
Nebela	1.3 ± 2.0 (3/0)	8.2 ± 4.7 (20/2)	9.0 ± 9.8 (46/6)
Tracheleuglypha	2.9 ± 5.5 (17/0)	10.0 ± 9.4 (50/3)	0.3 ± 0.7 (17/0)
Trigonopyxis	2.0 ± 1.4 (20/9)	4.8 ± 4.4 (55/23)	2.2 ± 3.0 (18/8)
Heleopera	0.4 ± 1.0 (n.e.)	0.5 ± 1.3 (n.e.)	0.3 ± 0.6 (n.e.)
Pseudodifflugia	1.0 ± 2.6 (n.e.)	0.0 (n.e.)	0.0 (n.e.)
undetermined	6.0 ± 4.9 (n.e.)	4.6 ± 4.2 (n.e.)	6.2 ± 4.7 (n.e.)

FIGURES

Figure 1: A TA shell loosely associated with the mycorrhizal root of *Rhododendron* cv. Azurro via fungal hyphae emerging from the root (white arrow). SEM; bar = 10µm. **Figure 2**: A TA shell tightly associated with the mycorrhizal root of *Rhododendron* cv. Azurro via fungal hyphae. SEM; bar = 50µm. The detail shows the hyphae connecting the shell with the mycorrhizal root (black arrows). SEM; bar = 25µm. **Figure 3**: Partially decomposed TA shell, surrounded by fungal hyphae (white arrows). SEM; bar = 50µm. **Figure 4**: A TA shell from the root surface of *Rhododendron* cv. Azurro. The shell is associated with dark septate hyphae (black arrow) and filled with septate multicellular object, which shows similarity to microsclerotia formed by DSE fungi either in TA shells (cf. Fig. 7) or rhizodermal cells of higher plants (cf. Fig. 11). DIC; bar = 50µm. **Figure 5**: A TA shell colonized by the mycelium of *R. ericae*, incubated on WA for 6 weeks. SEM; bar = 50µm. **Figure 6**: A TA shell colonized by the mycelium of *P. fortinii*, incubated on WA for 6 weeks. Contrary to *R. ericae*, there is only loose net of hyphae covering the shell's surface and the *P. fortinii* hyphae enter the shell's lumen via its aperture (white arrow). SEM; bar = 50µm. **Figure 7**: A detail of a TA shell intracellularly colonized by the mycelium of *P. fortinii*. The colonization pattern, i.e. dark, short and thick cells forming dense coiled hyphae, resembles microsclerotia formed by DSE fungi in the rhizodermal cells of higher plants (cf. Fig. 11). SEM; bar = 1µm. The detail shows general appearance of the colonized shell. DIC; bar = 10µm. **Figure 8**: A TA shell as a propagule carrier and a nutrient source for the *P. fortinii* mycelium. The pre-inoculated shell was cultivated on a nitrocellulose membrane placed on WA for two months. The mycelium emerges in all directions from the shell's lumen and completely disintegrates its structure and shape. SEM; bar = 100µm. The detail shows a sand grain, which served as a negative control. Nearly no mycelium developed from the pre-inoculated grain. SEM; bar = 100µm. **Figure 9**: A TA shell as a propagule carrier and a nutrient source for the *R. ericae* mycelium. The pre-inoculated shell was cultivated on a nitrocellulose membrane placed on WA for two months. The shell is completely covered by the *R. ericae* mycelium, which partly disintegrates its structure. SEM; bar = 50µm. **Figure 10**: A TA shell as a propagule carrier and a nutrient source for the *P. fortinii* mycelium. The pre-inoculated shell (black arrow) was cultivated

on a nitrocellulose membrane placed on moistened, serially washed quartz sand for two months. The mycelium radiates from the shell across the membrane. Binoculars; bar = 500µm. The detail shows the same situation using SEM. Bar = 100µm. **Figure 11**: Microsclerotia formed by *P. fortinii* in the rhizodermal cells of *Vaccinium myrtillus* in an aseptic culture. DIC; bar = 25µm. **Figure 12**: A TA shell collected from the rhizosphere of *V. myrtillus* from the field. Note dark septate hyphae attached to its surface (black arrows). DIC; bar = 50µm.

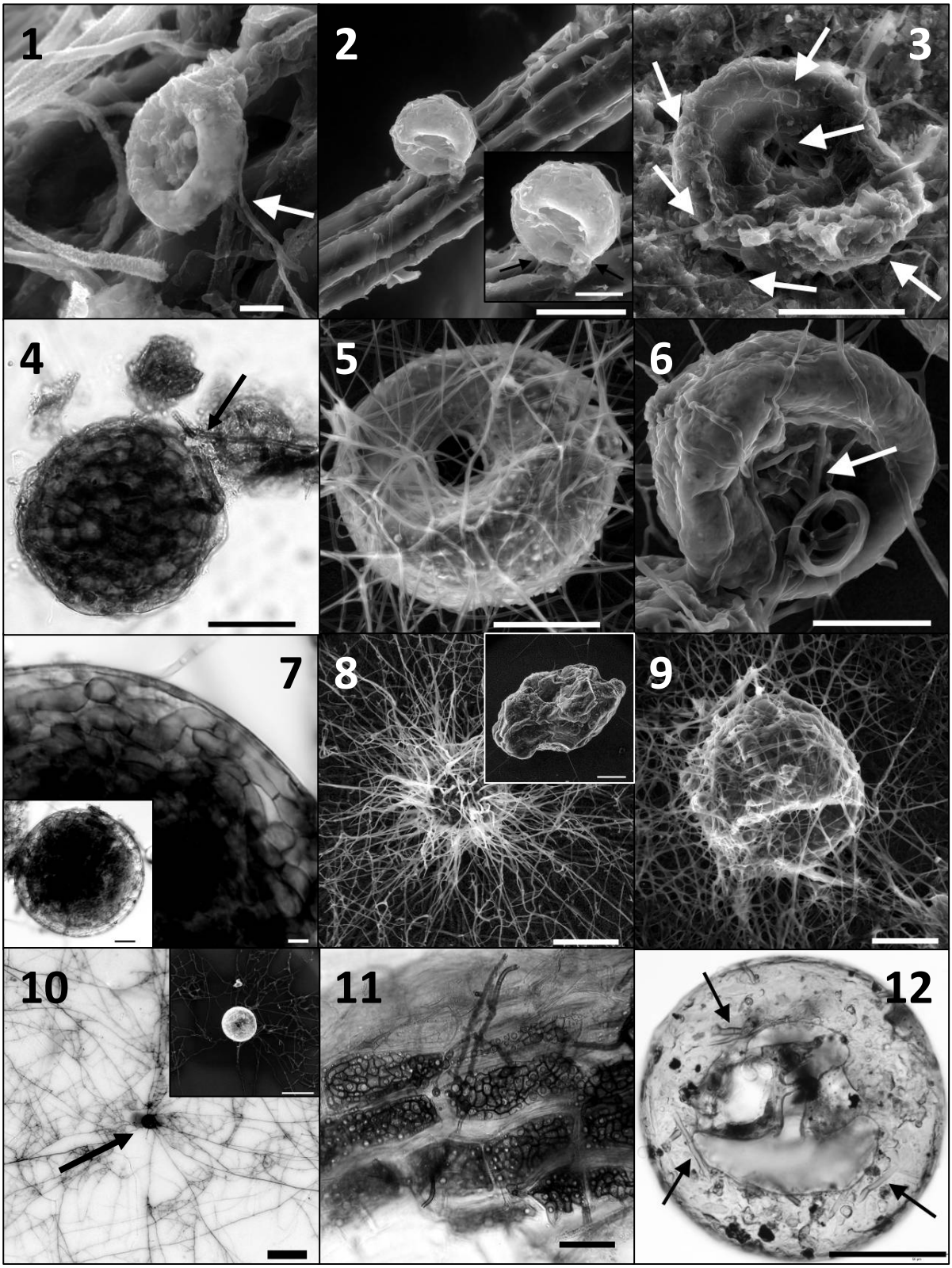
1
2
3
4
5
6
7
8
9
10
11
12

5.3. *ČLÁNEK 4: Interactions between testate amoebae and saprotrophic microfungi in a Scots pine litter microcosm (Microbial Ecology 61: 660–668, 2011)*

Interactions Between Testate Amoebae and Saprotrophic Microfungi in a Scots Pine Litter Microcosm

M. Vohník[1,2], Z. Burdíková[3,4], A. Vyhnal[4], O. Koukol[5]

(1) Department of Mycorrhizal Symbioses, Institute of Botany, Academy of Sciences of the Czech Republic, Lesní 323, 252 43 Průhonice, Czech Republic

(2) Department of Plant Physiology, Faculty of Science, Charles University in Prague, Viničná 5, 128 44 Prague, Czech Republic

(3) Department of Paleontology, Faculty of Science, Charles University in Prague, Albertov 6, 128 44 Prague, Czech Republic

(4) Department of Biomathematics, Institute of Physiology, Academy of Sciences of the Czech Republic, Vídeňská 1083, 142 20 Prague, Czech Republic

(5) Department of Botany, Faculty of Science, Charles University in Prague, CZ-112843

Abstract

In all terrestrial ecosystems, testate amoebae (TA) encounter fungi. There are strong indications that both groups engage in multiple interactions, including mycophagy and decomposition of TA shells, processes which might be fundamental in nutrient cycling in certain ecosystems. Here, we present the results of an experiment focusing on interactions between TA and saprotrophic microfungi colonizing Scots pine (*Pinus sylvestris* L.) litter needles. The needles were collected from a temperate pine forest and cultivated in damp chambers. Over a few weeks, melanized mycelium of *Anavirga laxa* Sutton started to grow out of some needles; simultaneously, the common forest-soil TA *Phryganella acropodia* (Hertwig & Lesser) Hopkinson reproduced and spread around the mycelium. We investigated whether a potential relationship between TA and saprotrophic microfungi exists by comparing the composition of TA communities on and around

the needles and testing the spatial relationship between the *A. laxa* mycelium and *P. acropodia* shells in the experimental microcosm. Additionally, we asked whether *P. acropodia* utilized the *A. laxa* mycelium as a nutrient source and screened whether *P. acropodia* shells were colonized by the microfungi inhabiting the experimental microcosm. Our results indicate that saprotrophic microfungi may affect the composition of TA communities and their mycelium may affect distribution of TA individuals in pine litter. Our observations suggest that *P. acropodia* did not graze directly on the *A. laxa* mycelium, but rather fed on its exudates or bacteria associated with the exudates. The fungus *Pochonia bulbillosa* (Gams & Malla) Zare & Gams was often found parasitizing encysted shells or decomposing already dead individuals of *P. acropodia*. TA and pine litter microfungi engage in various direct and indirect interactions which are still poorly understood and deserve further investigation. Their elucidation will improve our knowledge on fundamental processes influencing coexistence of soil microflora and microfauna.

Key words: testate amoebae, soil saprotrophic microfungi, pine liter

Introduction

Testate amoebae (TA) occupy various terrestrial and aquatic ecosystems. In some habitats, they represent an important part of the community of soil protists [20, 21] and play a significant role in biodegradation of organic matter [44] and nutrient cycling [1, 56, 58, 59]. Their frequency and biomass may exceed those of other important soil organisms, such as ciliates or earthworms [4, 38, 49]. TA mostly feed on bacteria but some species are carnivorous or mycophagous [22, 25, 44, 60].

TA inhabit coniferous [48] as well as deciduous forest soils [37, 38, 53]. Coniferous tree litter is colonized by a variety of soil fungi which play crucial roles in decomposition and nutrient sequestration and simultaneously represent an important food source for edaphic fauna and microorganisms [8, 34]. Fungi also represent a significant part of the soil microbial biomass; in boreal forests, ectomycorrhizal hyphae comprise over 30% of the microbial biomass [27], and

arbuscular mycorrhizal mycelium forms around 20% of the microbial biomass in prairie and pasture grasslands [39]. The presence and identity of the fungal mycelium may influence populations of soil protists: Ingham and Massicotte [30] and Timoten et al. [52] described significant variation in the composition of protist communities with different types of ectomycorrhizae. Napolitano and Flanagan [42] screened populations of amoebae in a sandy soil around fruitbodies of *Laccaria trullisata* (Ellis) Peck and coined the term "carphosphere effect" – the density of the amoebae decreased with an increasing distance from the fruitbodies and decreasing density of the soil mycelium. Feeding on fungi by soil protists may reduce colonization of plant roots by ectomycorrhizal fungi [7] or reduce the length of mycorrhizal hyphae in the mycorrhizosphere [6].

Interactions between TA and fungi in forest soil and litter are an intriguing and potentially important part of their ecology that has been only occasionally investigated. This might be due to the need for combining protozoological and mycological approaches; nevertheless, some simple and long-established mycological methods may be useful for understanding TA-fungi interactions. For example, damp chambers are a simple method for a long-term cultivation of saprotrophic microfungi [32, 62] and may offer optimal conditions for growth and reproduction of TA as well.

In our study, we used damp chambers to screen TA populations and saprotrophic microfungi colonizing *Pinus sylvestris* L. litter needles. During cultivation, a melanized mycelium of the anamorphic ascomycete *Anavirga laxa* Sutton radiated from pine needles in some chambers. Subsequently, *Phryganella acropodia* (Hertwig & Lesser) Hopkinson individuals multiplied in the chambers with *A. laxa* and their distribution was affected by the distribution of the *A. laxa* mycelium. *P. acropodia* is often found in association with saprophytic fungi on decaying pine needles [M.-M. Coûteaux, pers. comm., sec. in 44], but the nature of the association is unclear. It is unknown whether *P. acropodia* selectively feeds on certain guilds of fungi, utilizes hyphal fragments, hyphal exudates or bacteria in the hyphosphere, or a combination of both fungal and bacterial food sources. On the other hand, the fate of the dead *P. acropodia* individuals is also

unknown. In our previous report, we showed that TA shells were suitable nutrient source for some mycorrhizal and root endophytic fungi [56].

To address these questions, we tested whether a relationship between *P. acropodia* and other TA and pine needle microfungi existed in an experimental microcosm with pine litter needles. More specifically, we investigated the composition of TA communities on and around the needles and the spatial relationship between the *A. laxa* mycelium and *P. acropodia* shells. Additionally, we asked whether *P. acropodia* utilized the *A. laxa* mycelium as a nutrient source and screened whether *P. acropodia* shells were colonized by hyphae of the microfungi inhabiting the experimental microcosm.

Methods

Construction of damp chambers

Scots pine needles were collected from an unmanaged pine forest in National Park Bohemian Switzerland in North Bohemia (Czech Republic). Collections were taken from the top of a sandstone massif “Růžová zahrada”, about 450 m a. s. l. (50°53’20.28” N, 14°24’53.82” E). The forest (plant association *Dicrano–Pinetum*) has interspersed birch (*Betula pendula* Roth) and a herb layer that consists of *Vaccinium vitis-idaea* L. and *V. myrtillus* L. The soil is shallow (10–45 cm) and has an uppermost layer of more humus. Needles from the F1 layer were inserted into sterile plastic bags and transported to the laboratory.

Damp chambers consisted of glass 15-cm diameter Petri dishes with a piece of a plastic mesh overlain by a layer of cellular tissue and filter paper. They were moistened with distilled water and sterilized in an autoclave. Single intact needles were separated from the bulk samples and inserted equidistantly into sterile damp chambers (8–10 needles per each chamber). Ten damp chambers containing 91 needles were set up and maintained at ambient light and room temperature. The growth of fungi was observed periodically for three months.

A wide spectrum of microfungi was recovered from the pine needles and some of their mycelia were accompanied by TA shells (data not shown). With progressing time, the surface of one damp chamber became dominated by melanized mycelium of *A. laxa* accompanied by numerous *P. acropodia* shells (Figure 1). *A. laxa* was identified based on conidia morphology according to Sutton [51]. Confirmatory molecular identification was not possible as, at the time of publication, no nucleotide sequences of *A. laxa* were deposited in a public database (GenBank). Domination of the experimental system by a single fungal species was necessary for our study because interactions among different fungi would most likely hamper proper statistical analyses. Therefore, we used this chamber for subsequent investigations.

Testate amoebae communities

Eight pine needles and five + five squares (each 25 mm^2) of filter paper adjacent to the needles and colonized or non-colonized by the *A. laxa* mycelium were extracted from the damp chamber. Both the needles and the filter paper squares were screened with a FEI Quanta 200 scanning electron microscope in the Olympus ESEM^{TM} mode for the presence of TA shells. TA species were determined according to Balík [2, 3], Bartoš [5], Deflandre [15, 16], Ogden and Hedley [43] and Patterson *et al.* [45]. The total number of TA individuals and their density per mm^2 was calculated for the three scenarios, pine needles, and colonized or non-colonized filter paper. 1312 shells were identified in total. The Shannon H index was calculated for the three scenarios using PAST 1.4 [24]. Additionally, colonization of *P. acropodia* shells by fungi was documented using scanning electron microscopy, and the relative proportion of the *P. acropodia* shells occurring on and nearby the mycelium were calculated for the filter paper squares with the *A. laxa* mycelium.

Spatial correlation between A. laxa mycelium and P. acropodia shells

Next, the spatial correlation between the mycelium of *A. laxa* and the shells of *P. acropodia* was investigated. Specifically, we were interested in determining whether a statistically significant relationship between the mycelium and the shells could be inferred from their respective positions on the filter paper. The method used consisted of approximating the mycelium by a large number of discrete points, which were randomly distributed along the curves representing the mycelium, so that the essential details of the mycelium were reflected in the spatial relationship. We first approximated the mycelium by a number of line segments. Next we chose a fixed positive parameter λ and scattered uniformly and independently n (λ, l) points along each of these line segments; n (λ, l) was a random number with a Poisson distribution with mean λl where l is the length of the line segment. This resulted in a bivariate marked point process: we assigned the mark "1" to the points representing the mycelium and the mark "2" to the points representing the centers of the shells (Figure 2).

To perform an exploratory statistical analysis of the spatial correlation between the mycelium and the shells we estimated the partial pair correlation function $g_{12}(r)$ for the bivariate marked point process. The intuitive meaning of the partial pair correlation function $g_{12}(r)$ was as follows: $g_{12}(r)$dxdy described the normalized probability of finding a point of type "1" in an infinitesimally small sphere b(x) of volume dx and a point of type "2" in an infinitesimally small sphere b(y) of volume dy, where the distance between the two sphere centers was r. The convenient feature of the partial pair correlation function $g_{12}(r)$ as a tool of exploratory statistical analysis was its relatively straightforward interpretation, which in our context might be summarized as the following trichotomy: the value $g_{12}(r)$ =1 indicated no interaction between the mycelia and the shells, whereas $g_{12}(r)$ >1 indicated attraction and $g_{12}(r)$ <1 indicated repulsion.

To perform the confirmatory statistical analysis we tested the null hypothesis as the random superposition hypothesis, i.e., we tested if the two components of the marked point pattern, mark "1" representing the mycelia and mark "2" representing the shells, are independent. We used a Monte Carlo envelope test of random shifts on torus as detailed by Goreaud and Pelissier

[23]. For each of our marked point patterns we simulated other k ∈ N marked point patterns. In each of these k simulations all the points of type “1” were fixed and all the points of type “2” were shifted by a vector $\overrightarrow{OA}$, where A is a random uniform location in the observation window W, with a unique A for each individual simulation. In our analysis the observation window W was in all cases a rectangle, therefore we considered W to be a torus when performing the random shifts. For each simulated point pattern we estimated the bivariate L-function $L_{12}(r)$. Next, lower and upper envelopes $L_{12,\min}(r)$ and $L_{12,\max}(r)$, respectively, were constructed based on the k simulated patterns. If the estimate of the bivariate L-function $L_{12}(r)$ for the empirical marked point pattern was not within these envelopes, except the α fraction of the values r, the random superposition hypothesis was rejected. We assumed this general convention used in the context of point processes [29] to conform to the values k = 19 or k = 99, i.e., a statistical significance level of α=0.05 or α=0.01, respectively.

The input data set consisted of mycelium length and number of shells of *A. laxa* and *P. acropodia*, respectively. They were enumerated on five 2300 x 1700 µm microscopic images of the filter paper taken adjacent to the needles. The total length of the *A. laxa* mycelium and the number of *P. acropodia* shells were counted for each of the pictures using measuring tools in the Quick Photo Micro software. To perform the exploratory statistical analysis of the data we computed the kernel estimators of the partial pair correlation function $g_{12}(r)$ with translational edge-correction, the kernel being a simple box function with bandwidth h = 25 µm, for each of these five patterns. Since the observation windows of these five replicated patterns were congruent, we formed the averaged estimator of the partial pair correlation function by taking pointwise arithmetic means of these five estimators. To perform the confirmatory statistical analysis of the data we proceeded by testing the random superposition hypothesis as outlined above. All computations were performed in Mathematica (Wolfram Research, Inc., USA).

Results

The overall TA community in the damp chamber was dominated by members of Trinematidae, Phryganellidae and Euglyphidae. The most frequent species on the needles were *P. acropodia* and *Trinema lineare* Penard, while TA communities on the filter paper squares were dominated by *P. acropodia*. The ratio between the number of Trinematidae and *P. acropodia* individuals was 2.4 : 1 on the needles, and 1 : 5.9 on the colonized filter paper squares. There were no Trinematidae on the non-colonized filter paper squares (Table 1). The density of TA individuals and TA species richness and diversity were higher on the needles than on both *A. laxa*-colonized and non-colonized filter paper squares (Table 1). On the filter paper squares with the *A. laxa* mycelium, 53.8% of the *P. acropodia* shells were found on the mycelium with the remainder near but not in immediate contact with the mycelium.

Some of the *P. acropodia* shells were colonized by fungal hyphae with hyaline conidiophores bearing conidia (Figure 3), which was identified as *Pochonia bulbillosa* (W. Gams & Malla) Zare & W. Gams based on morphological characteristics [61]. Although *P. bulbillosa* occasionally formed conidiophores on the surface of the needles, conidiogenesis occurred mainly on *P. acropodia* shells.

In the first microscopic picture, there were 16 *P. acropodia* shells; the total length of the *A. laxa* mycelium (TLM) was 23804.4 µm which was approximated by 4475 points. In the second picture with 19 shells, TLM was 33052.8 µm and approximated by 6155 points. In the third picture with 22 shells, TLM was 34338.7 µm and the mycelium was approximated by 6478 points. In the fourth picture with 29 shells, TLM was 34711 µm and the mycelium was approximated by 6463 points. In the fifth picture with 22 shells, TLM was 27897.7 µm and TLM was approximated by 5170 points (Figure 2).

The estimators of the averaged partial pair correlation function indicated an attraction between the *A. laxa* mycelium and the *P. acropodia* shells at a range of up to 500 µm (Figure 4). The envelopes $L_{12,max}(r)$- $L_{12}(r)$ and $L_{12}(r)$- $L_{12,min}(r)$ resulting from 19 simulations of random shifts for the five patterns were created. Since the null line was above the confidence band for more than 5% of values of *r* for all five patterns, the hypothesis of random superposition was rejected for all

of these patterns (Figure 5), which indicates attraction between the *A. laxa* mycelium and the *P. acropodia* shells was statistically significant at $\alpha = 0.05$.

Discussion

Pine litter represents a considerable carbon pool which is primarily utilized by variety of soil fungi [17, 40, 54]. Some authors have attempted to link fungal succession on pine litter needles with faunal succession [46] and to determine the food substrate for microfauna inhabiting this ecosystem [47]. However, reports on the structure of TA communities found in coniferous litter are scarce and have not evaluated interactions between TA and decomposer fungi [48]. By contrast, by employing an experimental system traditionally used in mycological studies [26, 32, 55], we showed that TA are common inhabitants of the pine litter and their interactions with saprotrophic microfungi may significantly affect their fate, and potentially influence TA distribution, lifespan and turnover of their shells.

The composition of the TA community at the end of our experiment may have been influenced by the cultivation conditions, especially the constant high levels of humidity in the damp chamber. Lousier [35, 36] showed that an increase in soil moisture content caused a significant increase in active TA and a proportional decrease of their encysted forms. Interestingly, Lousier [36] pointed out that at high soil moisture, the proportion of encysted forms was enhanced to a greater degree for the large (>60 µm) compared to small TA, which dominated the TA community in the study. However, in our experiment, the generally smaller Trinematidae did not successfully colonize the filter paper, which was instead dominated by the large-diameter *P. acropodia*, suggesting that moisture did not influence TA activity and dispersion as previously described.

At the family level, the TA community on the needle surface roughly corresponded to the community observed by Schönborn [48] in raw humus of two Norway spruce forests in Thuringia (Germany). *P. acropodia* dominated both the surface of the needles (together with *Trinema* spp.)

and the filter paper. Congruently, *P. acropodia* has been reported as the most frequent TA in oak-beech and spruce forest soils in Europe [9, 10]. Therefore, it appears that the realized TA diversity in the damp chamber did not substantially differ from situations in the field. *A. laxa* was previously reported to colonize both deciduous [18] and coniferous litter [32] and *P. bulbillosa* has been commonly isolated from coniferous soils [57]. It is therefore likely that *P. acropodia* also comes into contact with these fungi under natural conditions.

The needle surface was the most suitable microhabitat for TA as opposed to the filter paper without the *A. laxa* mycelium, where the number of total TA individuals decreased by 20-fold and *P. acropodia* by 6-fold relative to the pine needles. However, when *A. laxa* mycelium was present, the TA numbers decreased only approximately 4 times (*P. acropodia* approx. 1.5 times) relative to the pine needles. Interestingly, *Trinema* spp. numbers decreased 34-fold on the *A. laxa*-colonized filter paper relative to the pine needles and decreased to zero in the absence of *A. laxa*. This, together with the significant affinity of the *P. acropodia* individuals to the *A. laxa* mycelium, clearly demonstrates the determining role of the fungal mycelium in the dispersion of TA in the microcosm. A similar result was also obtained in the field study carried out by Napolitano and Flanagan [42], who demonstrated that the amount of the mycelium was a primary determinant of the density of soil amoebae in the carphosphere of *L. trullisata*.

P. acropodia appears to be a mycophagous species that dominates TA communities in soils [13]. It is reported to associate with microfungi on decaying pine needles (M.-M. Coûteaux, pers. comm., sec. in 44; this study) and its occurrence is strongly correlated with ergosterol concentrations (a fungal biomass marker) along an altitudinal transect in tropical mountain rain forests in Ecuador [33]. Mycophagy of *P. acropodia* was originally proposed based on observations in two experimental studies. First, Coûteaux and Dévaux [11] added four sporulating saprotrophic microfungi into microcosms which contained soil humus naturally colonized by TA and observed a significant increase in the frequency of *P. acropodia* (but not other TA) in the experimental systems upon addition of saprophytic microfungi. Second, Coûteaux [12] added malt extract (ME) to induce fungal growth in a non-sterile soil and tracked the response of the TA community. In the study, the number of *P. acropodia* individuals

increased with time and *P. acropodia* shells were often attached to fungal hyphae. Although adding ME did not alter the fungal biomass and there were no signs of grazing on fungal hyphae, the author concluded that *P. acropodia* was mycophagous. Yet, its association with fungi is intriguing and unclear. Similarly to Coûteaux [12], we often observed *P. acropodia* shells directly attached to the *A. laxa* mycelium. On the other hand, there were no signs of grazing and approx. one half of the shells were found alongside, rather than in direct contact with the *A. laxa* mycelium, suggesting that association with the mycelium is not a conclusive evidence of mycophagy by TA.

It seems that *P. acropodia* has varying levels of affinity to different fungi; it was the only TA species that responded positively to the addition of four sporulating saprotrophic microfungi into a humus microcosm [11], but was completely absent from the ectomycorrhizosphere of six coniferous species investigated by Ingham and Massicotte [30], and the mycorrhizosphere of *Rhododendron* spp. investigated by Sutton and Wilkinson [50] and Vohník et al. [56], and its occurrence did not correlate with the presence of arbuscular mycorrhizal fungi in tropical mountain rain forests in Ecuador [33]. This raises a question: why would *P. acropodia* prefer saprotrophic to mycorrhizal fungi?

In principle, mycophagous TA can choose from two different substrates: fungal hyphae and spores. To our knowledge, there is only one published study showing that TA are actually able to ingest fungal mycelium [22], while ingested spores were confirmed by Gilbert et al. [22] via light microscopy and by Ogden and Pitta [44] with electron microscopy. A relatively large and continuous production of digestible spores might be a reason why mycophagous TA prefer saprotrophic fungi, because most mycorrhizal fungi produce spores seasonally in aboveground sporocarps.

Spores were the most likely food source for *P. acropodia* in the study of Coûteaux and Dévaux [11]. However, in our experimental system, most *A. laxa* mycelium did not produce conidia (asexual spores) and if conidia were present, they oversized the shells of *P. acropodia* by one order of magnitude. Additionally, thick melanized hyphae are relatively resistant to grazing.

Therefore, an alternative explanation of the *P. acropodia – A. laxa* relationship is that the testate amoeba utilized either exudates of hyphae, bacteria associated with the *A. laxa* hyphosphere, or both. In all cases, *P. acropodia* would be dependent on the presence of the *A. laxa* mycelium, but could spread in its hyphosphere over the surface of the filter paper. In our experiment, such attraction was significant in the range of up to 500 µm from the mycelium. Indeed, bacteria seem to be a common mediator of the TA – fungi interactions. Both Ingham and Massicotte [30] and Timoten *et al.* [52] concluded that the significant differences in composition of TA communities around different types of ectomycorrhizae were due to the differential effect of ectomycorrhizal fungi on bacterial growth, with bacteria as the primary nutrient source for the observed protists. If we suppose that the fungal diversity was considerably higher on the needles than the filter paper, a differential effect of *A. laxa* on the assemblages of bacteria associating with its hyphosphere may explain why *Trinema* spp. and other bacteriophagous TA prospered on the needle surface, but were unable to spread on the filter paper surface.

The hundreds to thousands of *P. acropodia* shells that developed in our experimental systems represented a significant nutrient pool. Congruently, under natural conditions, TA constitute a significant part of the community of soil protists. They represented 48% of the total microbial biomass (excluding fungi) in a *Sphagnum* peatland [20] and nearly 14% of the total microbial biomass (including fungi) in a *Sphagnum fallax – Carex rostrata* fen [21]. The processes involved in the decomposition of the TA shells are, however, largely unknown. Couteaux [14] found no significant decomposition of TA shells in a sterilized organic acid soil five weeks after inoculation with a mixed bacterial inoculum. This suggests that bacteria are not the primary decomposers of dead TA shells. On the other hand, decomposition of litter and soil TA shells may be relatively fast: Lousier and Parkinson [38] found that within two weeks, 89-98% of empty tests made of self-secreted plates (idiosomes) and 47-83% of empty tests made of agglutinated organic or mineral particles (xenosomes) may decompose under controlled experimental conditions. Vohník et al. [56] observed that TA shells collected from the *Rhododendron* mycorrhizospheres were frequently colonized by fungal hyphae; up to 45% of the *Trigonopyxis* shells were found in association with fungal hyphae. Additionally, the authors showed that *Cyclopyxis* and

Trigonopyxis shells were regularly decomposed by two root-symbiotic fungi *in vitro*. This suggests that soil fungi rather than bacteria might be the primary decomposers of TA shells under natural conditions.

An increased incidence of *P. bulbillosa* on *P. acropodia* shells suggests a direct trophic interaction. Most probably, *P. bulbillosa* parasitized *P. acropodia* encysted cells or decomposed already dead individuals. To our knowledge, there is no published information on fungal parasites of testate amoebae. However, selective fungal parasitization of encysted TA shells may significantly affect the lifespan of TA and the structure of TA communities in soils. *Pochonia* spp. are producers of numerous secondary metabolites that mediate their parasitism of invertebrates and mycoparasitism [31]. For example, Fassatiová and Lysek [19] isolated *P. bulbillosa* from *Ascaris* (Nematoda) eggs and Moosavi *et al.* [41] successfully tested the infectivity of several *Pochonia* spp. on eggs of root-knot nematode. On the other hand, *P. bulbillosa* is used as a food source by some plant parasitic nematodes [28], suggesting that the relationship between the fungus and nematodes is ambivalent. Similarly, *P. bulbillosa* spores may be ingested by soil TA.

To conclude, saprotrophic/parasitic fungi seem to be frequent partners of testate amoebae in soils. Their most notable direct interactions involve mycophagy, fungal parasitism and decomposition of TA shells. Additionally, soil fungi may indirectly influence TA populations through their influence on bacterial communities in the hyphosphere. However, these potentially significant processes are currently poorly understood and undoubtedly deserve further investigation.

Acknowledgement

This study was supported by the Academy of Sciences of the Czech Republic (research projects AV0Z60050516 and AV0Z50110509), Ministry of Education, Youth and Sports (research program LC06063) and Grant Agency of the Czech Republic (206/09/P295). The authors thank David M. Wilkinson and Humphrey G. Smith for valuable comments on the results of the experiment, four

anonymous reviewers for their valuable effort and Jesse J. Sadowsky for a stylistic revision. MV thanks the foundation “Nadání Josefa, Marie a Zdenky Hlávkových” for funding his stay at Liverpool John Moores University, Liverpool, UK.

References

1. Aoki Y, Hoshino M, Matsubara T (2007) Silica and testate amoebae in a soil under pine-oak forest. Geoderma 142:29-35
2. Balík V (1992) Testate amoebae fauna (Protozoa, Rhizopoda, Testacea) from the marsh habitats in the Krkonoše Mountains National Park (Czechoslovakia). Opera Corcontica 29: 139-154
3. Balík V (1994) Testaceenfauna (Protozoa, Rhizopoda, Testacea) aus dem Naturschutzgebiet Žofínský prales (Novohradské hory Gebirge) in Südböhmen (Tschechische Republik). Act Mus Boh Meridion Č Budějovice 34: 55-67
4. Bamforth SS (1971) Numbers and proportions of Testacea and Ciliates in litters and soils. J Protozool 18: 24-28
5. Bartoš E (1954) Koreňonožce radu Testacea. Vydavaťelstvo Slovenskej Akadémie Vied, Bratislava. 1-185
6. Bonkowski M, Jentschke G, Scheu S (2001) Contrasting effects of microbial partners in the rhizosphere: interactions between Norway Spruce seedlings (*Picea abies* Karst.), mycorrhiza (*Paxillus involutus* (Batsch) Fr.) and naked amoebae (protozoa). Appl Soil Ecol 18: 193-204
7. Chakraborty S, Theodorou C, Bowen GD (1985) The reduction of root colonization by mycorrhizal fungi by mycophagous amebas. Can J Microbiol 31: 295-297
8. Coleman DC (2008) From peds to paradoxes: Linkages between soil biota and their influences on ecological processes. Soil Biol Biochem 40: 271–289
9. Coûteaux MM (1975) Écologie des thécamoebiens de quelques humus bruts forestiers. Rev Ecol Biol Sol 12: 421-447
10. Coûteaux MM (1976) Dynamisme de l'equilibre des thécamoebiens dans quelques sols climaciques. Mem Mus Natl Hist Nat, Ser A Zool 96: 1-183

11. Coûteaux MM, Dévaux J (1983) Effet d'un enrichissement en champignons sur la dynamique d'un peuplement thécamoebien d'un humus. Rev Écol Biol Sol 20: 519-545
12. Coûteaux MM (1985) Relationships between testate amebas and fungi in humus microcosms. Soil Biol Biochem 17: 339-345
13. Couteaux MM, Darbyshire JF (1998) Functional diversity amongst soil protozoa. Appl Soil Ecol 10: 229-237
14. Couteaux MM (1992) Decomposition of cells and empty shells of testate amebas (Rhizopoda, Testacea) in an organic-acid soil sterilized by propylene-oxide fumigation, autoclaving, and gamma-ray irradiation. Biol Fert Soil 12: 290-294
15. Deflandre G (1929) Le genre *Centropyxis* Stein. Arch Protistenkd 67: 322-375
16. Deflandre G (1936) Etude monographique sur le genre *Nebela* Leidy. Annals de Protistologie 5: 201-286
17. De Santo AV, Rutigliano FA, Berg B, Fioretto A, Puppi G, Alfani A (2002) Fungal mycelium and decomposition of needle litter in three contrasting coniferous forests. Acta Oecol 23: 247-259
18. Ellis MB, Ellis JP (1997) Microfungi on land plants. Richmond Publishing
19. Fassatiová O, Lysek H (1982) Ovicidal fungi in soil ecological system. Acta Univ Carol Biol 9: 297–334
20. Gilbert D, Amblard C, Bourdier G, Francez A-J (1998a) The microbial loop at the surface of a peatland: structure, function, and impact of nutrient input. Microb Ecol 35: 83-93
21. Gilbert D, Amblard C, Bourdier G, Francez A-J (1998b) Short-term effect of nitrogen enrichment on the microbial communities of a peatland. Hydrobiologia 373/374: 111-119
22. Gilbert D, Mitchell EAD, Amblard C, Bourdier G, Francez A-J (2003) Population dynamics and food preferences of the testate amoeba *Nebela tincta major-bohemica-collaris* complex (Protozoa) in a *Sphagnum* peatland. Acta Protozool 42: 99-104
23. Goreaud F, Pelissier R (2003) Avoiding misinterpretation of biotic interactions with the intertype K12-function: Population independence vs. random labeling hypotheses. J Veget Sci 14: 681–692

24. Hammer Ř, Harper DAT, Ryan PD (2001) PAST: Palaeontological Statistics software package for education and data analysis. Palaeontologia Electronica 4:9
25. Han BP, Wang T, Lin QQ, Dumont HJ (2008) Carnivory and active hunting by the planktonic testate amoeba *Difflugia tuberspinifera*. Hydrobiologia 596: 197-201
26. Hayes AJ (1965) Some microfungi from Scots pine litter. Trans Br Mycol Soc 48:179-185
27. Hogberg MN, Hogberg P (2002) Extramatrical ectomycorrhizal mycelium contributes one-third of microbial biomass and produces, together with associated roots, half the dissolved organic carbon in a forest soil. New Phytol 154: 791–795
28. Hasna I, Rämert L (2007) Food attraction and population growth of fungivorous nematodes with different fungi. Ann Appl Biol 151: 175-182
29. Illian J, Penttinen A, Stoyan H, Stoyan D (2008) Statistical Analysis and Modelling of Spatial Point Patterns. Wiley-Interscience
30. Ingham ER, Massicotte HB (1994) Protozoan communities around conifer roots colonized by ectomycorrhizal fungi. Mycorrhiza 5: 53-61
31. Koehn FE, Kirsch DR, Feng X, Janso J, Young Y (2008) A cell wall-active lipopeptide from the fungus *Pochonia bulbillosa*. J Nat Prod 71: 2045–2048
32. Koukol O (2007) Effect of *Pinus strobus* L. invasion on the mycoflora of pine litter needles in the Bohemian Switzerland National Park (Czech Republic). In: Sandstone Landscapes (Härtel H et al Eds). Academia, 493 pp
33. Krashevska V, Bonkowski M, Maraun M, Ruess L, Kandeler E, Scheu S (2008) Microorganisms as driving factors for the community structure of testate amoebae along an altitudinal transect in tropical mountain rain forests. Soil Biol Biochem 40: 2427-2433
34. Lindahl BD, Ihrmark K, Boberg J, Trumbore SE, Högberg P, Stenlid J, Finlay R (2007) Spatial separation of litter decomposition and mycorrhizal nitrogen uptake in a boreal forest. New Phytol 173: 611–620
35. Lousier JD (1974a) Effects of experimental soil-moisture fluctuations on turnover rates of Testacea. Soil Biol Biochem 6: 19-26

36. Lousier JD (1974b) Response of soil Testacea to soil-moisture fluctuations. Soil Biol Biochem 6: 235-239
37. Lousier JD (1982) Colonization of decomposing deciduous leaf litter by Testacea (Protozoa, Rhizopoda) - species succession, abundance, and biomass. Oecologia 52: 381-388
38. Lousier JD, Parkinson D (1984) Annual population dynamics and production ecology of Testacea (Protozoa, Rhizopoda) in an aspen woodland soil. Soil Biol Biochem 16: 103-114
39. Miller RM, Reinhardt DR, Jastrow JD (1995) External hyphal production of vesicular-arbuscular mycorrhizal fungi in pasture and tallgrass prairie communities. Oecologia 103: 17–23
40. Mitchell CP, Millar CS, Minter DW (1978) Studies on decomposition of Scots pine needles. Trans Br Mycol Soc 71: 343-348
41. Moosavi M-R, Zare R, Zamanizadeh H-R, Fatemy S (2010) Pathogenicity of *Pochonia* species on eggs of *Meloidogyne javanica*. J Invertebr Pathol 104: 125-133
42. Napolitano JJ, Flanagan VD (1981) Occurrence of amebas in and around the mushroom *Laccaria trullisata*. J Protozool 28: 494-497
43. Ogden CG, Hedley RH (1980) An atlas of freshwater testate amoebae. Oxford University Press, Oxford. 222 pp
44. Ogden CG, Pitta P (1990) Biology and ultrastructure of the mycophagus, soil testate ameba, *Phryganella acropodia* (Rhizopoda, Protozoa). Biol Fert Soils 9:101-109
45. Patterson RT, Dalby A, Kumar A, Henderson LA, Boudreau EA (2002) Arcellaceans (thecamoebians) as indicators of land-use change: settlement history of the Swan Lake area, Ontario as a case study. J Paleolimn 28: 297-316
46. Ponge JF (1991a) Succession of fungi and fauna during decomposition of needles in a small area of Scots pine litter. Plant Soil 138: 99-113
47. Ponge JF (1991b) Food resources and diets of soil animals in a small area of Scots pine litter. Geoderma 49: 33-62

48. Schönborn W (1986) Population dynamics and production biology of testate amebas (Rhizopoda, Testacea) in raw humus of 2 coniferous forest soils. Arch Protistenkd 132: 325-342
49. Schönborn W (1992) Comparative studies on the production biology of protozoan communities in freshwater and soil ecosystems. Arch Protistenkd 141**:** 187-214
50. Sutton CA, Wilkinson DM (2007) The effects of *Rhododendron* on testate amoebae communities in woodland soils in north west England. Acta Protozool 46: 333-338
51. Sutton BC (1975) Hyphomycetes on cupules of *Castanea sativa*. Trans Br Mycol Soc 64: 405-426
52. Timoten S, Christensen S, Ekelund F (2004) Distribution of protozoa in Scots pine mycorrhizospheres. Soil Biol Biochem 36: 1087-1093
53. Todorov M (2001) Testate amoebae (Protozoa: Rhizopoda) in soil and litter of beech forests (*Fagus sylvatica* L.) from Bulgaria. Act Zool Bulg 53: 19-36
54. Tokumasu S, Aoki T, Oberwinkler F (1994) Fungal succession on pine needles in Germany. Mycoscience 35: 29-37
55. van Maanen A, Gourbière F (1997) Host and geographical distribution of *Verticicladium trifidum*, *Thysanophora penicillioides*, and similar fungi on decaying coniferous needles. Can J Bot 75:699–710
56. Vohník M, Burdíková Z, Albrechtová J, Vosátka M (2009) Testate amoebae (Arcellinida and Euglyphida) vs. ericoid mycorrhizal and DSE fungi: a possible novel interaction in the mycorrhizosphere of ericaceous plants? Microb Ecol 57: 203-214
57. White JF, Bacon CW, Hywel-Jones NL, Spatafora JW (2003) Clavicipitalean fungi: evolutionary biology, chemistry, biocontrol, and cultural impacts. CRC Press, 575 pp.
58. Wilkinson DM (2008) Testate amoebae and nutrient cycling: peering into the black box of soil ecology. Trend Ecol Evol 23: 596-599
59. Wilkinson DM, Mitchell EAD (2010) Testate amoebae and nutrient cycling with particular reference to soils. Geomicrobiol J 27: 520-533

60. Yeates GW, Foissner W (1995) Testate amebas as predators of nematodes. Biol Fert Soils 20: 1-7
61. Zare R, Gams W, Evans HC (2001) A revision of *Verticillium* section *Prostrata*. V. The genus *Pochonia*, with notes on *Rotiferophthora*. Nova Hedwigia 73: 51-86
62. Zucconi L, Pasqualetti M (2007) Microfungal assemblage on *Quercus ilex* leaf litter in Tuscany, central Italy. Plant Biosystems 141: 305-313

Figure 1 The dark *Anavirga laxa* mycelium radiates from a *Pinus sylvestris* needle (N) and supports the growth of *Phryganella acropodia* (its shells visualized as black dots). Bar corresponds to 1 mm.

Figure 2 One of the five transformed microscopic pictures used to investigate the spatial correlation between the *Anavirga laxa* mycelium and the shells of *Phryganella acropodia*. The *A. laxa* mycelium radiating from *Pinus sylvestris* needles is approximated by 4475 black points; the centers of the TA shells are represented by 16 blue dots. The total length of the mycelium is 23804.4 µm. For details on the exploratory and confirmatory statistical analyses see Methods.

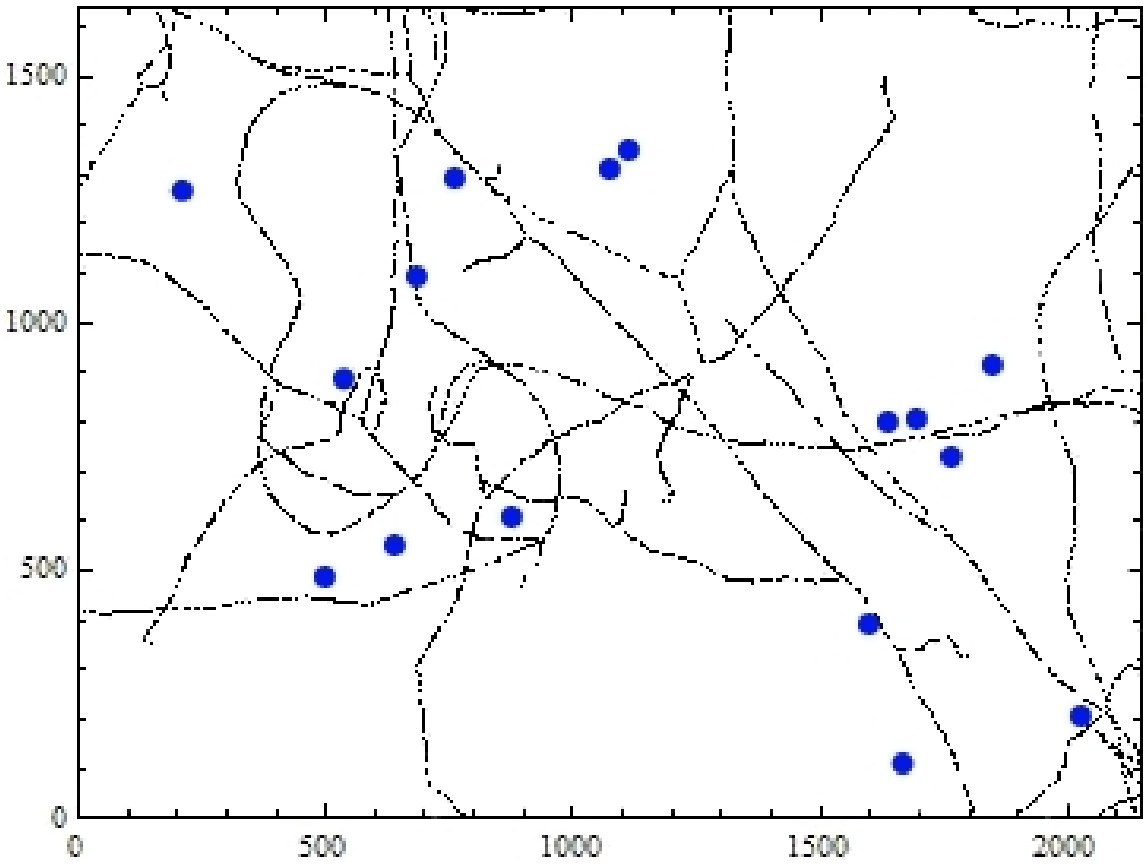

Figure 3 Conidiophores of *Pochonia bulbillosa* emerging from *Phryganella acropodia* shells. Bars correspond to 50 µm.

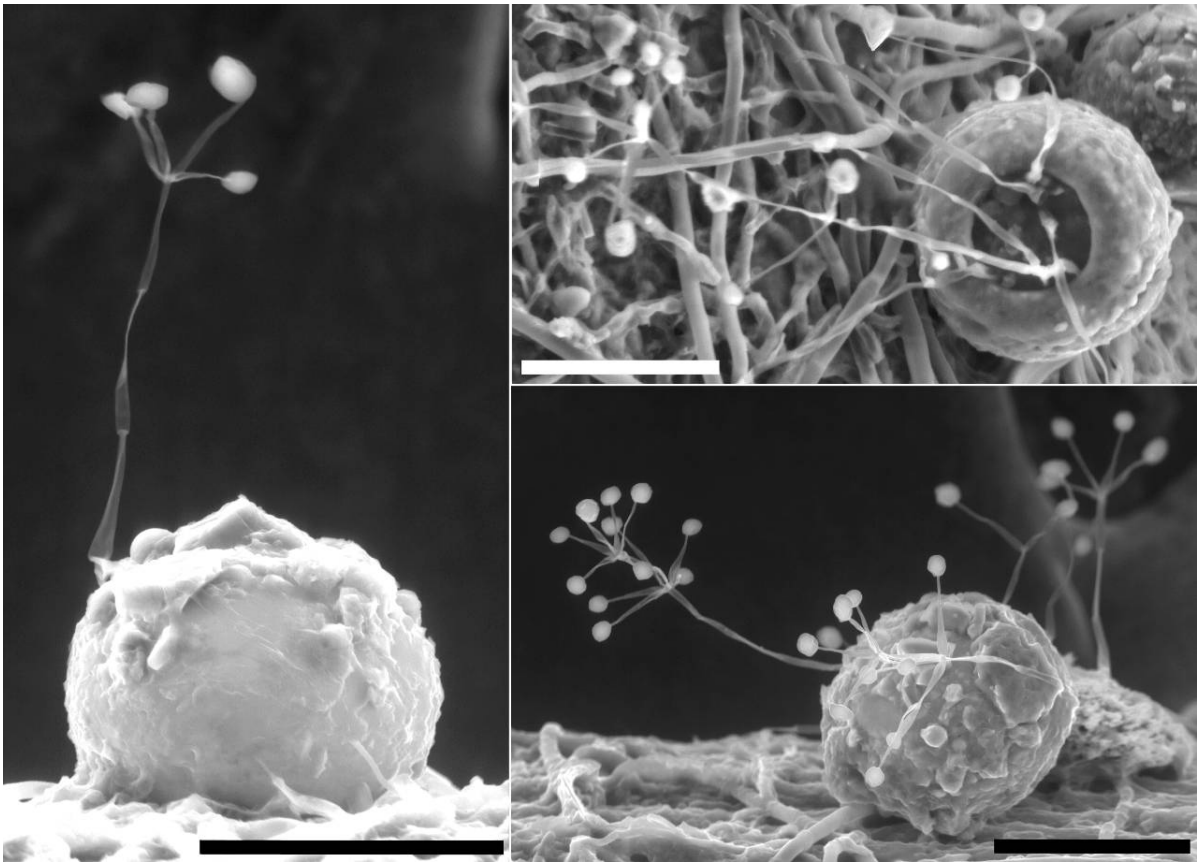

Figure 4 The averaged estimated partial pair correlation function for the dataset of the five transformed microscopic pictures (See Figure 2). It indicates attraction between the *Anavirga laxa* mycelium and the shells of *Phryganella acropodia* in the range of up to 500 µm.

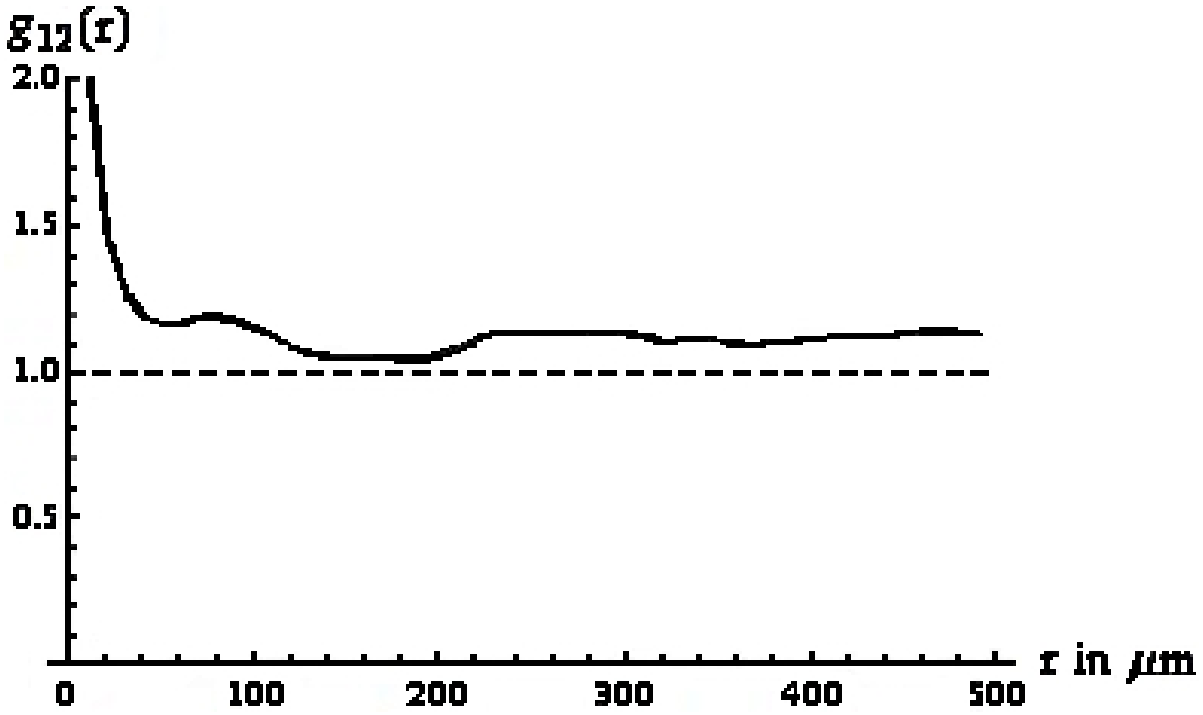

Figure 5 The envelope $L_{12,max}(r)$- $L_{12}(r)$ and $L_{12}(r)$- $L_{12,min}(r)$ resulting from 19 simulations of random shifts for a transformed microscopic picture (Figure 3). Since the null line is outside the confidence band for many more than 5% values of r, the hypothesis of random superposition is rejected. This means that the attraction between the *A. laxa* mycelium and the *P. acropodia* shells was confirmed by the confirmatory statistical analysis at the significance level $\alpha = 0.05$.

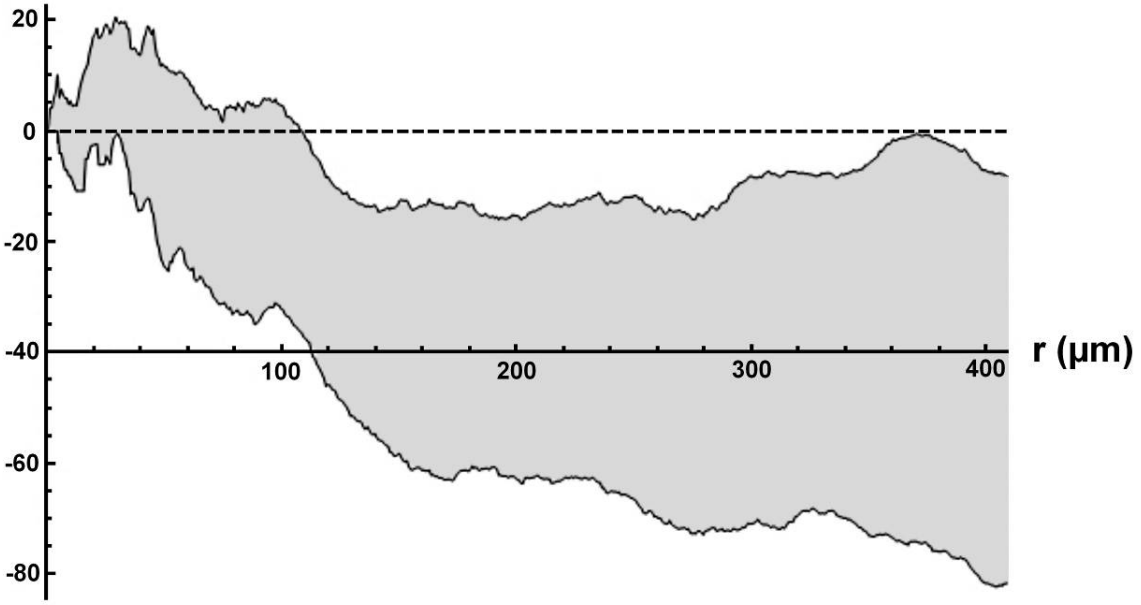

Table 1 The spectra and numbers of testate amoebae found on the *Pinus sylvestris* needles and on the filter paper colonized (Paper + myc) and non-colonized (Paper - myc) by the *Anavirga laxa* mycelium. The density of the respective species per mm^2 is in parentheses. For further details see Methods.

	Needles (45 mm^2)	**Paper + myc** (125 mm^2)	**Paper - myc** (125 mm^2)
EUGLYPHIDA			
Assulinidae			
Assulina muscorum	15 (0.34)	6 (0.05)	
Euglyphidae			
Euglypha compressa	1 (0.02)		
Euglypha rotunda	13 (0.29)		
cf. *Euglypha*	8 (0.18)	1 (0.01)	1 (0.01)
Trinematidae			
Corythion dubium	43 (0.96)	15 (0.12)	
Trinema complanatum	28 (0.63)		
Trinema enchelys	27 (0.60)	1 (0.01)	
Trinema lineare	266 (5.95)	10 (0.08)	
cf. *Trinema*	325 (7.28)	8 (0.06)	
ARCELLINIDA			

Centropyxidae *Centropyxis aerophila*	2 (0.05)		
Hyalospheniidae cf. *Nebela*	1 (0.02)		
Phryganellidae *Phryganella acropodia*	290 (6.45)	199 (1.59)	49 (0.39)
Plagiopyxidae *Bullinularia indica*	1 (0.02)		
Trigonopyxidae cf. *Trigonopyxis*	1 (0.02)		1 (0.01)
TOTAL	1021 (22.80)	240 (1.92)	51 (0.41)
Shannon index (H)	1.595	0.712	0.193

5. SHRNUTÍ A DISKUSE

Analýza krytének novými mikroskopickými technikami

Pro aplikaci výsledků pozorování krytének do ekologického výzkumu je důležité přesné taxonomické zařazení, rozlišení mrtvých / živých jedinců; s příchodem a aplikací molekulárních dat, však je nutné toto hodnocení obohatit o další parametry. Pro studium parametrů společenstev krytének jsme použili konfokální a dvoufotonovou mikroskopii. Celkem jsme vyzkoušeli 16 fluorescenčních barev pro zvýraznění různých buněčných struktur, z toho 10 úspěšně. Díky fluorescenčnímu barvení, konfokální a dvoufotonové mikroskopii jsme byli schopni zobrazit jádro, cytoplasmu, membrány, některé organely (mitochondrie, endoplasmatické retikulum) a symbiotické řasy u mixotrofních druhů. Rovněž rozlišení živých a mrtvých jedinců díky fluorescenčnímu barvení propidium jodidem a BCECF-AM bylo úspěšné a do budoucna by mohlo nahradit doposud používané nespolehlivé barvení Bengálskou růžovou (Bernhard, 2000). U několika jedinců jsme zkoumali také autofluorescenci chlorofylu symbiotických řas uvnitř schránky. Pro proostření menších rodů krytének (např. Trinema, Euglypha) postačilo použití klasické konfokální mikroskopie. Pro rody s typickou velikostí nad 100 μm a rody s aglutinovanou schránkou bylo pro úspěšné proostření celého živočicha nutné použít dvoufotonovou mikroskopii. Obě tyto zobrazovací metody byly použity pro studium krytének poprvé a poprvé byly takto detailně zobrazeny buněčné struktury krytének. Na takto získaná data je možné aplikovat stereologické metody např. pro výpočet biomasy či prostorovou vizualizaci. Ve spojení s 3D rekonstrukcemi a stereologickými metodami jsou tyto zobrazovací metody zajímavé zejména pro taxonomii, ekofyziologii a ekotoxikologii krytének.

Sezónní variabilita krytének a jejich závislost na limnologických parametrech prostředí v Komořanských tůňkách

Druhové složení společenstva krytének v Komořanských tůních se během roku výrazně mění. Nejhojněji jsou v lokalitě zastoupeny rod *Arcella*, *Centropyxis* a *Difflugia*. Na počátku roku převládá ve společenstvu rod *Arcella*. V letních měsících je nejpočetnější rod *Difflugia*. Rod *Centropyxis* je přítomen během celého roku. Zdá se tedy, že rod *Arcella* a *Difflugia* mají opozitní životní strategie a ekologické preference.

Porovnáním významnosti jednotlivých limnologických ukazatelů pro společenstvo krytének v průběhu roku jsme zdokumentovali další poznatky o jejich ekologii. Mitchell (2004) tvrdí, že změny ve společenstvu krytének jsou způsobeny změnou abiotických faktorů prostředí. Z mého pozorování vyplývá, že rod *Arcella* upřednostňuje vody s nízkou koncentrací organického materiálu a nižší teplotou. *Difflugia* preferuje vody eutrofního charakteru, což odpovídá zjištěním Qina (2009), který popisuje druh *Difflugia oblonga* jako excelentní indikátor eutrofizace vodního systému. Obecně rod *Centropyxis* nevykazoval statisticky významné valence k jednotlivým limnologickým parametrům. Reinhardt (1998) popisuje výskyt rodu *Centropyxis* z vod kontaminovaných a organicky bohatých. Další autoři charakterizují rod *Centropyxis* jako oportunistický (Roe, 2010; Scott, 2001). Významnými limnologickými ukazateli jsou ionty NH_4^+a NO_3^- (Gilbert, 1998). Krashevska et al. (2010) studovala dopad dusíku na hustotu krytének a jeho dopad na specifické druhy. Z mého pozorování vyplývá statisticky významná korelace s ionty NH_4^+a NO_3^- . Podle RDA analýzy ovlivňují komunitu krytének v tůňkách: těžké kovy (As, Pb, Cd, Mn, Ni) a PAH.

Těžké kovy jsou intenzivně sledovanými znečišťovateli životního prostředí z důvodů jejich vysoké toxicity a dopadu na mikroorganismy (Nguyen-Viet, 2008). Davis a Wilkinson (se domnívají, že rod Centropyxis je tolerantní ke znečištění těžkými kovy a výsledky RDA analýzy tomu odpovídají. RDA analýzy u většiny druhů krytének dokazují negativní korelaci s těžkými kovy. Např. rod *Centropyxis* vykazuje citlivost vůči kontaminaci arsenu avšak relativní necitlivost ke koncentraci niklu. Vysokou citlivost krytének vůči arsenu potvrzuje Patterson (2002). Z přítomných druhů vykazuje v tůňkách statisticky signifikantní citlivost rod *Arcella* negativního charakteru. *C. discoides*, *D. oblonga*, *D. bartosi* a *D. oviformis* mají naopak pozitivní toleranci k přítomnosti arsenu. Esenciální živina a komponenta schránky pro kryténky je železo (Fe). Extracelulární ukládání železa může být také spojeno s detoxifikačními mechanismy, jež umožní buňce ponechat všechny kovy včetně železa na vnější straně buněčné membrány (Payne, 2011). V našem výzkumu se ukázalo, že rod *Arcella* má mírně pozitivní korelaci s Fe a rod *Difflugia* mírně negativní.

Interakce mezi kryténkami a mykorhizními a saprotrofními houbami

Mykorhizní a saprotrofní houby se liší v mnoha ohledech, pravděpodobně nejdůležitějším rozdílem je ale způsob, jakým ze svého okolí získávají uhlík. Zatímco saprotrofní houby ho získávají z odumřených částí jiných organizmů, původ uhlíku využívaného houbami mykorhizními je ve fotosyntéze a tedy de facto ve vzdušném oxidu uhličitém. Na jedné straně tedy saprotrofní houby limituje přítomnost organického substrátu, na druhé jsou mykorhizní houby limitovány svou realizovanou schopností interagovat s rostlinami, tedy autotrofními organismy, které většinou nejsou zdrojem uhlíku limitovány. To má velký důsledek i pro kryténky, které s oběma druhy půdních hub běžně interagují. Zatímco v organickém opadu většinou bývá houbového mycelia dostatek, a to jak saprotrofního, tak mykorhizního, v čistě minerálních substrátech se vyskytují pouze houby, které čerpají uhlík z jiných organizmů. O krytenkách je známo, že dokážou pro svou výživu využívat mycelium půdních hub; mykorhizní rostliny tak mohou nepřímo ovlivňovat distribuci a abundanci krytének ve své mykorhizosféře právě přes své symbiotické houby.

V Článku 1 jsme ukázali, že tento vztah může být velmi komplexní. Kryténky mohou ke své výživě využívat jak mycelium půdních hub, tak jeho exudáty a pravděpodobně i baktérie asociované s jejich hyfosférou. Ve rhizosféře mykorhizních rostlin tedy mají velkou evoluční výhodu skupiny krytének, které se naučily využívat přítomnosti mycelia mykorhizních hub. Na druhou stranu představuje biomasa odumřelých krytének v některých půdách podstatný zdroj živin, přičemž se jedná zejména o rašeliniště a vřesoviště, tedy habitaty většinou dominované vřesovcovitými rostlinami. Jak již bylo vysvětleno v úvodu, asociují vřesovcovité rostliny se zvláštní skupinou půdních hub, se kterými tvoří erikoidní mykorrhizy. Erikoidně mykorhizní houby přitom dokážou z celé skupiny mykorhizních hub asi nejlépe využívat chitin jako zdroj dusíku. Dusík je vedle fosforu nejdůležitějším makroprvkem, který podstatně ovlivňuje rozšíření a druhovou pestrost a bohatost rostlin a řada rostlin při jeho získávání spoléhá právě na mykorhizní houby. Uvědomíme-li si, že dusíkem bohatý chitin tvoří velmi důležitou složku schránek řady krytének, nemůžeme si nepovšimnout velmi zajímavého momentu: interakce mezi kryténkami a myceliem mykorhizních hub může být oboustranná, jedny konzumují druhé, aby byly posléze svou předchozí potenciální potravou “navráceny” do koloběhu živin v rhizosféře, přičemž do této sítě interakcí přirozeně vstupují rostliny jako primární zdroj uhlíku, který tento

hypotetický minicyklus dusíku pohání. V Článku 1 jsme podali řadu nepřímých důkazů o jeho možné existenci.

Článek 2 se naproti tomu zabývá interakcemi krytének a saprotrofních hub, které jsme zkoumali ve zjednodušeném mikrokosmu simulujícím podmínky panující v opadu borovice lesní. Opad obecně je rozkládán celou řadou specializovaných saprotrofních hub, přičemž je v případě jehličnatých stromů možno zjednodušeně konstatovat, že jako první nastupují houby vřeckovýtrusé, které jsou postupně v sukcesi vystřídány houbami stopkovýtrusými. Narážíme zde na další z hlediska výživy krytének významný rozdíl mezi saprotrofními a mykorhizními houbami – první skupina totiž tvoří velmi ochotně obrovské množství spór, a to často přímo v substrátu, který kolonizují, tedy pod povrchem půdy. Zdá se, že pro řadu krytének je snazší využívat jako zdroj potravy právě spóry, nikoliv aktivní mycelium, a lze tak předpokládat, že bude řada krytének přizpůsobena interakci právě se saprotrofními houbami tvořícími ochotně spóry. V Článku 2 jsme ukázali, že jedna z nejhodnějších krytének kolonizujících jak listnatý tak jehličnatý opad, *Phryganella acropodia*, umí na rozdíl od jiných krytének efektivně využívat přítomnost mycelia saprotrofní houby *Anavirga laxa*. Mycélium této houby signifikantně ovlivňovalo distribuci kryténky *P. acropodia*, ta se také v jeho přítomnosti úspěšně rozmnožovala a postupně opanovala celý experimentální systém, na úkor ostatních krytének. Zjistili jsme přitom, že zdrojem potravy pro *P. acropodia* velmi pravděpodobně není přímo tlustostěnné melanizované mycelium *A. laxa*, ale spíše jeho produkty, tedy hyfové exudáty, nebo baktérie živící se těmito exudáty. Opět se tedy může jednat o značně komplexní, z části zprostředkovanou interakci mezi několika zcela odlišnými skupinami organizmů (kryténky, houby, baktérie). V Článku 2 jsme opět ukázali, že schránky odumřelých krytének představují v půdním prostředí bohatý koktejl živin, který je nejspíše hojně využíván houbami: odumřelé, popř. dormantní schránky *P. acropodia* byly totiž na konci našeho pokusu hojně kolonizovány houbou *Pochonia bulbillosa*, přičemž tato houba tvořila konidiofory především na myceliu vyrůstajícím ze schránek *P. acropodia*. Není bez zajímavosti, že rod *Pochonia* obsahuje druhy, které jsou specializovanými predátory půdních háďátek.

6. ZÁVĚR

V metodické studii jsem použila pokročilé mikroskopické techniky - CLSM a TPEM. Použití těchto technik přineslo nové poznatky o vnitřních strukturách krytének, pomohlo přesněji rozlišit živé/mrtvé jedince ve vzorku, než doposud běžně používané metodiky a po aplikaci stereologických metod se ukázala tato metodika vhodná i pro výpočet biomasy uvnitř schránky. Celoročním pozorováním se podařilo zachytit změny v druhovém společenstvu krytének. Pozorovala jsem nejdříve rozvoj rodu *Arcella* následovaný rodem *Centropyxis* v jarních měsících. Během letních měsíců došlo k nástupu rodu *Difflugia* a postupnému ústupu rodu *Arcella*. Statistická analýza korelovala signifikantně společenstva krytének s teplotou, koncentrací fosforu, NH_4^+, NO_3^-, As, Pb, Cd, Mn, Ni, PAH a Fe.

Dokumentovala jsem s kolegy interakci mezi kryténkami a kořeny rododendronu asociovanými s mykorhizními houbami, spojenou myceliem s mykorhizními kořeny. Naše pozorování a zjištění spolu s publikovanými články přináší podporu hypotéze, že kryténky mohou být zdrojem živin pro hostitelskou rostlinu.

Zjistila jsem, že saprofytické/parazitické houby interagují s kryténkami ve smrkovém opadu. Půdní houby nepřímo ovlivňují populaci krytének, díky jejich vlivu na bakteriální populaci v hyphosféře. Tato interakce zahrnuje mykofagy, houbové parazity a dekompozici schránek krytének.

7. SEZNAM POUŽITÉ LITERATURY

1. Bubík M, (1997) What is *Rothina silesica*? A taxonomic revision of the genus Rothina. (Foraminiferida) Ann. Societas geologum. Poloniae, 67(2-3): 175-182.

2. Cázares E, Trappe JM, Jumpponen A (2005) Mycorrhiza-plant colonization patterns on a subalpine glacier forefront as a model systém of primary succesion. Myccorhiza 15: 405-416

3. Charman DJ, Roe HM, Gelhels WR (1998) The use of testate amoebae in studies of sea level change: a case study from the Taf estuary, South Wales, UK. The Holocene 8: 209-218

4. Dallimore A, Schro¨der-Adams CJ, Dallimore SR. 2000. Holocene environmental history of thermokarst lakes on Richards Island, Northwest Territories, Canada: thecamoebians as paleolimnological indicators. Journal of Paleolimnology 23: 261–283.

5. Escobar J, Brenner M, Whitmore TJ, Kenney WF, Curtis JH (2008) Ecology of testate amoebae (thecamoebians) in subtropical Florida lakes. Journal of Paleolimnology 40: 715-731

6. Gortari MC, Hours RA (2008) Fungal chitinases and their biological role in the antagonism onto nematode eggs. Mycological progress, 7 (4): 221-238

7. Lamentowicz M, Mitchell EAD (2005) The ecology of testate amoebae (protists) in Sphagnum in North-Western Poland in relation to peatland ecology. Microbial Ecology 50 (1), 48-63

8. Lorencová M (2009) Thecamoebians from recent lake sediments from the Sumava Mts, Czech Republic. Bulletin of geosciences, 84 (2): 359-376

9. Moraczewski J (1969) Composition chimique, structure et formation de la coque d'Arcella In Strelkov A.A., Sukhanova K.M., Raikov I. B. (Ed.) Progress in Protozool. (Proc. 3rd Int. Congr. Protozool.). Nauka Leningrad. Pp. 32-33

10. Ogden CG. (1983) Observations on the systematics of the genus Difflugia in Britain (Rhizopoda, Protozoa). Bulletin of. British Natural History, 44(1): 1-73

11. Patterson RT, Mackinnon KD, Scott DB, Medioli FS (1985) Arcellaceans ("Thecamoebians") in small lakes of New Brunswick and Nova Scotia: modern distribution and Holocene stratigraphic changes. Journal of Foraminiferal Research, 15(2):114-137

12. Patterson RT, Kumar A (2000) Assessment of arcellacean (thecamoebian) assemblages, species, and strains as contaminant indicators in James Lake, northeastern Ontario, Canada. Journal of Foraminiferal Research 30:310-320

13. Penard E. (1902) Faune rhizopodique du bassin du Léman. H. Kündig, Geneve

14. Porter SM, Knoll AH (2000) Testate amoebae in the Neoproterozoic Era: evidence from vase-shaped microfossils in the Chuar Group, Grand Canyon Paleobiology, 26(3) :360-385

15. Reinhardt ED, Daldy AP, Kumar A, Patterson RT (1998) Arcellaceans as pollution indicators in mine tailing contaminated lakes near Cobalt, Ontario, Canada. Micropaleontology 44:131-148

16. Sageman BB, Bina CR (1997) Diversity and species abundance patterns in Late Cenomanian black shale biofacies, Western Interior, US. Palaios, 12 (5):449-466

17. Scott DB, Medioli FS (1980) Living vs. total foraminiferal populations: their relative usefulness in paleoecology. Journal of Paleontology, 54:814–831

18. Scott DB, Medioli FS, Schafer CT (2001) Monitoring in coastal environments using foraminifera and thecamoebian indicators. Cambridge University Press, Cambridge.

19. Tolonen K. (1986) Rhizopod analysis. In: Berlund BE (eds) Handbook of holocene palaeoecology and palaeohydrology. Wiley, Chicchester :645-666

20. Vašíček M, Růžička B (1957) Namurian Thecamoebina from the Ostraxa-Karvina coal district: Sbornik Narodního Muze v Praze, Rada B, Přírodní Vědy Acta Musei Nationalis Pragae, Series B, Historia Naturalis, v. 13, p. 333–340.

21. Warner BG, (1990) Methods in Quaternary Ecology Testate Amoebae (Protozoa). Geoscience Canada, 15:251-260.

22. Warner BG, Charman, D (1994) Holocene changes on a peat land in northwestern Ontario interpreted from testate amoebae (Protozoa) analysis. Boreas, 23: 270-279

23. Wanner M (1999) a review on the variabilityof testate amoebae: methodical aproaches, environmental influences and taxonomical implications. Acta Protozoologia 38:15-29